Diplodiosis: Cytotoxicity and ultrastructural changes induced by diplodiatoxin, dipmatol and diplonine, toxic metabolites isolated from *Stenocarpella maydis*

MXOLISI GOODWILL MASANGO

Diplodiosis: Cytotoxicity and ultrastructural changes induced by diplodiatoxin, dipmatol and diplonine, toxic metabolites isolated from *Stenocarpella maydis*

By

MXOLISI GOODWILL MASANGO

Submitted in fulfillment of the requirement for the degree

Doctor of Philosophy

in the

Department of Paraclinical Sciences,

Faculty of Veterinary Science,

University of Pretoria

Date submitted: October 2014

DECLARATION

I, **Mxolisi Goodwill Masango**, declare that the thesis, which I hereby submit for the degree **Doctor of Philosophy** at the University of Pretoria, is my own work and has not previously been submitted by me for a degree at this or any other tertiary institution.

Signature: ……..

ACKNOWLEDGEMENTS

- I am sincerely grateful to my supervisor Prof Christo Botha for his invaluable contribution and guidance throughout this critical step of my scientific development.
- I would like to thank my co-supervisor Dr. Charlotte Ellis for her consistent support.
- Dr. Louis Ackerman for providing me with diplodiatoxin and dipmatol as well as drawing the chemical structures of the toxins.
- Dr. Leendert Snyman and Ms. Anitra Schultz for providing me with diplonine.
- Ms Arina Ferreira for her technical assistance in the cytotoxicity assays.
- Dr. Mirinda Van Kleef for her help with the flow cytometer readings.
- Ms. Erna Van Wilpe and Dr. Lizette Du Plessis for preparation of the EM samples.
- Ms. Nicolene Thiebaut for statistical analyses and interpretation.
- Prof. B.C. Flett for his scientific contribution on the literature review.
- Onderstepoort Biological Products (OBP) for permission to use their xCELLigence instrument.
- Agricultural Research Council (ARC) for allowing me time and resources to undertake this study.
- Toxicology personnel for their support.
- University of Pretoria for allowing me to register for my studies.

❖ The following funding bodies for their financial support: International Foundation for Science (IFS), Joy Liebenberg Trust Fund and National Research Foundation (NRF).

❖ My grandmother, the late Mrs. N.E. Masango (1924-2006), for believing in my vision and my mother, Ms. T.E. Masango, for being a strong pillar in my life for all these years.

❖ My wife, Lesego Modibedi, for her love, patience and understanding.

❖ God Almighty for his faithfulness always.

SUMMARY

Diplodiosis: Cytotoxicity and ultrastructural changes induced by diplodiatoxin, dipmatol and diplonine, toxic metabolites isolated from *Stenocarpella maydis*

By

MXOLISI GOODWILL MASANGO

Supervisor:	Prof. C.J. Botha
Co-supervisor:	Dr. C.E. Ellis
Department:	Paraclinical Sciences
Degree:	PhD

Stenocarpella maydis (previously known as *Diplodia maydis*) is one of the most prevalent ear and stalk rot pathogens of maize globally, causing reductions of grain quality and yield. Ingestion of *S. maydis* infected maize causes diplodiosis, a neuromycotoxicosis of cattle and sheep. To date, diplodiatoxin, dipmatol, diplonine and chaetoglobosins (K, L, M and O) have been isolated from *S. maydis* infected cultures.

The mechanism of action of these metabolites is poorly understood and consequently, it is not known whether these metabolites play a role in the aetiology of diplodiosis.

The toxicity and mechanism of action of the three *S. maydis* metabolites (i.e. diplodiatoxin, dipmatol and diplonine) were evaluated for the first time in this study using *in vitro* cell cultures, namely the mouse neuroblastoma (Neuro-2a), Chinese hamster ovary (CHO-K1) and Mardin-Darby bovine kidney (MDBK) cells.

The cytotoxicity was firstly evaluated after exposure of the three cell lines to various concentrations of diplodiatoxin, dipmatol and diplonine for 24, 48 and 72 h. The xCELLigence, tetrazolium 3-(4,5-dimethylthiazol-2-yl)-2,5-diphenyltetrazolium bromide (MTT) and protein measurement assays were used. To better understand the mechanism(s) involved in the observed cytotoxicity, necrotic and apoptotic cell death pathways were investigated. The lactate dehydrogenase (LDH) and propidium iodide (PI) flow cytometry assays were used to assess necrotic changes, and the caspase-3/7 and Annexin V-FITC flow cytometry assays were used for apoptosis. Finally, transmission electron microscopy (TEM) was used to evaluate the subcellular changes induced by the *S. maydis* toxins *in vitro*.

Results obtained in this study indicate that both diplodiatoxin and dipmatol induced a concentration-dependent cytotoxicity in Neuro-2a, CHO-K1 and MDBK cells and also affected the activity of the mitochondrial succinate dehydrogenase enzyme. Conversely, diplonine was not cytotoxic at comparable concentrations. Diplodiatoxin and dipmatol, at

high concentrations, exerted their toxicity via the necrotic and the caspase-dependent apoptotic cell death pathways. Mitochondrial damage, cytoplasmic vacuolation and nuclear fragmentation were the major subcellular changes induced by diplodiatoxin and dipmatol. Except for the elongation of mitochondria, no major subcellular changes were observed following exposure of MDBK cells to diplonine. Collectively, these results indicate that mitochondrial damage could be central in the toxicity of the two *S. maydis* metabolites and possibly in the development of diplodiosis.

Keywords: *apoptosis, cell culture, cytotoxicity, diplodiatoxin, diplodiosis, diplonine, dipmatol, maize, necrosis, neuromycotoxicosis, ruminants, Stenocarpella maydis*.

LIST OF ABBREVIATIONS

β	: beta
γ	: gamma
µ	: micro
°C	: degrees Celsius
>	: greater than
%	: percentage
Ac-DEVD-AMC	: acetyl-Asp-Glu-Val-Asp-7-amino-4-methylcoumarin
Apaf1	: apoptotic protease activating factor 1
ARC	: Agricultural Research Council
AST	: aspartate aminotransferase
ATCC	: American Type Culture Collection
ATP	: Adenosine-5´-triphosphate
Bak	: Bcl-2 homology antagonist/killer protein
Bax	: Bcl-2 associated X protein
Bcl-2	: B-cell lymphoma 2
BH3	: Bcl-2 homology 3
Bid	: BH3-interacting domain
BSA	: bovine serum albumin
Cd	: cadmium
CHO-K1	: Chinese hamster ovary
CI	: cell index

Cm	: centimeter
Cm^2	: square centimeter
Da	: Dalton
CO_2	: Carbon dioxide
DISC	: death-inducing signalling complex
DMEM	: Dulbecco's modified Eagle's medium
DMSO	: dimethyl sulphoxide
DNA	: deoxyribonucleic acid
EC_{50}	: effective concentration, 50%
FADD	: Fas-associated death domain
FITC	: fluorescein isothiocyanate
Fwd	: forward
g	: gram
GCI	: Grain Crops Institute
GGT	: γ-glutamyl transferase
h	: hour
$HgCl_2$	: mercuric chloride
k	: kilo
L	: litre
LC-MS	: liquid chromatography-mass spectrometry
LC-ESIMS	: liquid chromatography-electrospray ionization mass spectrometry
LDH	: lactate dehydrogenase
LD_{50}	: lethal dose, 50%

LEM : leukoencephalomalacia

m : milli

M : molar

MDBK : Mardin-Darby bovine kidney

MDCK : Mardin-Darby canine kidney

min : minute

MRC : Medical Research Council

MTT : tetrazolium 3-(4,5-dimethylthiazol-2-yl)-2,5-diphenyltetrazolium bromide

n : nano

NaOH : sodium hydroxide

Neuro-2a : mouse neuroblastoma

NMR : nuclear magnetic resonance

OVI : Onderstepoort Veterinary Institute

p : probability

PBS : phosphate buffered saline

PCR : polymerase chain reaction

PDA : potato dextrose agar

PI : propidium iodide

PS : phosphatidylserine

PT : permeability transition

qRT : quantitative reverse transcription

r : Pearson's correlation

R^2	: correlation coefficient
RAP	: random amplified polymorphic
rev	: reverse
RTCA	: real-time cell analyzer
RT-CES	: real-time cell electronic sensing
SAS	: statistical analysis system
S. maydis	: *Stenocarpella maydis*
TCA	: trichloroacetic acid
TEM	: transmission electron microscopy
TNF	: tumor necrosis factor
TRAIL	: TNF-related apoptosis-inducing ligand
UV	: ultraviolet
XTT	: 2,3-bis(2-methoxy-4-nitro-5-sulphophenyl)-5-carboxanilide-2H-tetrazolium

TABLE OF CONTENTS

LIST OF FIGURES

LIST OF TABLES

CHAPTER 1

INTRODUCTION

1.1 BACKGROUND

Maize (*Zea mays* L.) is produced worldwide and is cultivated in more areas than any other crop. It is regarded as the most important grain crop in South Africa since it is the major feed grain and staple food for the majority of the South African population (DAFF, 2013). Thus, a constant supply of good quality maize that is safe for human and animal consumption is required (Barros et al., 2008). Two major types of maize are produced in South Africa, namely the white maize which is primarily used for human consumption and the yellow maize which is mainly used for animal feed production (DAFF, 2013). During the 2012/13 season, a total of 2.78 million hectares were planted in South Africa with a total maize production of 11.69 million tons (DAFF, 2014).

In South Africa, maize is usually planted from late spring to early summer, with highest planting in November and December. Planting of maize can also start as early as October and extend to January. In a particular season, the planting period and length of the growing season is determined by the rainfall pattern and other weather conditions. In most cases, maize is harvested from late May up to the end of August (DAFF, 2013).

1.2 PROBLEM STATEMENT

Stenocarpella maydis (Berk.) Sutton (previously named *Diplodia maydis* (Berk.) Sacc.) is one of the most prevalent ear and stalk rot pathogens of maize globally, causing reductions of grain quality and yield as well as lodging of plants with infected ears and stalks (Flett & McLaren, 1994). *S. maydis* is known to cause diplodiosis, a neuromycotoxicosis of cattle and sheep (Riet-Correa et al., 2013).

Diplodiosis is considered as the last major veterinary mycotoxicosis of which the causative mycotoxin is still uncertain (Marasas et al., 2012). Over the last three decades in South Africa, various reports of diplodiosis in livestock were received from veterinarians and farmers (Kellerman et al., 1996; 2005). These outbreaks have unfortunately not been confirmed to be caused by *S. maydis* contaminated residues.

Since the first description of diplodiosis in 1914 by Van der Bijl, efforts have been made to isolate the principal toxin(s) responsible for this mycotoxicosis. To date, different metabolites (i.e. diplodiatoxin, dipmatol, chaetoglobosins K, L, M and O and diplonine) have been isolated from *S. maydis* contaminated cultures (Steyn et al., 1972; Ackerman et al., 1995; Snyman et al., 2011; Wicklow et al., 2011; Rogers et al., 2014).

The major drawback with all these *S. maydis* metabolites isolated thus far is that none of them has been administered to ruminants in an attempt to reproduce diplodiosis. Consequently it is not known whether these metabolites play a role in the aetiology of

diplodiosis. In addition, there is limited information available on the mechanism of action of these toxic metabolites, especially diplodiatoxin, dipmatol and diplonine purified from South African fungal isolates. Understanding how these *S. maydis* metabolites exert their cellular effects will be valuable in solving the conundrum of diplodiosis.

1.3 OBJECTIVES

The main objectives of this study were:

- To evaluate the cytotoxicity of diplodiatoxin, dipmatol and diplonine on continuous cell lines.
- To expand our understanding of the mechanism of action of diplodiatoxin, dipmatol and diplonine.

CHAPTER 2

LITERATURE REVIEW

2.1 INTRODUCTION

Modern mycotoxicology probably began in the early 1960's as a result of a rare veterinary crisis in the United Kingdom, which was characterized by death of a large number of turkey poults (Blount, 1961). Consumption of peanut meal, contaminated with secondary metabolites from *Aspergillus flavus*, induced the mycotoxicosis known as Turkey "X" disease. Subsequent studies led to the discovery of aflatoxins and the elucidation of their mechanism of action (Ciegler & Bennett, 1980). Research was conducted, on many of the mycotoxins that are currently known, between 1960 and 1975, a period that has been termed the '*mycotoxin gold rush'* (Maggon et al., 1977). Nearly 400 compounds are currently recognized as mycotoxins, of which a small percentage is considered as a threat to human and animal health (Atanda et al., 2012).

2.2 MYCOTOXINS

Mycotoxins are defined as toxic secondary metabolites synthesized by filamentous fungi. The term mycotoxin has been constructed from the Greek word '*mykes*' which means fungus and the Latin word '*toxicum*' which means poison. Mycotoxins are low-molecular weight natural compounds synthesized by fungi that grow on crops during pre-harvest or post-harvest (Bennett, 1987).

Not all metabolites synthesized by fungi are referred to as mycotoxins. Antibiotics, such as penicillin, are fungal products and are predominantly toxic to bacteria (Turner et al., 2009). In general, mycotoxins are toxic to vertebrates and other animal species when ingested, inhaled or after dermal contact. The most important factors contributing to a mycotoxicosis include the animal species and concentration of the metabolite (Bennett & Klich, 2003).

Various crops are potential substrates for mould growth and mycotoxin formation when stored for more than a couple of days under specific optimal conditions. Cereals, nuts, dried fruits, coffee, cocoa, spices, oil seeds, dried peas, maize, beans and fruits are the most common food commodities affected (Beasely, 2011). Beer and wine produced from contaminated barley and grapes may also contain mycotoxins (Coulombe, 1993). Mycotoxins can also enter the human food chain via edible products of animal origin, such as meat, eggs, milk and cheese, sourced from livestock exposed to contaminated feed (Turner et al., 2009).

2.3 MYCOTOXICOSES

Mycotoxicoses are generally defined as diseases caused by mycotoxins. The majority of mycotoxicoses are attributed to feeds stored under high moisture conditions that favour the growth of fungi. Various mycotoxins have been implicated in numerous fatal intoxications in humans and animals (Ciegler & Bennett, 1980). Mycotoxicoses caused by mouldy maize, such as aflatoxicosis, leukoencephalomalacia (LEM), diplodiosis and zearalenone poisoning, are important veterinary mycotoxicoses in South Africa. However, this literature review focuses on diplodiosis, regarded as the most important neuromycotoxicosis of ruminants in South Africa.

2.4 DIPLODIOSIS

The discussion on *Stenocarpella maydis*, its toxic metabolites and diplodiosis has been published (Masango et al., "In Press"). Refer to the back of the thesis for the complete article.

Diplodiosis is defined as a nervous disorder of cattle and sheep grazing in winter on harvested maize fields infected by *Stenocarpella maydis*. Although this neuromycotoxicosis is most common in southern Africa (Kellerman et al., 2005), it has also been reported in Australia (Darvall, 1964), Argentina (Odriozola et al., 2005) and Brazil (Riet-Correa et al., 2013).

2.4.1 Historical perspectives

The first record of diplodiosis in South Africa is a report by Van der Bijl in 1914 in the region of Mooi River in KwaZulu-Natal province. He reported an outbreak of '*sickness*' in cattle which was characterized by paralysis following grazing on harvested maize fields (Van der Bijl, 1914).

Later in 1919, Mitchell (Fig. 1) confirmed that maize ears infected with *S. maydis* causes diplodiosis in cattle. He was able to induce diplodiosis in cattle by feeding naturally infected maize ears as well as a culture of *S. maydis* grown on sterile maize kernels. The clinical signs elicited by feeding with naturally infected maize ears collected from previously harvested maize fields were indistinguishable from those obtained by feeding with *S. maydis* cultures grown on maize kernels (Mitchell, 1919). The disease was also reproduced experimentally by

Theiler (1927) in cattle and sheep fed sterilized maize kernels artificially infected with *S. maydis*.

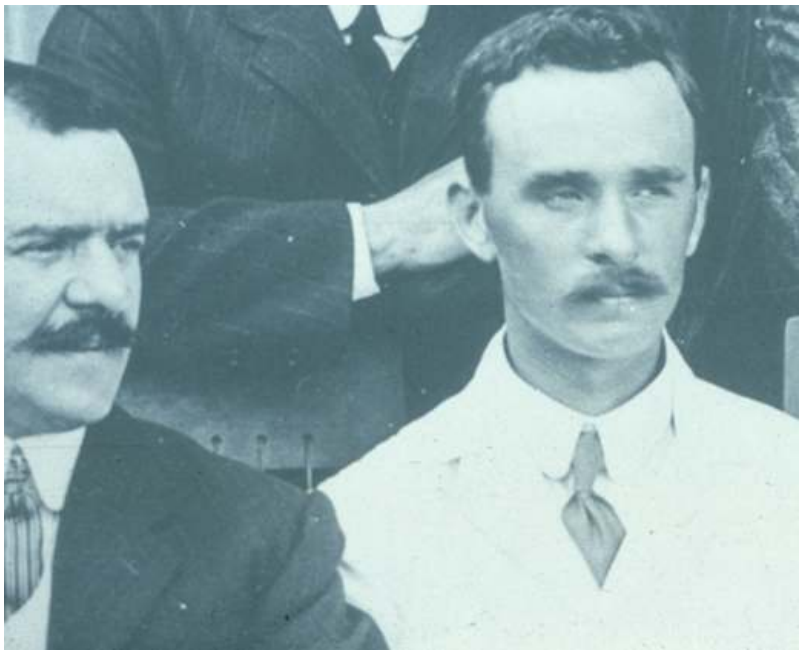

Figure 1. Sir Arnold Theiler (left) and D.T. Mitchell (right). Photographic collection of Toxicology Division, ARC-OVI**.**

2.4.2 *Stenocarpella maydis*

To date no teleomorphic state of the *Diplodia* ear and stalk rot fungus has been identified. The anamorphic stage was a controversial issue for many years. This is obvious from the many synonyms of *Stenocarpella maydis* (Berk.) Sutton which include *Diplodia maydis* (Berk.) Sacc., *Diplodia zeae* (Schw.) Lev., *Sphaeria maydis* Berk., *Sphaeria zeae* Schw., *Diplodia maydicola* Speg., *Diplodia zeae-maydis* Mechtij., *Macrodiplodia zeae* (Schw.) Petrak and Syd., *Hendersonia zeae* (Schw.) Hazsl. and *Phaeostagonosporopsis zeae* (Schw.) Woron. Sutton (1964) suggested the species be accommodated in a distinct genus and later placed both *Diplodia maydis* and *Diplodia macrospora* Earle into the genus

Stenocarpella after typification of *Diplodia* and related genera (Sutton, 1980). The genus was described by Sutton (1980) based primarily on conidiogenesis. The conidiogenic cells of the genus *Stenocarpella* are enteroblastic, phialidic, determinate, discrete (only rarely integrated on one septate conidiophore), cylindrical, colarette and channel minute, periclinal wall is thickened and formed from the inner cells of the pycnidial wall. The revised typification of the genus *Diplodia* and related genera meant that *Stenocarpella* became the acceptable generic name to use in this context (Sutton, 1980).

The genus *Stenocarpella* contains two species known as *Stenocarpella maydis* (Berk.) Sutton and *Stenocarpella macrospora* (Earle) Sutton (formerly referred to as *Diplodia macrospora*). The two *Stenocarpella* species are encountered throughout the world as economically important ear rot pathogens of maize (Wicklow et al., 2011). The global distribution of *S. maydis* is shown in Figure 2. A South African study reported *S. maydis* ear rot to be the most prevalent of the two *Stenocarpella* species with *S. macrospora* being more common in parts of KwaZulu-Natal (Flett & Wehner, 1991). *S. macrospora* therefore appears to be restricted to the lower altitude maize production areas in South Africa, whereas *S. maydis* is widespread in all maize production areas. In KwaZulu-Natal, where both species occur, it is important to determine which *Stenocarpella* spp. is most prevalent in a specific area.

Figure 2. Global distribution (green circles) of *Stenocarpella maydis* (http://www.plantwise.org/KnowledgeBank/PWMap).

2.4.3 Symptoms of *Stenocarpella* stalk and ear rot

The *S. maydis* fungal pathogen causes a seedling blight, stalk and ear rot of maize (Fig. 3 A & 3 B). *S. maydis* seedling blight root symptoms appear as necrotic lesions and lead to dwarfing and stunting together with other organisms making up the root rot complex (Chambers, 1982). Crown infections develop from seed- or soil-borne inoculum. Symptoms of crown infection include straw brown discolouration of the crown, lower internode and root tissues (McNew, 1937). *S. maydis* stalk rot manifests itself after flowering, resulting in plants wilting and eventually dying prematurely, resembling frost injury. Under stress conditions the lower stalk internodes become brown or straw coloured, soft and spongy and are easily crushed. Stalk pith tissue disintegrates and discolours until only the vascular bundles remain intact (Shurtleff, 1980). *S. maydis* ear rot symptoms generally develop from the base of the maize ear growing up to its tip, and are visible as white-grey-brownish mycelia over the husk and kernels. Silk infections occur with downward mycelial ramification but such infections are less frequent (Koehler, 1942). Later season ear infections may show no external symptoms, but removal of kernels exposes discoloured embryos (Shurtleff, 1980).

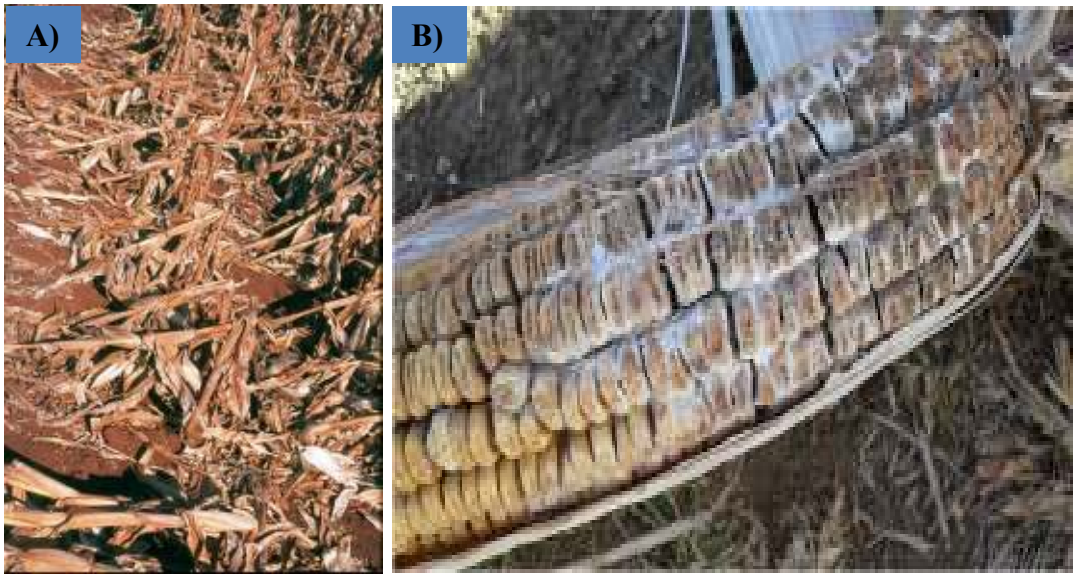

Figure 3. Maize stalks (A) and ear (B) infected by *Stenocarpella maydis*. Photographs 3 A and 3 B were provided by B.C. Flett (ARC-GCI) and C.J. Botha (University of Pretoria), respectively.

2.4.4 Inoculum development and infection of maize stalks and ears by *Stenocarpella maydis*

Stenocarpella maydis overwinters on maize stubble as viable pycnidia which are produced on the infected husks, kernels and rotted stalks (Fig. 4 A & 4 B) (Flett & Wehner, 1991; Flett et al., 1992). Pycnidia are flask-shaped and are 150-350 µm in diameter. Conidiophores, which are elongated, straight or curved, are formed from cells of the inner pycnidial wall. Conidia are formed from the apex of the conidiophores and are cylindrical or ellipsoidal, narrowing at both ends to a round apex and truncate base (Marasas, 1977; Kellerman et al., 1985). Conidia are released from pycnidia in cirrhi under warm moist conditions and are wind- or rain-borne (Shurtleff, 1980; Del Rio & Del Rio, 1991). *S. maydis* conidia infect through leaf attachments on the maize stalk (Durrel, 1923) where ear rot infections occur through ear tips and leaf shanks (Koehler, 1942). Miller (1952) determined that after germination mycelium ramifies from the shank through the cob to the grain

attachment, filling cavities between the embryo, scutellum, coleoptile and plumule. Ramification into kernels begins at embryonic tissues and proceeds into the starchy and horny endosperm and pericarp (Miller, 1952; Bensch, 1995).

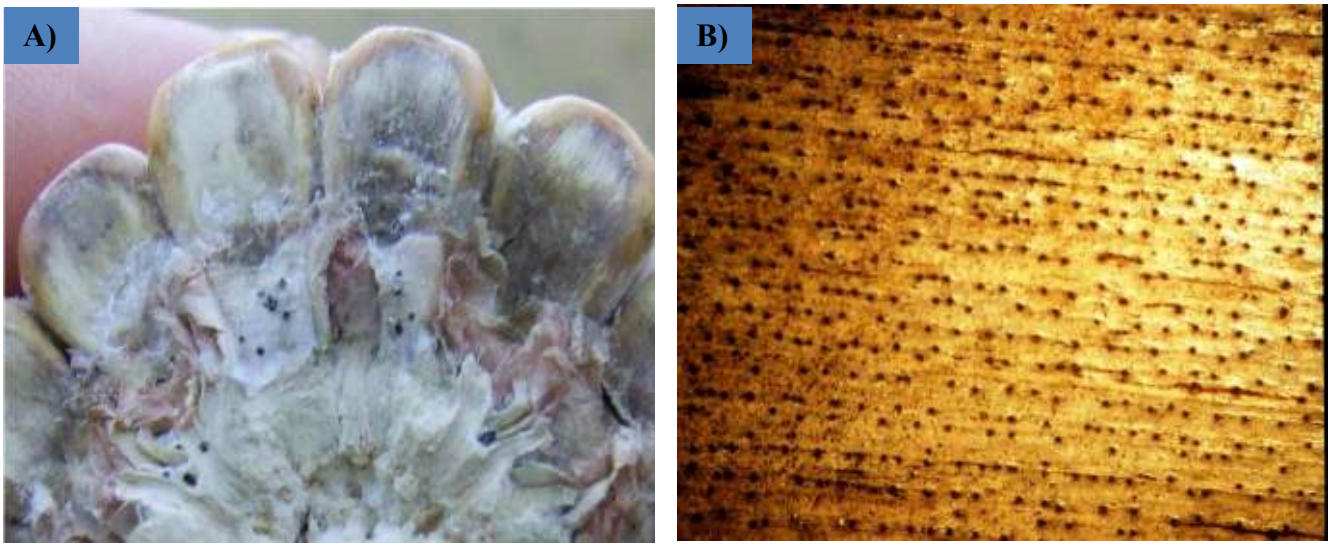

Figure 4. *Stenocarpella maydis* pycnidia (black spots) on a maize cob (A) and stalk (B). Photographs 4 A and 4 B were provided by C.J. Botha (University of Pretoria) and B.C. Flett (ARC-GCI), respectively.

2.4.5 Isolation and characterization of *Stenocarpella* spp.

Stenocarpella spp. are easily isolated by placing pieces of infected maize tissue on artificial agar. The fungus grows readily on media such as cornmeal, potato dextrose, or malt extract agars where it produces a thick, coarse, white, woolly aerial mycelium. Dark brown to black pycnidia containing conidia eventually develop on and in the agar (Rabie et al., 1977; Flett & McLaren, 1994). Snyman (1991) reported that pycnidium and conidium production under black light on half-strength potato dextrose agar (PDA) was 0.41 pycnidia/cm^2 and 245 conidia per 9 cm Petri dish, respectively, whereas on cornmeal agar (CMA) it was 0.05

pycnidia/cm^2 and 21 conidia per 9 cm Petri dish, respectively. Eight isolates used in this study did not differ significantly regarding pycnidium and conidium development on these standard agars. Snyman (1991) developed a maize kernel medium onto which *Stenocarpella* spp. isolates could be plated and extensive pycnidial development and sporulation occurred after incubation for 14 days under black light at 28 °C. Black light increased pycnidium and conidium development on the maize kernel medium from 0.41 to 1.99 pycnidia/cm^2 and 123 to 1 926 conidia per 9 cm Petri dish, respectively, using a mean of eight *S. maydis* isolates. This maize kernel medium increased *S. maydis* and *S. macrospora* sporulation under black light which enabled researchers to distinguish between the two *Stenocarpella* spp. isolated from maize ears (Snyman, 1991).

Cultural characteristics of the two fungi on isolation agars are almost identical. On agar, *S. macrospora* grows slower than *S. maydis*, and pycnidia are also formed less rapidly and abundantly. Another characteristic difference is that *S. maydis* grows well on synthetic media whereas *S. macrospora* requires biotin-like growth factors (Marasas, 1977; Latterell & Rossi, 1983). The main characteristic distinguishing *S. macrospora* from *S. maydis* is the size of the conidia. Conidia of *S. macrospora* are two to three times (43-98 x 6-14 µm) larger than the *S. maydis* conidia and have two to three celled conidia. *S. maydis* conidia are one to two celled, straight or curved and 15-34 µm long x 5-8 µm wide (Sutton, 1980).

2.4.6 Detection of *Stenocarpella maydis* in affected maize commodities

Visual ear damage symptoms caused by *S. maydis* are very similar to those caused by *S. macrospora* and it is extremely difficult to distinguish which species is the cause of ear rot in the field. Methods commonly used for the detection of fungal contamination are based on phenotypic and physiological characteristics that make use of standard culture and biochemical or serological tests (Lezar & Barros, 2010). Traditionally, *S. maydis* infected grains are identified by competent maize graders who perform visual inspections of maize consignments at the grain silos where the grains are stored (Flett & McLaren, 1994). The major disadvantage of visual grading inspections, in the context of diplodiosis, is that they do not provide the true level of infestation or toxin production since growth of this fungus is not limited to the surface area of the maize kernels and in certain cases may be difficult to detect for the untrained eye. *S. maydis* ear rot symptoms are normally easily visible in the field unless infections occur late and are restricted to the embryo. These symptoms have been termed '*hidden diplodia*' (Flett et al., 1996).

Severity of *S. maydis* infected ears may be quantified by determining the percentage of infected ears, by plating out of 200 kernels per sample and identification of colonies in a random sample. Alternately infected kernels in a 250 g randomly selected sample can be sorted visually and infected kernels expressed as a percentage of the total (Flett & Wehner, 1991; Flett et al., 1998, 2001). Although these techniques generally correlated with one another, each technique has its own shortcomings. Firstly, the percentage of infected ears was done by harvesting a research plot and counting total ears and rotten ears irrespective of spread of the fungus on the ear. If infections occurred late in the season some infected ears could not be seen due to the '*hidden diplodia*' symptoms and this may underestimate the

amount of infection as only part of the ear is rotten. Secondly, the plating out of 200 kernels as a representative for an entire plot or field may result in identifying all kernels infected, but due to sample size may lead to high statistical variation. Thirdly, the technique of taking a 250 g sample and sorting rotten kernels and expressing these as a percent of the total 250 g sample may include grains infected by numerous other ear rot fungi. In epidemic seasons these three techniques were shown to correlate significantly but in seasons where *S. maydis* infections occurred late or in seasons/localities where other ear rot pathogens predominated, these techniques did not always correlate (Flett, B.C. unpublished data). The greatest disadvantage of these methods are that the quantification of *S. maydis* in grain samples becomes costly and lengthy (Barros et al., 2008).

Recently, various molecular methods have been developed for the identification of *S. maydis* infestation in maize grain. These methods include Random Amplified Polymorphic DNA (RAPD)-PCR (Blakemore et al., 1994) where the primer 5'-CGGTTTGGTC-3' produced a single major band common for all 15 isolates tested. Although little polymorphism was obtained, the single main band could be used as a probe for *S. maydis*. Since then, other PCR-based techniques (Xia & Achar, 2001; Barros et al., 2008; Barrocas et al., 2012) and oligonucleotide microarrays (Lezar & Barros, 2010) have been developed to identify *S. maydis* DNA within a host substrate. These methods increased accuracy and speed of determining the presence of *S. maydis* in host tissue, but could not be used to quantify the fungus in a sample. Mouton (2014) developed a quantitative reverse transcription (qRT)-PCR using primers *Maydis3 fwd*/*Maydis3 rev* for the detection and quantification of the *S. maydis* biomass in a root, stalk or grain maize sample.

2.4.7 *Stenocarpella maydis* metabolites

Different toxic metabolites have been isolated from *S. maydis* contaminated cultures using various organic solvent systems. These mycotoxins include diplodiatoxin (Steyn et al., 1972), dipmatol (Ackerman et al., 1995), diplonine (Snyman et al., 2011) and chaetoglobosins K and L (Wicklow et al., 2011).

2.4.7.1 Diplodiatoxin

Diplodiatoxin ($C_{18}H_{28}O_4$; molecular weight: 308 g/mol) contains a β-ketol side chain and the rare β,γ-unsaturated acid unit (Fig. 5). This metabolite has been isolated and characterized from *S. maydis* infected maize cultures using bioassay-guided isolation from chloroform-methanol extracts. Steyn et al. (1972) reported that diplodiatoxin accounted for only 10% of the total toxicity of the maize culture material based on toxicity studies in chickens. Administration of diplodiatoxin (265 mg/kg) to chickens induced liver degeneration (Louw, 1969). Using a highly stereo-controlled strategy, Ichihara et al. (1986) successfully synthesized diplodiatoxin. The authors reported the synthetic diplodiatoxin as being identical to the natural diplodiatoxin based on spectroscopic data.

The toxicity of diplodiatoxin has also been evaluated in rats (Rahman et al., 2002; Rao et al., 2003). In rats, diplodiatoxin causes a decrease in body weight and feed intake, dullness, irritability, tremors and convulsions when administered at a single oral dose of 5.7 mg/kg or daily at 0.27 mg/kg (for 21 days) to male and female rats. In addition, evidence was provided for liver damage (increased alkaline and acid phosphatases as well as aspartate and alanine aminotransferase activities) and inhibition of the brain acetylcholinesterase activity.

Diplodiatoxin induced significant lesions in maize leaves after it was tested for phytotoxicity using the leaf puncture wound assay (Wicklow et al., 2011).

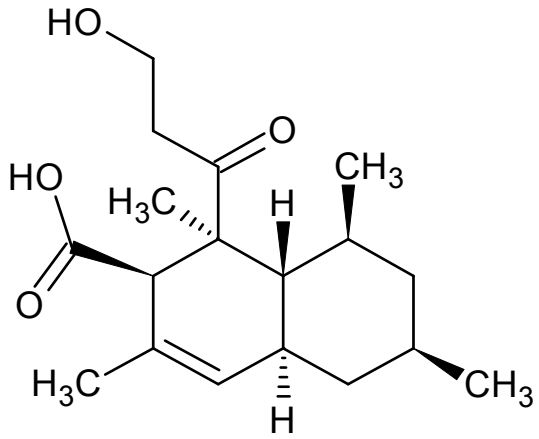

Figure 5. Chemical structure of diplodiatoxin (Steyn et al., 1972).

Diplodiatoxin was detected in naturally infected field maize ears (Wicklow et al., 2011) and in a field outbreak of *S. maydis* ear rot in Illinois, North America (Rogers et al., 2014). Liquid chromatography-mass spectrometry (LC-MS) was used by Rogers et al. (2014) to detect diplodiatoxin at 200 ng extract per injection of the acetonitrile-soluble portion of the infected maize kernels. The LC-MS analysis performed by Wicklow et al. (2011) did not provide quantitative data of the concentrations of diplodiatoxin.

2.4.7.2 Dipmatol

Dipmatol ($C_{15}H_{27}O_5$; molecular weight: 287 g/mol) has been characterized as a trihydroxyhexadecanoic acid (Fig. 6), and it was isolated from *S. maydis* infected cultures using chloroform-hexane. Not much is known about this *S. maydis* metabolite except that its toxicity has been evaluated in broiler chickens (Ackerman et al., 1995). The stereochemistry

of the three chiral centers of the molecule is currently being determined (L.G.J. Ackerman, personal communication, 2013).

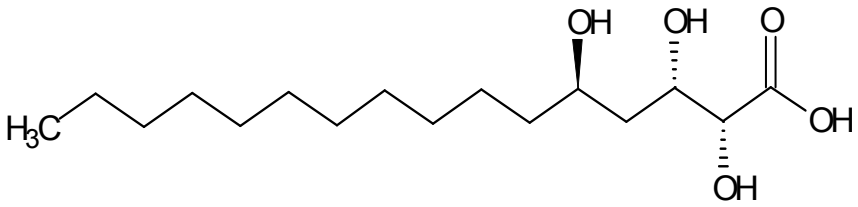

Figure 6. Chemical structure of dipmatol (Ackerman et al., 1995).

2.4.7.3 Diplonine

Diplonine ($C_6H_{11}NO_3$; molecular weight: 145 g/mol), has been classified as a substituted β-cyclopropylamino acid (Fig. 7). This neurotoxin has been isolated using methanol extraction from *S. maydis* cultures that had been used previously to induce diplodiosis in sheep (MRC 2829 and ARC-GCI 6) (Snyman et al., 2011). The cultures and subsequent column chromatography fractions were evaluated for toxicity using the guinea pig as model (Schultz et al., 2009).

Guinea pigs gavaged with 1 580 mg diplonine per kg body weight exhibited incoordination, imbalance, paresis in the hindquarters, frequent falling and lateral recumbency which were followed by recovery. These authors suggested that the clinical signs were similar to the neurological signs observed in cattle and sheep with diplodiosis and that diplonine may therefore be the toxic metabolite responsible for this disease or may at least contribute significantly to intoxication (Snyman et al., 2011).

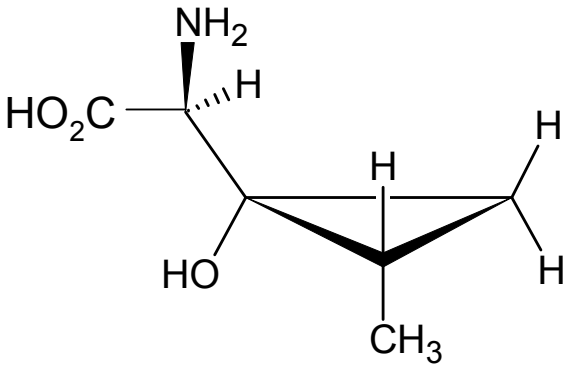

Figure 7. Chemical structure of diplonine (Snyman et al., 2011).

Diplonine was detected for the first time in a field outbreak of *S. maydis* ear rot by Rogers et al. (2014) using ^{1}H nuclear magnetic resonance (NMR)-based analysis. Approximately 75-350 µg of diplonine in a 320 mg sample of a methanol extract was detected.

2.4.7.4 Chaetoglobosins

Chaetoglobosins are metabolites that belong to the family of cytochalasins and include chaetoglobosin K, L, M and O and other compounds. Chaetoglobosins K and L are isomers with the characteristic molecular formula $C_{34}H_{40}N_2O_5$ and molecular weight of 557 g/mol (Fig. 8 A & 8 B). These metabolites have been isolated from fermented rice cultures of *S. maydis* (NRRL 53565, 53566 and 53567) using ethyl-acetate (Wicklow et al., 2011).

Chaetoglobosin K has significant anti-fungal activity when tested against *Aspergillus flavus* and *Fusarium verticillioides* (Wicklow et al., 2011). In addition, this mycotoxin demonstrated significant insecticidal activity against the fall armyworm, *Spodoptera frugiperda*, in dietary assays. Cutler et al. (1980) isolated chaetoglobosin K from maize infected with *S. macrospora* and reported that this metabolite was toxic to day-old chickens with an LD_{50} ranging from 25 to 62.5 mg/kg.

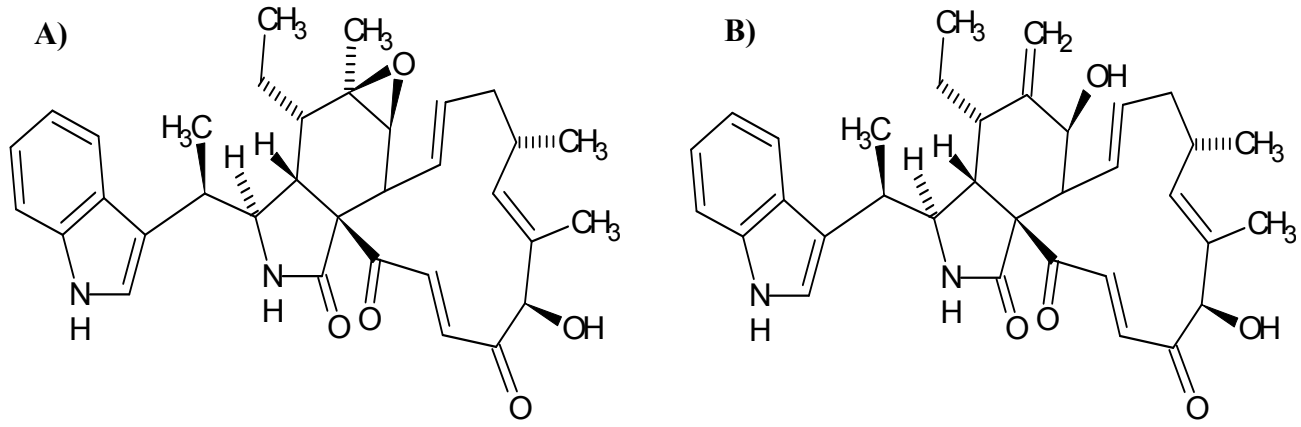

Figure 8. Chemical structures of chaetoglobosin K (A) and L (B) (Wicklow et al., 2011).

Chaetoglobosins K, M and O were detected in a field outbreak of *S. maydis* ear rot using LC-MS analysis (Rogers et al., 2014). Approximately 2 µg of chaetoglobosins K, M and O was detected in the ethyl-acetate extracts prepared from *S. maydis* infected ears.

Wicklow et al. (2011) proposed that chaetoglobosins, including chaetoglobosin K and L, are likely to be the major component in the 'unidentified toxin' mixture that is responsible for diplodiosis in cattle and sheep. Since this mycotoxicosis is characterized by degeneration of

myelin in neonates, these authors have based their argument on the fact that chaetoglobosins disrupt actin polymerization and therefore interferes with the myelination process.

2.4.8 Factors influencing the occurrence of diplodiosis

Diplodiosis in southern Africa is not observed every year. The field outbreaks of the disease occur sporadically and are believed to be favoured by heavy late rains (for ear rot infections) and early rains followed by severe mid-season droughts (for stalk rot infections) (Louw, 1969; Marasas, 1977). Diplodiosis is limited to the late winter months, namely July to September. This is the period when the field grazing is scarce and it is common practice for farmers to allow their cattle to graze in harvested maize fields to utilize the stover (Kellerman et al., 2005). In years past, the occurrence of diplodiosis was most likely due to the practice of discarding all malformed maize ears by either leaving them on the stalks or dropping them to the ground during hand reaping. Thus, when the cattle were introduced to the harvested maize fields, there were a considerable number of infected maize ears lying around and these were readily ingested by cattle (Mitchell, 1919; Marasas, 1977).

Not all isolates of *S. maydis* cause diplodiosis (Rabie et al., 1977; 1985). Variability in the toxigenic potential between *S. maydis* strains from different geographical areas has also been suggested as another reason for the sporadic occurrence (Marasas, 1977). The incubation period of the fungus is also important in inducing diplodiosis. In all the reported cases where diplodiosis was experimentally reproduced successfully, the *S. maydis* cultures used were incubated for at least 6-8 weeks at 27-28 °C (Mitchell, 1919; Theiler, 1927; Kellerman et al., 1985). Under field conditions, this period may be less due to the exposure of

plant material to numerous biotic and abiotic environmental conditions which could limit the build-up of toxins.

Stenocarpella epidemics differ due to climatic variations and presence of inoculum which are conducive to disease outbreaks. Flett and McLaren (1994) referred to this interaction between available inoculum and conducive climatic conditions as disease potential which interacts with various genotypes resulting in inconsistent disease reactions. Susceptibility of the predominant genotypes in specific areas influences the severity of epidemics of *Stenocarpella* ear rot. Van Rensburg and Ferreira (1997) reported the most consistent infection levels in seasons with extreme droughts after flowering, high summer temperatures and late season rains, whereas lowest average infection rates occurred in seasons with cool and humid conditions. During the 1985/86 to 1988/89 seasons, serious *Stenocarpella* ear rot epidemics occurred in South Africa resulting in reductions of grade one maize (primarily yellow) of up to 60% and an increase in grade three maize of up to 30% nationally (Nowell, 1997; Flett, 1999). These epidemics have become localized and restricted to certain areas particularly where reduced tillage and maize monoculture has been practised (Flett, 1999).

Relatively large quantities of naturally infected maize ears or culture material must be consumed to induce diplodiosis (Marasas, 1977; Kellerman et al., 2005). Hence the degree of ear rot caused by *S. maydis* probably plays a role, with a greater risk during more severe epidemics or when greater levels of residues remain in the field. The agricultural practice of using harvested maize fields for winter foraging and grazing by cattle is another important factor in diplodiosis (Marasas, 1977; Odriozola et al., 2005). Prior to the use of

mechanization, maize fields were harvested by hand and infected ears were discarded onto the land where livestock, both cattle and sheep, could pick up and ingest the ears. With the use of modern combine harvesters, *S. maydis* infested grain (lightly infected kernels which are heavy enough to be sorted with healthy grain) either goes into the bin with the rest of the grain, or the heavily rotten ears are broken in the process and are scattered onto the field in smaller pieces. These small pieces are more difficult for cattle to pick up; however, smaller ruminants such as sheep may still be able to ingest these infected kernels or pieces of kernels.

2.4.9 Species affected

Under field conditions diplodiosis is limited to sheep and cattle. No cases have been reported in equidae or pigs (Mitchell, 1919; Theiler, 1927; Marasas, 1977). Goats fed with maize kernels infected with *S. maydis* (15 g/kg) developed signs of diplodiosis within 2-3 days (Kellerman et al., 1985).

Maize kernels infected with *S. maydis* were reported to be acutely toxic to ducklings and rats (Rabie et al., 1977). The major lesion observed in rats was a toxic degenerative myocarditis and no neurological signs were observed. In a subsequent study, no correlation was reported between the toxicity of *S. maydis* strains in ducklings and their ability to induce diplodiosis in cattle and sheep (Rabie et al., 1985).

Schultz et al. (2009) suggested the guinea pig as an appropriate bio-assay model for the identification of the principal toxin(s) in crude extracts of *S. maydis* cultures. Following

dosing of guinea pigs with approximately 75 g of *S. maydis* crude extracts, these authors reported neurological signs resembling diplodiosis in cattle and sheep.

2.4.10 Clinical signs

Under field conditions, diplodiosis occurred from 6 days to 2 weeks after the animals were introduced to harvested maize fields with infected maize ears and stalks. During experimental trials, the animals developed clinical signs from 2-8 days after feeding with *S. maydis* infected maize kernels (Kellerman et al., 1985; 1991). The clinical signs typically last for 1- 4 days. In the beginning the animals' back is slightly arched, there is a slight quivering of the muscles of the flank and shoulders which are accompanied by lacrimation and salivation. The animal stands with its legs further apart than normal and is reluctant to move (Fig. 9 A & 9 B). Locomotory effects, such as ataxia with high-stepping gait, hypermetria and falling, are noticed (Fig. 9 C & 9 D). These signs become more pronounced with time and eventually the animal is unable to rise (Fig. 9 E & 9 F). At this stage the animal still feeds and drinks occasionally while lying on the ground, becomes constipated and the hard faecal balls are covered with blood-tinged mucus. Death is preceded by complete muscular paralysis (Fig. 10).

Recovery is rapid and complete if stock are removed from the maize fields when distinct clinical signs develop. There is no increase in body temperature throughout the course of the disease (Mitchell, 1919; Marasas, 1977; Kellerman et al., 2005).

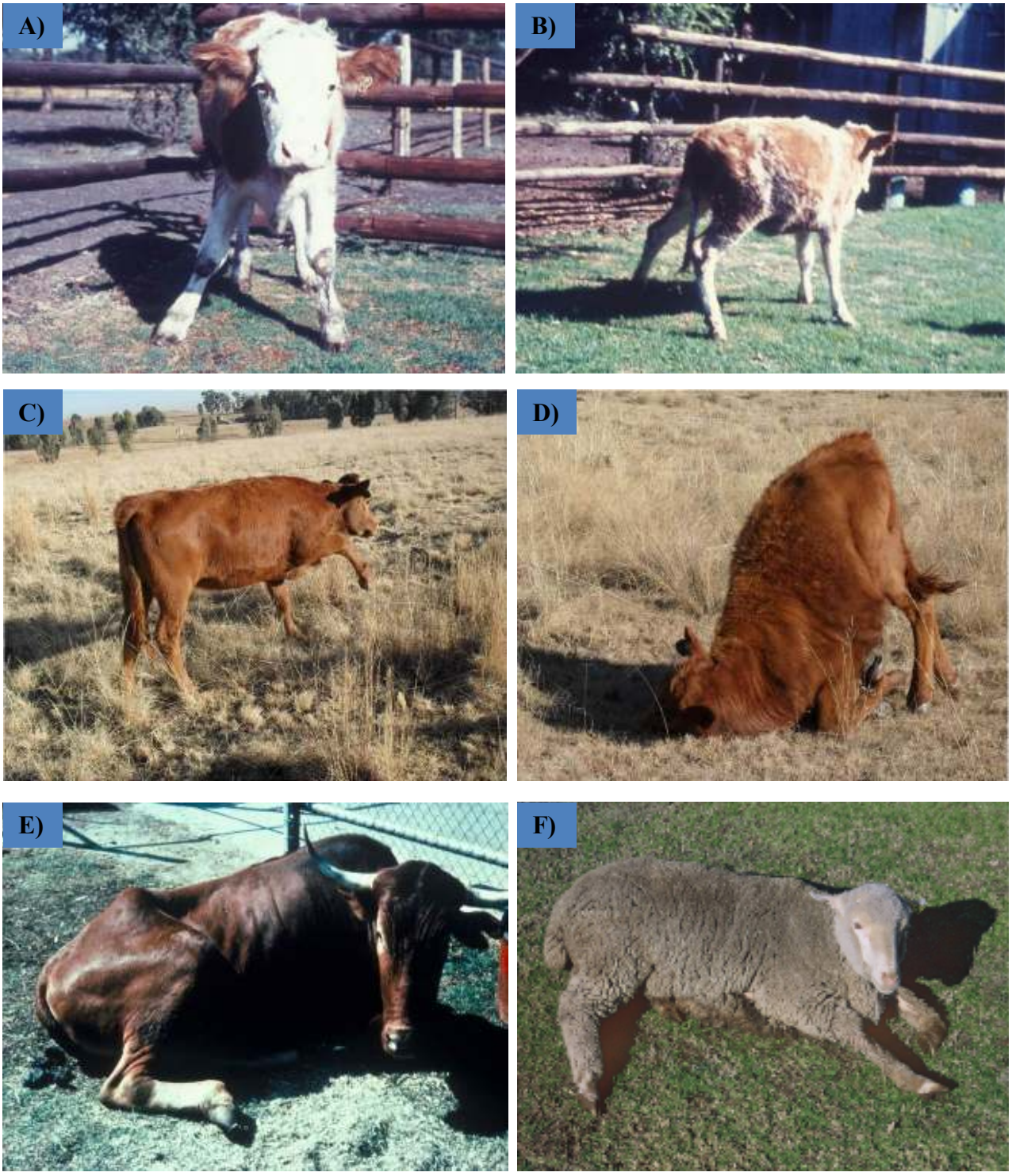

Figure 9. Diplodiosis: Heifer standing with legs wide apart (A & B); ataxia with high stepping gait, hypermetria (C) and falling (D); paretic/paralytic ruminants (E & F). A, B, E & F - Photographic collection of Toxicology Division, ARC-OVI (T.S. Kellerman & L.D. Snyman). Photographs C & D were provided by C.J. Botha (University of Pretoria).

Figure 10. Diplodiosis: Paretic/paralytic young animal. Photographic collection of Toxicology Division, ARC-OVI.

2.4.11 Reproductive effects

Perinatal losses were reported in sheep flocks and cattle herds that had been exposed to diplodiosis (Fig. 11 A) (Kellerman et al., 1991). Sixty-six and 87% of the offspring of ewes exposed to toxic cultures of *S. maydis* during the second and third trimester of gestation, respectively, were either stillborn or non-viable and died soon after birth (Fig. 11 B) (Prozesky et al., 1994). Kellerman et al. (1991) concluded that the developing foetuses are much more susceptible to diplodiosis.

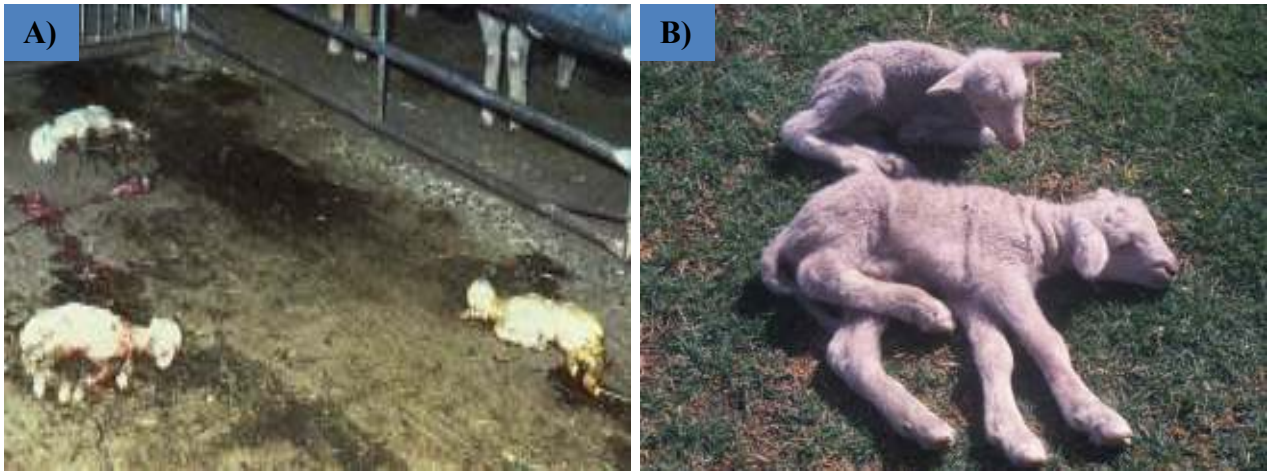

Figure 11. Diplodiosis – reproductive effects: Stillborn lambs produced by ewes exposed to cultures of *Stenocarpella maydis* (A) (Kellerman et al., 1991). Paretic lambs born after ewes were exposed to *S. maydis* (B). Photographic collection of Toxicology Division, ARC-OVI.

2.4.12 Pathology

Gross lesions are usually not present in naturally affected adult cattle. Mitchell (1919) reported catarrhal enteritis, diffuse hyperaemia of the kidneys and congestion of the lungs in one experimentally induced case of bovine diplodiosis.

Microscopically, spongiform degeneration of the white matter of the cerebellum and cerebrum is rarely seen. In dosing trials with pure *S. maydis* cultures, widespread laminar subcortical *status spongiosis* was observed in the brain of a sheep that had been paralyzed for a number of days and in a steer that had permanent locomotory disturbances (Kellerman et al., 1985). In contrast to adult animals, stillborn and non-viable lambs exhibited pronounced *status spongiosis* in the brain and spinal cord. In lambs, the *status spongiosis* is mainly characterized by the presence of vacuoles within myelin sheaths which sometimes develop into large cystic areas, separated myelin lamellae at the intraperiod line, enlargement of the extracellular space and swelling of astrocytes (Fig. 12) (Prozesky et al., 1994).

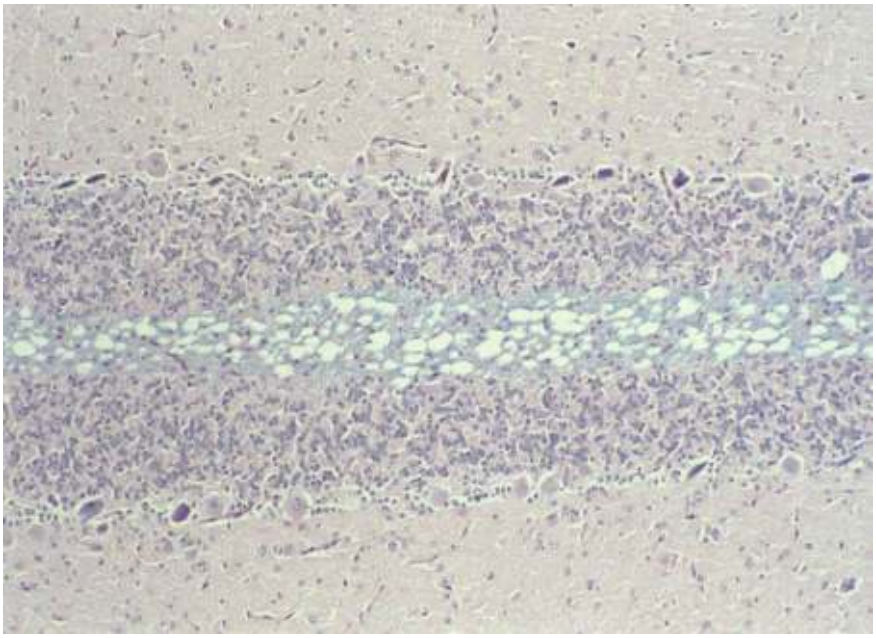

Figure 12. Spongiform degeneration (*status spongiosis*) of the cerebellar white matter of an affected lamb. Brain sections were stained with luxol-fast-blue periodic-acid-Shiff haematoxylin (Prozesky et al., 1994).

Odriozola et al. (2005) recorded an outbreak in Argentina of high mortality (37%) of heifers after they grazed on harvested maize fields infected by *S. maydis*. The clinical signs were consistent with those reported previously for diplodiosis. No gross lesions were observed in this study, however histopathological examination revealed moderate to severe degeneration of myelin sheaths in the white matter of the cerebellum (*status spongiosis*) (Odriozola et al., 2005).

No notable chemical pathological changes (i.e. packed cell volume, haemoglobin concentration, γ-glutamyl transferase (GGT) and aspartate aminotransferase (AST) serum activities and serum concentrations of urea, sodium, potassium, calcium and magnesium) have been reported in the recorded cases of diplodiosis (Kellerman et al., 1985).

2.4.13 Diagnosis

A diagnosis of diplodiosis could be considered where nervous signs in cattle and sheep grazing on harvested maize fields during winter are observed. The main differential diagnoses are tremorgenic diseases caused by indole-diterpenoid mycotoxins such as *Paspalum* staggers and Bermuda grass staggers (Uhlig et al., 2009). Diplodiosis in the initial stages bears some resemblance to heartwater (*Ehrlichia ruminantium*), however, it is most easily confused with botulism when the animals become paralytic (Kellerman et al., 2005). Poisoning by *Aspergillus clavatus* shares similar signs with diplodiosis, but can be distinguished from diplodiosis by the high mortality rate (Sabater-Vilar et al., 2004). A detailed microscopical examination of the central nervous system could aid in the diagnosis, mainly in cases of neonatal mortality when the dams do not exhibit clinical signs.

2.4.14 Treatment and prevention

There is no specific treatment for diplodiosis. This disease can be controlled by removing the animals from harvested maize fields as soon as the first signs of diplodiosis are noticed. Most, if not all, of the affected animals should recover with good nursing care after removal from the toxic fields. Care should be taken when dosing affected animals orally with electrolyte-containing solutions and other remedies as the deglutition muscles may be affected (Kellerman et al., 2005).

In order to decrease the prevalence of diplodiosis in the following winter season, all mouldy maize ears and stalks should be removed from the field by deep early ploughing and burning. Agronomic practices such as the use of resistant maize hybrids, removal of infested stubble and crop rotation, aimed at reducing the levels of *S. maydis* infection of the maize

plants, should be considered as preventative measures to reduce *Stenocarpella* ear rot epidemics and in turn the potential for outbreaks of diplodiosis (Van Rensburg & Flett, 2010).

2.5 CYTOTOXICITY TESTING

The use of non-animal test methods such as *in vitro* studies plays a critical role in enhancing our understanding of the harmful effects caused by toxins or chemicals in animals and humans (Freshney, 2001). *In vitro* systems are focussed primarily on screening and generating more comprehensive data on the toxicological profiles of chemicals. In addition, they are important in studying tissue- and target-specific effects as well as providing information about the mechanism of action of toxins.

When cells are experiencing toxic stress, they respond by changing their metabolic rates, cell growth or gene transcription, thus resulting in the phenomenon of cytotoxicity. Cytotoxicity can be described as the quality of being toxic to cells (Horvath, 1980). In *in vitro* studies, a compound or treatment is considered to be cytotoxic if it affects cell growth rate, cellular attachment and morphology or cause cell death (Niles et al., 2008). *In vitro* cytotoxicity tests are important in defining the concentration range required to undertake further and other more detailed *in vitro* testing methods; in order to provide valuable information on parameters such as mechanism of cell death, induction of mutations (mutagenicity) or genotoxicity and possibly carcinogenicity. Cytotoxicity tests allow quantitative comparison of single or several compounds in individual or different systems by estimating the dose at which 50% of the cells are affected (EC_{50}) (Eisenbrand et al., 2002).

Data generated from cytotoxicity studies may have negative implications (e.g. death of cells following exposure to toxic substances) or positive implications (e.g. development of anticancer drugs) (Valentin et al., 2000). Advantages of the cytotoxicity assays include the ability to control the physico-chemical and physiological environment during the course of the experiments. In addition, cytotoxicity assays provide reproducible data. The toxin concentration and the duration of exposure can be regulated more accurately compared to *in vivo* systems. *In vitro* assays are usually relatively simple to perform, analysis of the results is straightforward and the consumables and labour costs are low, especially with the microtitre-plate systems. The major disadvantage of *in vitro* assays is that they do not fully mimic the *in vivo* environment and lack some of the *in vivo* features, such as the pharmacokinetic parameters of absorption, distribution, metabolism and excretion. Genetic instability is most common in cultured cells, especially continuous cell lines. Additionally, a cell population different to the tissue from which the cells were derived may result from selection pressure. Cultured cells also lack the unique cell and matrix interaction needed to sustain the differentiated phenotypes (Borenfreund & Puerner, 1985; Freshney, 2001).

There are several important factors to consider when performing cytotoxicity assays. In most cytotoxicity studies, cytotoxicity and viability measures are inversely proportional, meaning that cytotoxicity measures are high when viability measures are low, and *vice versa* (Niles et al., 2008). In short-term exposure experiments (4h or less), toxins may adversely affect metabolism markers before changes in membrane integrity are detected. In long-term exposure experiments (24h or more), measurement of cytotoxicity may be underestimated as a result of degradation of the marker enzyme activity after release into the extracellular environment (Riss & Moravec, 2004). The last main consideration when performing cytotoxicity testing is the manner in which cells die. There are three main types of cell deaths,

namely the apoptosis (type I), autophagy (type II) and necrosis (type III) (Loos & Engelbrecht, 2009).

Cell death is an essential part of normal development and survival, and death of cells is determined by cellular responses to physiological conditions. These processes are strictly regulated to maintain normal development and tissue homeostasis, as well as to protect against a variety of diseases such as ischaemia, viral infection, neurodegeneration and tumours (Saikumar et al., 1999; Han et al., 2008). Apoptosis is one particular form of cell death that is most common. The three main types of cell death have traditionally been distinguished in mammalian cells based on their unique morphological criteria (Schweichel & Merker, 1973). The determining factor of whether cells die by apoptosis, necrosis or other default mechanisms is dependent on the cell type or the nature and duration of cell injury. In most cases, apoptosis can be induced when harmful stimuli such as radiation or anticancer drugs are administered at low doses, but the same stimuli can result in necrosis at higher doses. Therefore, in most cases cell death does not occur as a straight forward process (Schulze-Osthoff, 2008).

2.5.1 Apoptosis

Apoptosis is morphologically distinguished by cell shrinkage, changes in nuclear morphology (i.e. chromatin condensation and nuclear fragmentation), blebbing of plasma membrane and formation of apoptotic bodies that contain nuclear or cytoplasmic material (Collins et al., 1997; Loos & Engelbrecht, 2009). Apoptosis occurs in a well-orchestrated sequence of morphological events (Fig. 13 A & 14 c). This process usually begins with the blebbing of the plasma membrane which breaks up into membrane-bound apoptotic bodies

that contain cytoplasmic organelles as well as portions of the nucleus (Kerr et al., 1972). Phagocytes and neighbouring cells recognise and ingest these apoptotic bodies. Apoptosis takes place without any leakage of cellular contents and therefore does not induce inflammatory response.

Condensation of the nucleus and its fragmentation into smaller pieces is considered as the most noticeable and defining feature of apoptosis, which is not seen in any other forms of cell death. Hydrolysis of nuclear DNA into internucleosomal fragments is another characteristic feature of apoptosis (Fig. 13 A). Apoptotic changes are stereotypical and similar in all cell types irrespective of the death stimulus, hence the biochemical mechanisms responsible for these changes also follow a similar built-in process (Schulze-Osthoff, 2008).

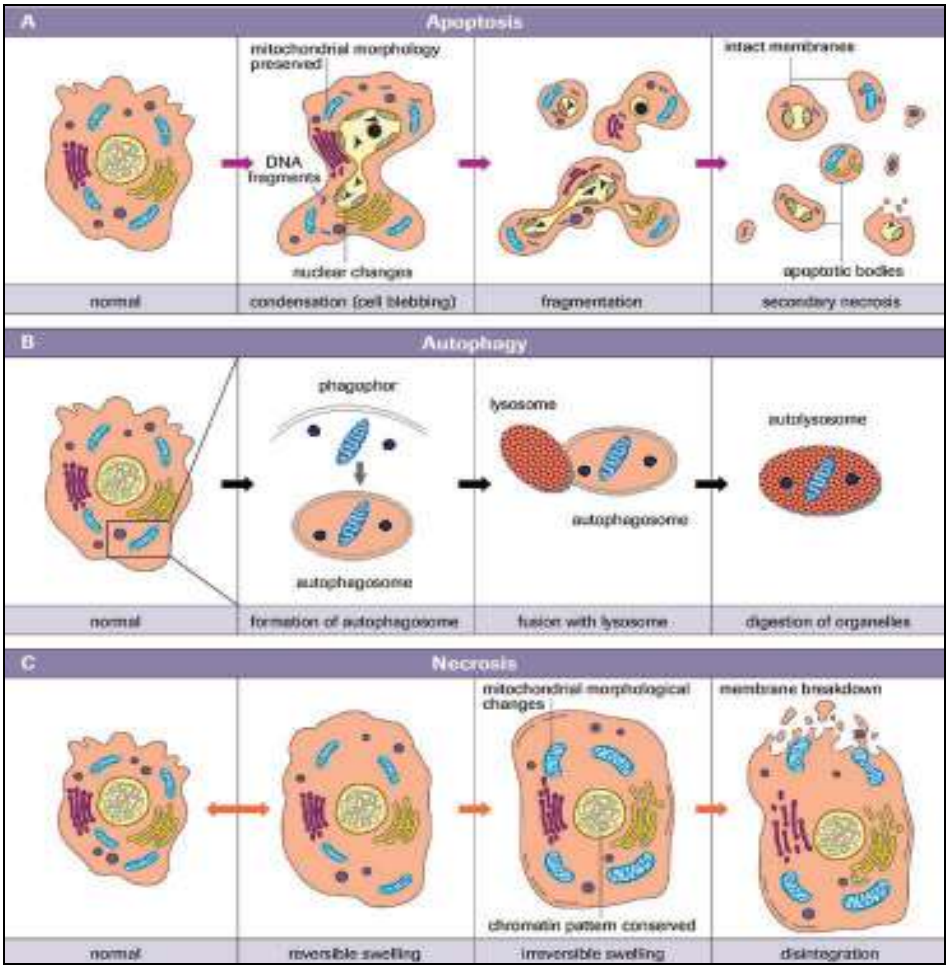

Figure 13. Schematic illustration of the three main types of cell deaths: Apoptosis (A), autophagy (B) and necrosis (C) (Schultze-Osthoff, 2008).

When activated, caspases (a unique class of intracellular proteases) mediate morphological changes of apoptosis (Taylor et al., 2008). Caspase proteases form the core engine of apoptosis and play a major role in the initiation, execution and regulatory phases of this pathway. Caspases become activated in the early stages of apoptosis. These proteases are divided into upstream initiators and downstream effectors of apoptosis based on their structure and sequence in cell death pathways (Los et al., 1999). Effector caspases such as caspase-3, -6 and -7 are made up of a short prodomain and cleave diverse cellular proteins and substrates. Initiator caspase-2, -8, -9 and -10 consist of a long prodomain and exert

regulatory roles by activating downstream effector caspases (Fuentes-Prior & Salvesen, 2004).

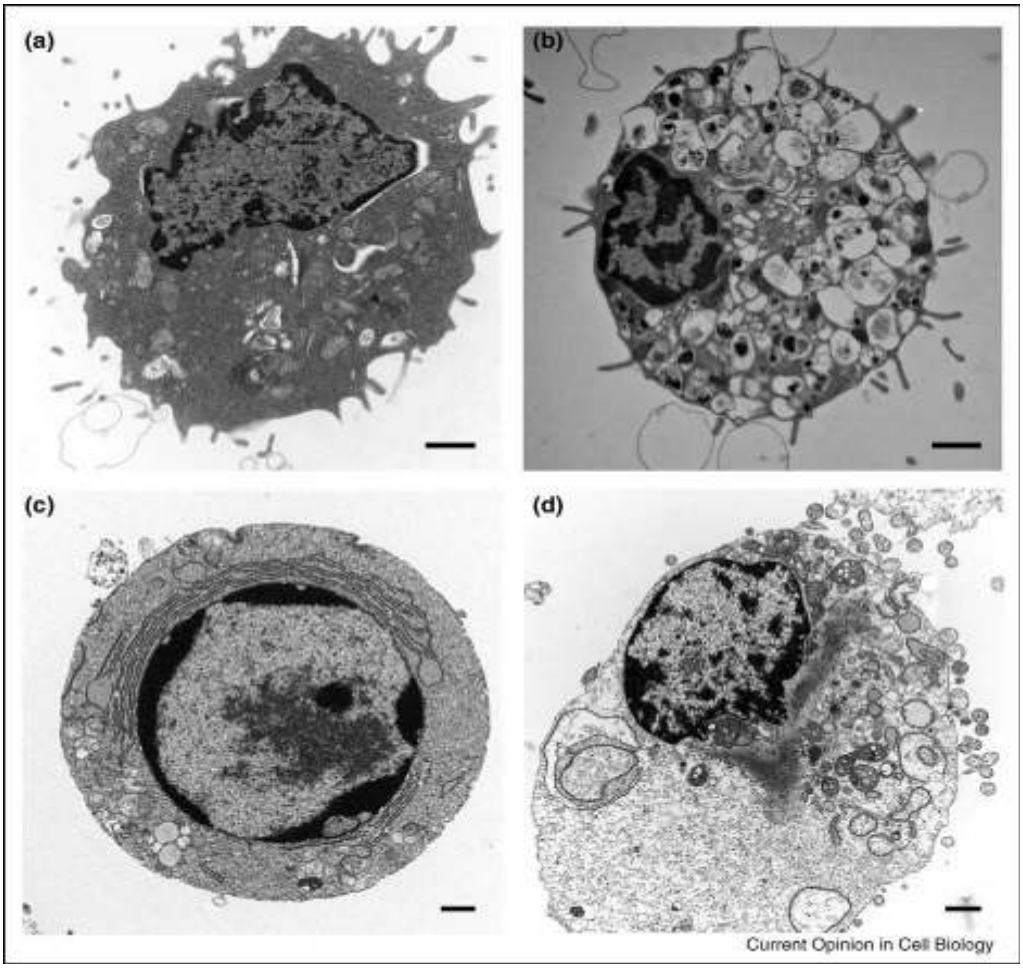

Figure 14. Morphological characteristics of cells undergoing autophagy, apoptosis and necrosis. Normal (a), autophagic (b), apoptotic (c), and necrotic (d) cells (Edinger & Thompson, 2004).

Apoptosis can be induced in cells through a number of different pathways, namely the extrinsic death receptor pathway and the intrinsic mitochondrial pathway. The extrinsic death pathway is characterized by the involvement of extrinsic stimuli whereby death inducing ligands bind to cell surface receptors known as death receptors. This pathway is most

commonly employed when cytotoxic T-lymphocytes recognise damaged or virus infected cells via the death ligands. The intrinsic mitochondrial pathway is characterized by the involvement of mitochondria following cellular stress such as DNA damage, loss of adhesion, growth factor withdrawal or exposure to chemicals (Danial & Korsmeyer, 2004; Meier & Vousden, 2007).

Death receptors are cell surface receptors responsible for the transmission of apoptotic signals initiated by specific ligands such as the Fas ligand, tumour necrosis factor (TNF) alpha and TNF-related apoptosis-inducing ligand (TRAIL). All death receptors contain the intracellular structure called the death domain, which is responsible for transmission of the apoptotic signal. Following ligand binding, the death receptors communicate via their death domain with a corresponding protein interaction structure, termed the death effector domain of adapter proteins, which in turn facilitates binding to the prodomain of the initiator caspase-8 (Fig. 15). The resulting protein complex is called the death inducing signalling complex (DISC), which recruits caspase-8 and ultimately initiates apoptosis via the subsequent activation of downstream effector caspases (Danial & Korsmeyer, 2004; Debatin & Krammer, 2004).

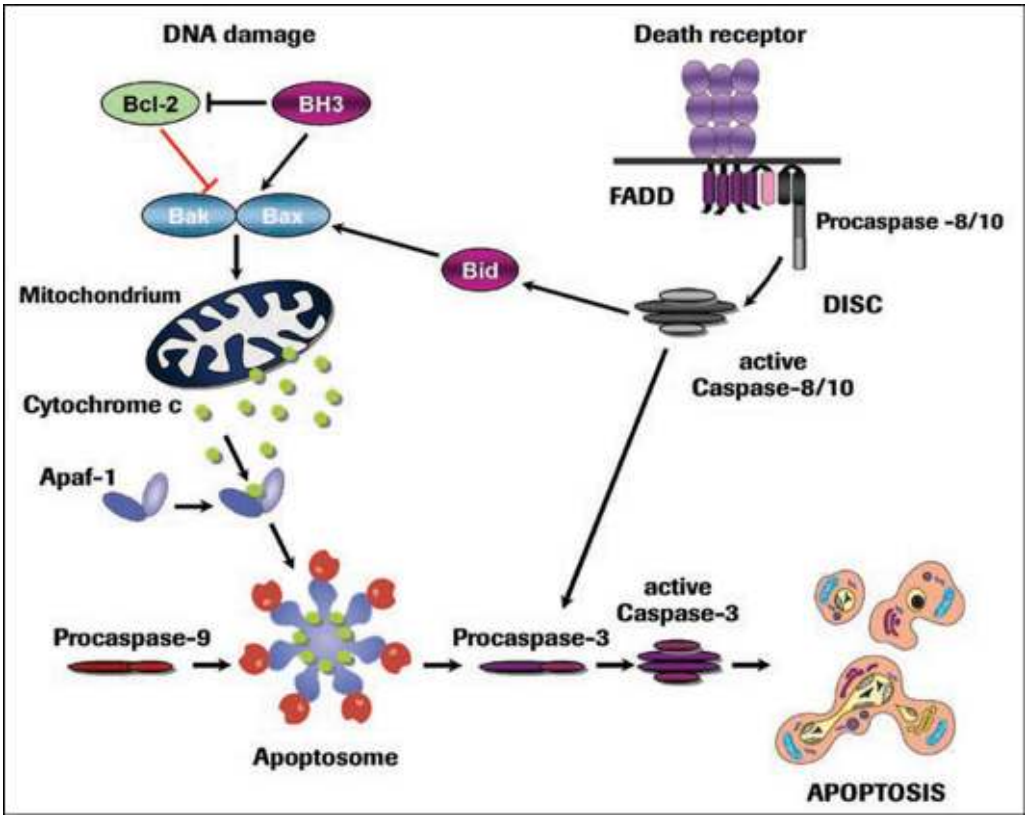

Figure 15. Schematic illustration of the major pathways of apoptosis. FADD = Fas-associated death domain; DISC = death inducing signalling complex; Bid = BH3 interacting domain; BH3 = Bcl-2 homology 3; Bcl-2 = B-cell lymphoma 2; Bak = Bcl-2 homology antagonist/killer protein; Bax = Bcl-2-associated X protein; Apaf1 = apoptotic protease activating factor 1 (Schultze-Osthoff, 2008).

Mitochondria play a critical role in the regulation of cell death. They contain many pro-apoptotic co-factors including cytochrome c. In the electron transport processes of the respiratory chain, cytochrome c is normally involved in the generation of ATP. However, it serves as a co-factor for the adapter protein Apaf-1 in the cytoplasm of apoptotic cells. The interaction between cytochrome c and Apaf-1 leads to the recruitment of pro-caspase-9 to form a multi-protein complex known as apoptosome (Fig. 15). Formation of the apoptosome results in the activation of caspase-9 and the subsequent induction of apoptosis. Cytochrome c is released from the mitochondria through special pores called the permeability transition

(PT) pores. The PT pores are formed as a result of the action of the pro-apoptotic members of the Bcl-2 family of proteins. The Bcl-2 proteins are activated by apoptotic signals such as cell stress, DNA damage, free radical damage or growth factor deprivation. Mitochondria also play a critical role in amplifying the apoptotic signal from the death receptor through activation of Bid, a pro-apoptotic Bcl-2 protein, by caspase-8 (Adams & Cory, 1998; Shimizu et al., 1999).

The most common assays used to study apoptosis include electron microscopy, DNA fragmentation, caspase activity (e.g. caspase-3/-7), Annexin V flow cytometry and Western blot assays. Some of the apoptosis assays used in this study are discussed in detail in Chapter 5.

2.5.2 Autophagy

Autophagy, which literally mean 'self-eating', is a highly conserved catabolic process for a large variety of long-lived proteins and organelles (Bergmann, 2007). Nutrient starvation and metabolic or hypoxic stress are the most common inducers of autophagy. This type of cell death is morphologically characterized by the appearance of a number of double-membrane vacuoles or vesicles, known as autophagosomes, in the cytoplasm (Fig 13 B & 14 b). The autophagosomes encapsulates whole organelles and cytoplasmic materials and eventually fuse with the lysosome whereby the autophagosome contents are degraded and recycled (Edinger & Thompson, 2004).

In addition to the classical function of autophagy in turnover of cytoplasmic components, promoting cell adaptation and survival during stress, it is involved in programmed or autophagic cell death and tissue-specific processes (Mariño & Lopez-Otín, 2004). Deficiencies in autophagy are implicated in a number of diseases, including myopathies, neurodegenerative diseases, liver diseases and some forms of cancer (Levine & Kroemer, 2008).

2.5.3 Necrosis

Necrosis has been traditionally described as a consequence of physical and chemical stress, which does not require energy and believed to be accidental (Festiens et al., 2006; Hamacher-Brady et al., 2006). However, recent evidence suggests that necrosis is a consequence of a well-orchestrated process involving various signalling cascades (Saberi et al., 2008). Necrosis is morphologically characterized by cytoplasmic swelling, vacuolation of the cytoplasm, breakdown of the plasma membrane, dilation of organelles (e.g. mitochondria, endoplasmic reticulum and Golgi apparatus), moderate chromatin condensation and induction of inflammation around the dying cell caused by the release of cytoplasmic contents and pro-inflammatory molecules (Fig. 13 C & 14 d) (Edinger & Thompson, 2004; Festiens et al., 2006).

This type of cell death is biochemically characterized by massive energy depletion, increase in intracellular calcium, generation of reactive oxygen species and activation of non-apoptotic proteases (Orrenius et al., 2003). In conditions where there is inhibition of specific proteins, such as caspases, the mechanism of cell death switches from apoptosis to necrosis resulting in caspase-independent necrotic cell death (Lockshin & Zakeri, 2004). It has

therefore been suggested that necrosis might act as a backup cell death mechanism when apoptosis or autophagic cell death fails (Kitanaka & Kuchino, 1999).

The most common assays used to study necrosis include electron microscopy and assays based on the alteration of the plasma membrane permeability (e.g. lactate dehydrogenase leakage and propidium iodide uptake assays). These assays are discussed in greater detail in Chapter 4.

CHAPTER 3

CYTOTOXICITY OF DIPLODIATOXIN, DIPMATOL AND DIPLONINE

Parts of the cytotoxicity results presented in this chapter have been published (Masango et al., 2014). Refer to the back of the thesis for the complete article.

3.1 INTRODUCTION

A variety of *in vitro* assays have been used to assess cellular viability and/or cytotoxicity (Riss & Moravec, 2004; Fotakis & Timbrell, 2006; Ellis et al., 2010). A majority of these experimental assays are based on the exclusion of dyes from cells and uptake of dyes into cells.

Tetrazolium 3-(4,5-dimethylthiazol-2-yl)-2,5-diphenyltetrazolium bromide (MTT) was the first tetrazolium dye to be used in the development of a multi-well viability assay for mammalian cells (Mosmann, 1983). This assay is based on the principle that cellular damage results in loss of the ability of the cell to maintain and provide energy for the metabolic functions and growth. The experimental procedure involves the addition of a small volume of MTT, dissolved in phosphate-buffered saline (PBS), to the cultured cells. The yellow MTT dye is transported into viable cells via endocytosis (Kim et al., 2009) where it is reduced to a purple formazan product by cellular mitochondrial and cytosolic enzymes, after incubation for 1- 4 h at 37 °C (Gonzalez & Tarloff, 2001). Formazan is an aqueous insoluble product, hence, a second additional step of dimethyl sulphoxide (DMSO) is required to solubilize and

disperse it for maximum absorbance (Mosmann, 1983). The MTT assay is well characterized and is often considered as the '*gold standard*' that new viability or cytotoxicity assays are compared with (Niles et al., 2008). The major advantage of this colorimetric assay is that it is very rapid, cheap and convenient (Fotakis & Timbrell, 2006).

The protein assay is an indirect determination of cell viability since it measures the protein content of cells following exposure to toxic substances (Shopsis & Eng, 1985). This assay is based on the relative growth of treated cells compared to the control cells to show differences in toxicity. Depending on the incubation time with the test compound, the termination of cell replication may also contribute to the overall difference in protein content (Harbell et al., 1997). The Bradford assay is a common spectrophotometric method used to determine protein concentrations. The assay depends on the change in absorbance of the Coomassie reagent after binding with proteins (Bradford, 1976). The reaction is very rapid, however, the results of this assay are influenced by non-protein sources such as detergents (Compton & Jones, 1985; Husøy et al., 1993). The results are also protein-dependent and vary with the composition of the protein (Forsby et al., 1991).

Cellular changes in response to toxic substances are dynamic with multivariate parameters. Certain cellular effects such as morphological and adhesive changes, which may not lead to ultimate cell death, are transient and occur only at the early or late stages of toxin exposure (Xing et al., 2005; 2006). Most conventional cell-based assays (such as the MTT and Bradford protein assays) that are currently available use labelling or dye based endpoint detection that provides only single information such as cell viability, at one given time point in the entire cellular dynamic process. Thus, to accurately assess toxin-induced cellular

damage and to understand the mechanism of action of toxic compounds, it is important to examine multiple parameters in real time (Kustermann et al., 2013).

In recent years, new technological approaches have emerged thus enabling label-free detection methods for cell-based assays. One of the most sophisticated new technologies is the real-time cell electronic sensing (RT-CES) system, based on a special micro-electronic sensor-based platform (Ózsvári et al., 2010). This system utilizes a microtitre plate station, which is kept inside a CO_2 incubator that is maintained at 37 °C. The electrode sensor array is specifically designed and integrated onto the bottom of the microtitre plate and is sensitive to cells directly growing on the sensor surface. The basic principle of the RT-CES system is to monitor the changes in electrode impedance induced by the interaction between cultured cells and electrodes. The presence of the cells results in an increase in the electrode impedance. The more cells attach to the sensor, the higher the impedance that can be monitored with RT-CES. Because the test is label-free, the RT-CES assay allows real-time, automatically and continually monitored cellular changes during the whole process of the cell-toxin interaction.

In this chapter, the cytotoxicity of diplodiatoxin, dipmatol and diplonine was evaluated on the mouse neuroblastoma (Neuro-2a), Chinese hamster ovary (CHO-K1) and Mardin-Darby bovine kidney (MDBK) cell lines. Cytotoxicity of the *S. maydis* metabolites was assessed using the real-time cell analyzer (RTCA) xCELLigence, MTT and Bradford protein assays.

3.2 MATERIALS AND METHODS

3.2.1 Materials

All the materials used in the cytotoxicity experiments were purchased from Sigma Aldrich, South Africa, unless otherwise stated.

3.2.2 *Stenocarpella maydis* metabolites

Diplodiatoxin ($C_{18}H_{28}O_4$; molecular weight: 308 g/mol) (Steyn et al., 1972), dipmatol ($C_{15}H_{27}O_5$; molecular weight: 287 g/mol) (Ackerman et al., 1995) and diplonine ($C_6H_{11}NO_3$; molecular weight: 145 g/mol) (Snyman et al., 2011) were utilized.

3.2.3 Maintenance of cell cultures

The Neuro-2a, CHO-K1 and MDBK cells (Fig. 16) were obtained from the American Type Culture Collection (ATCC). The cells were grown in DMEM (Dulbecco's modified Eagle's medium) (Neuro-2a cells) or DMEM and Ham's F-12 Nutrient Mixture (CHO-K1 and MDBK cells) supplemented with 10% foetal calf serum, 100 U/mL penicillin, 100 µg/mL streptomycin and 2.5 µg/mL amphotericin B (Fungizone) in a humidified atmosphere of 5% CO_2 at 37 °C. The cells were cultured in 75 cm^2 cell culture flasks.

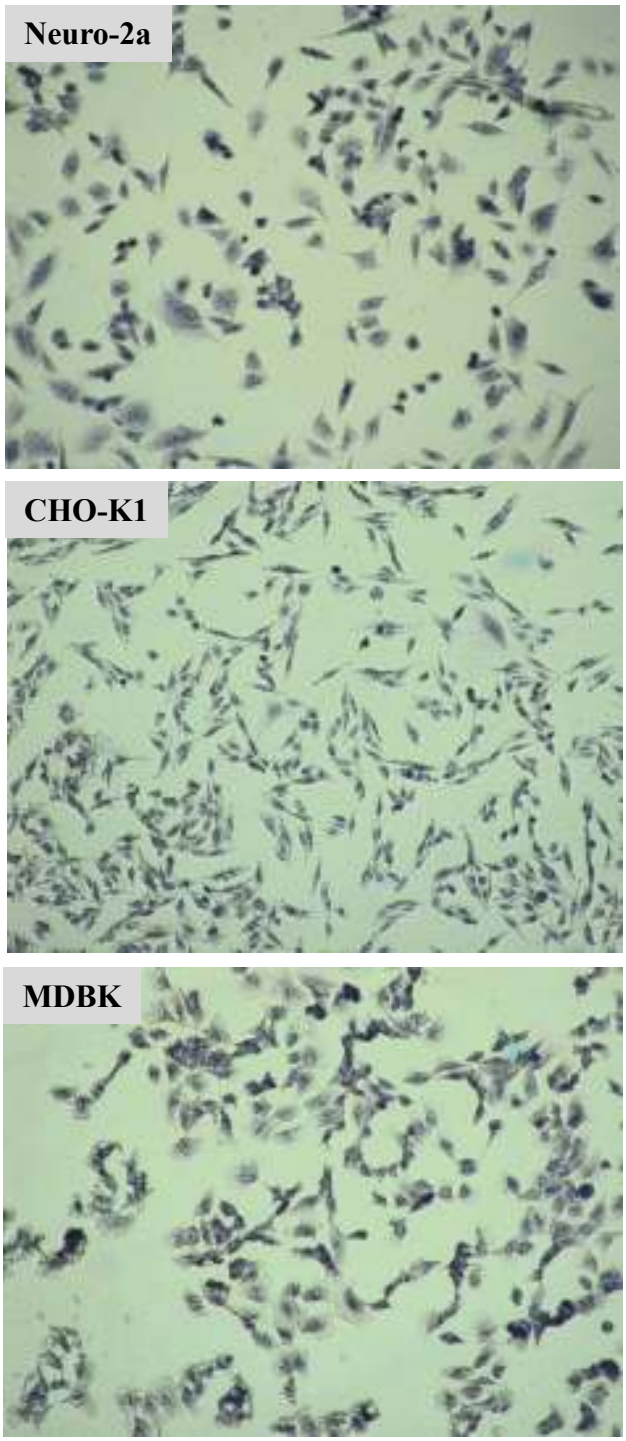

Figure 16. Photographs showing the characteristic morphology of Neuro-2, CHO-K1 and MDBK cells. Cells (100 000 cells/slide) were plated on glass slides and incubated overnight in a humidified atmosphere of 5% CO_2 at 37 °C. Cells were washed with PBS and fixed with acetone (100%) for 15 min at -20 °C. Fixed cells were incubated with trypan blue for 24 h, washed with PBS and observed under UV light microscope.

3.2.4 Cell proliferation studies using the xCELLigence system

Proliferation curves for the Neuro-2a, CHO-K1 and MDBK cells were initially determined in order to establish the appropriate cell densities (in growth area of ±0.32 cm^2) to be used in the cytotoxicity assays. Before cells were seeded on the E-plate, 50 µL of cell culture media was added and background impedance was recorded for each well. The cells were resuspended in cell culture media and densities were adjusted to 5 000, 10 000, 20 000 and 40 000 cells/mL. The cell suspensions (200 µL) were added to the 50 µL media-containing wells on the E-plate. Growth and proliferation of the cells were monitored for a period of up to 96 h, without changing the cell culture media, via the incorporated sensor electrode arrays of the E-plate. The electrical impedance was measured by the RTCA-integrated software of the xCELLigence system as a unit less cell index (CI) value. Appendix 1 provides the xCELLigence programming used during the experiments.

A cell index is derived to represent the cell status based on the measured relative change in electrical impedance that occurs in the presence and absence of cells in the wells. The CI is calculated based on the following formula: $CI = (Z_i - Z_0)/15$, where Z_i is the impedance at an individual point of time during the experiment; Z_0 is the impedance at the start of the experiment and 15 is the impedance factor. When there are no cells on an electrode surface, the sensor's electronic feature will not be affected and the impedance will be zero. The impedance will increase when more cells attach to the electrodes and this will lead to a higher CI value. However, cell death or toxicity induces cell detachment which will lead to a decreased CI value (RTCA SP instrument operator's manual).

3.2.5 Cytotoxicity assays

Based on results obtained from the proliferation studies, cell lines seeded at a density of 20 000 cells/mL were exposed to the *S. maydis* toxic metabolites. After attaching to the wells (24 h post culturing), cells were exposed to diplodiatoxin, diplonine and dipmatol at concentrations of 10, 100, 250, 350, 500 and 750 µM (750 µM concentrations were not included in xCELLigence assays for CHO-K1 cells). The stock solutions of the toxic metabolites were prepared in DMSO. The working solutions of the toxins were prepared in the corresponding cell culture media. Control wells were prepared by adding 200 µL of the corresponding culture medium.

3.2.5.1 xCELLigence cytotoxicity assay

The cytotoxic effect of the three *S. maydis* toxins was evaluated and monitored in real time by using the RTCA xCELLigence 16-well plate system (Roche Applied Sciences). The different toxin dilutions (200 µL) were added to the wells on the E-plate. The dynamic growth of the three different cell lines was then measured at 1 h intervals over 72 h. Two independent experiments were carried out with two replicate wells for each toxin concentration.

3.2.5.2 MTT assay

Assessment of cell viability was carried out using the method of Mosmann (1983). At the end of the exposure period, 10 µL of MTT (5 mg/mL in PBS) was added into each well and the cells were further incubated for 4 h. Thereafter, cells were lysed with DMSO for 30 min in order to dissolve the formazan crystals. The formation of colour (formazan) was measured

with a microtitre plate spectrophotometer (Bio-Tek µQuant) at 570 nm. Results were analyzed with GraphPad Prism software (version 4.0). Cell viability was estimated as the percentage absorbance of the toxins tested relative to control cells. Three independent experiments were carried out with three replicate wells for each toxin concentration.

3.2.5.3 Protein measurement assay

Protein determination was based on the modified Bradford method (Bradford, 1976) using the Coomassie Bradford reagent. At the end of the exposure period, cells were washed with PBS and 6.5% trichloroacetic acid (TCA) was used to precipitate the proteins for 10 min. NaOH (1 M) was used in the dissolution of proteins overnight at room temperature. The assay was performed in 96-well microtitre plates and each test was carried out in duplicate. A standard curve was constructed using bovine serum albumin (BSA) at concentrations of 10, 20, 30, 40, 50 and 100 µg/mL (GraphPad Prism Software), and concentrations of the toxin samples were determined from this standard curve. Preparation of the BSA standards, toxin samples and blank, are summarized in Table 1. Results were presented as percentage of control values.

Table 1

Preparation of BSA standards, blank and toxin samples for the Bradford protein assay

Sample	Sample Vol (µL)	Water (µL)	Bradford Reagent (µL)
Blank	0	40	160
BSA Standard - 10 µg/mL	4	36	160
BSA Standard - 20 µg/mL	8	32	160
BSA Standard - 30 µg/mL	12	28	160
BSA Standard - 40 µg/mL	16	24	160
BSA Standard - 50 µg/mL	20	20	160
BSA Standard - 100 µg/mL	24	16	160
Toxin Samples	20	20	160

3.2.6 Statistical analysis

A factorial analysis of variance (ANOVA) was used for analysis of the MTT assay data with exposure duration (24, 48 and 72 h), toxin (diplodiatoxin, dipmatol and diplonine), concentration (10, 100, 250, 350, 500 and 750 µM) and cell type (Neuro-2a, CHO-K1 and MDBK). The data was normally distributed with homogeneous treatment variances and therefore, the means were separated using Fisher's unprotected *t*-test (least significant difference-LSD) tested at the 5% level of significance (SAS/STAT version 9.2).

3.3 RESULTS AND DISCUSSION

3.3.1 Proliferation studies

Proliferation of Neuro-2a, CHO-K1 and MDBK cells was investigated before the cells were exposed to the *S. maydis* toxins. The three cell lines were characterized by their unique proliferation profiles as shown in Fig. 17. In general, cell densities ranging between 10 000 – 20 000 cells/mL were suitable for culturing the three cell lines for up to 72 h without cell death from starvation or accumulation of toxic by-products. After 24 h of culturing (20 000 cells/mL), the CI of the three cell lines was above 0.5 indicating that the cells were suitable for the cytotoxicity studies.

Neuro-2a cells cultured at density of 40 000 cells/mL reached their growth peak at approximately 56 h and started dying after 60 h of culturing. The CI of Neuro-2a cells cultured at 5 000 cells/mL was below 1.0 throughout the growth period.

CHO-K1 cells cultured at density of 40 000 cells/mL reached their growth peak at approximately 70 h and started dying after 80 h of culturing. The CI of CHO-K1 cells cultured at 5 000 cells/mL exceeded 0.5 after 46 h of culturing.

MDBK cells cultured at 40 000 cells/mL reached their plateau at approximately 80 h with a CI value of 8.0, whereas the CI of cells cultured at 5 000 cells/mL only exceeded 0.5 after 48 h of culturing.

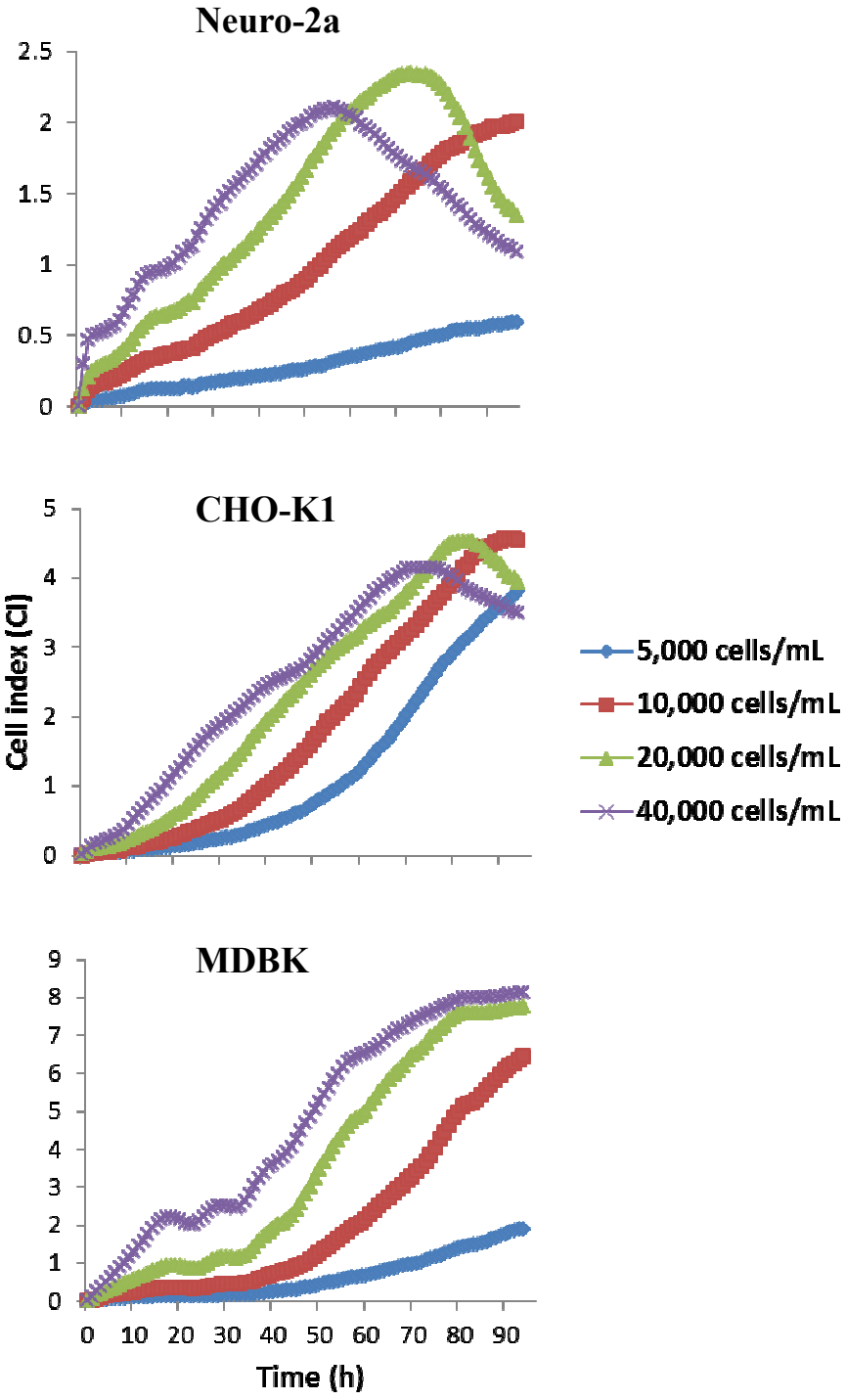

Figure 17. Dynamic monitoring of growth and proliferation of the Neuro-2a, CHO-K1, and MDBK cells using the xCELLigence system. Cells were cultured for up to 96 h without changing culture media at the densities of 5 000, 10 000, 20 000 and 40 000 cells/mL.

3.3.2 xCELLigence cytotoxicity assay

The xCELLigence assay provided valuable and real-time information regarding the cell-toxin interactions. The dynamic cytotoxic responses of the Neuro-2a, CHO-K1 and MDBK cells after exposure to diplodiatoxin, dipmatol and diplonine are shown in Fig. 18. A concentration-dependent cytotoxic response was observed when the three cell lines were exposed to diplodiatoxin (Fig. 18 A-C) and dipmatol (Fig. 18 D-F). Real-time analysis showed that at the highest concentrations (500-750 µM), diplodiatoxin and dipmatol induced a cytotoxic response that was irreversible on the three cell lines tested and most of the cells were unable to recover from the cytotoxic effects induced by the two toxins. However, partial concentration-dependent recovery of the three cell lines was observed at the lower toxin concentrations (10-350 µM). There was no concentration-dependent cytotoxic response observed on the three cell lines after exposure to diplonine (Fig. 18 G-I).

3.3.3 MTT assay

Assessment of cell viability following exposure of Neuro-2a, CHO-K1 and MDBK cells to diplodiatoxin, dipmatol and diplonine is shown in Fig. 19. A concentration-dependent cytotoxic response was observed when the three cell lines were exposed to diplodiatoxin and dipmatol. In addition, the cytotoxic response observed with diplodiatoxin on CHO-K1 and MDBK cells was time-dependent. A significant difference ($p < 0.05$) in the cytotoxic response was only recorded for the CHO-K1 and MDBK cells exposed to diplodiatoxin at the different exposure periods. There was no significant difference ($p > 0.05$) in the cytotoxic response of the three cell lines exposed to dipmatol at the different exposure periods.

There was no concentration-dependent cytotoxic response observed on the three cell lines exposed to diplonine. In general, the cell viability measured for all the toxin concentrations at the different exposure periods was above that of the control cells (> 100%), implying that diplonine did not induce cytotoxicity on the three cell lines at the different concentrations and exposure periods used.

Depicted in Table 2 are the EC_{50} values obtained after exposure of Neuro-2a, CHO-K1 and MDBK cells to diplodiatoxin, dipmatol and diplonine. The EC_{50} could be calculated following exposure of Neuro-2a and CHO-K1 cells to diplodiatoxin for 48 and 72 h, whereas EC_{50} values were obtained at all the time periods (24, 48 and 72 h) when the MDBK cells were exposed to diplodiatoxin. An EC_{50} of ± 686 µM was determined when MDBK cells were exposed to dipmatol for 48 and 72 h. No EC_{50} could be obtained after the three cell lines were exposed to diplonine, indicating that this *S. maydis* metabolite was not cytotoxic at the concentration range used in this study. The lowest EC_{50}, following exposure to the three toxins, was recorded for diplodiatoxin (EC_{50} = 147±8.6 µM) when MDBK cells were exposed for 72 h.

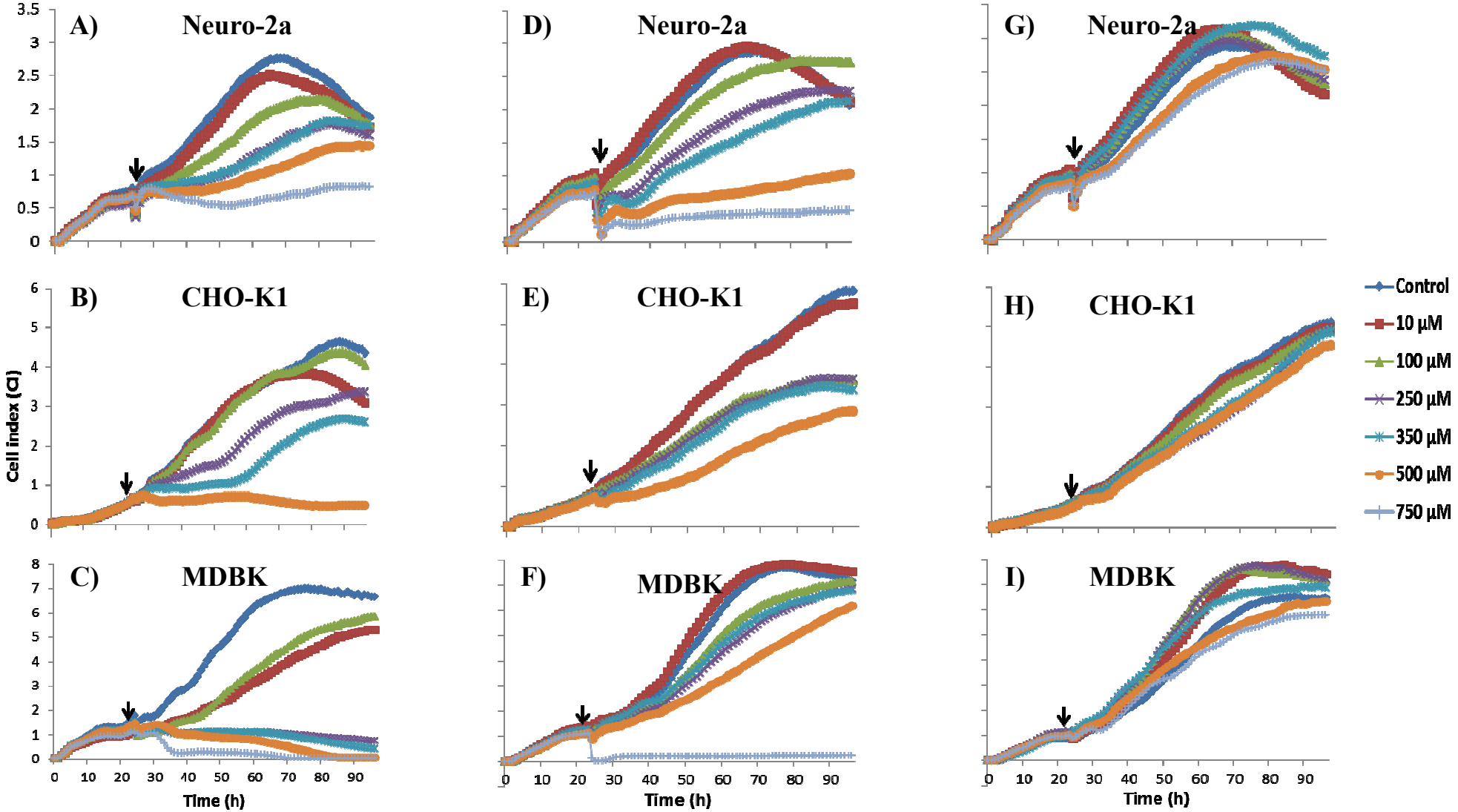

Figure 18. Cytotoxic responses of Neuro-2a, CHO-K1 and MDBK cells monitored in real-time (xCELLigence) following exposure for 72 h to diplodiatoxin (A-C), dipmatol (D-F) and diplonine (G-I). The *Stenocarpella maydis* metabolites were added to the cultured cells after 24 h (↓).

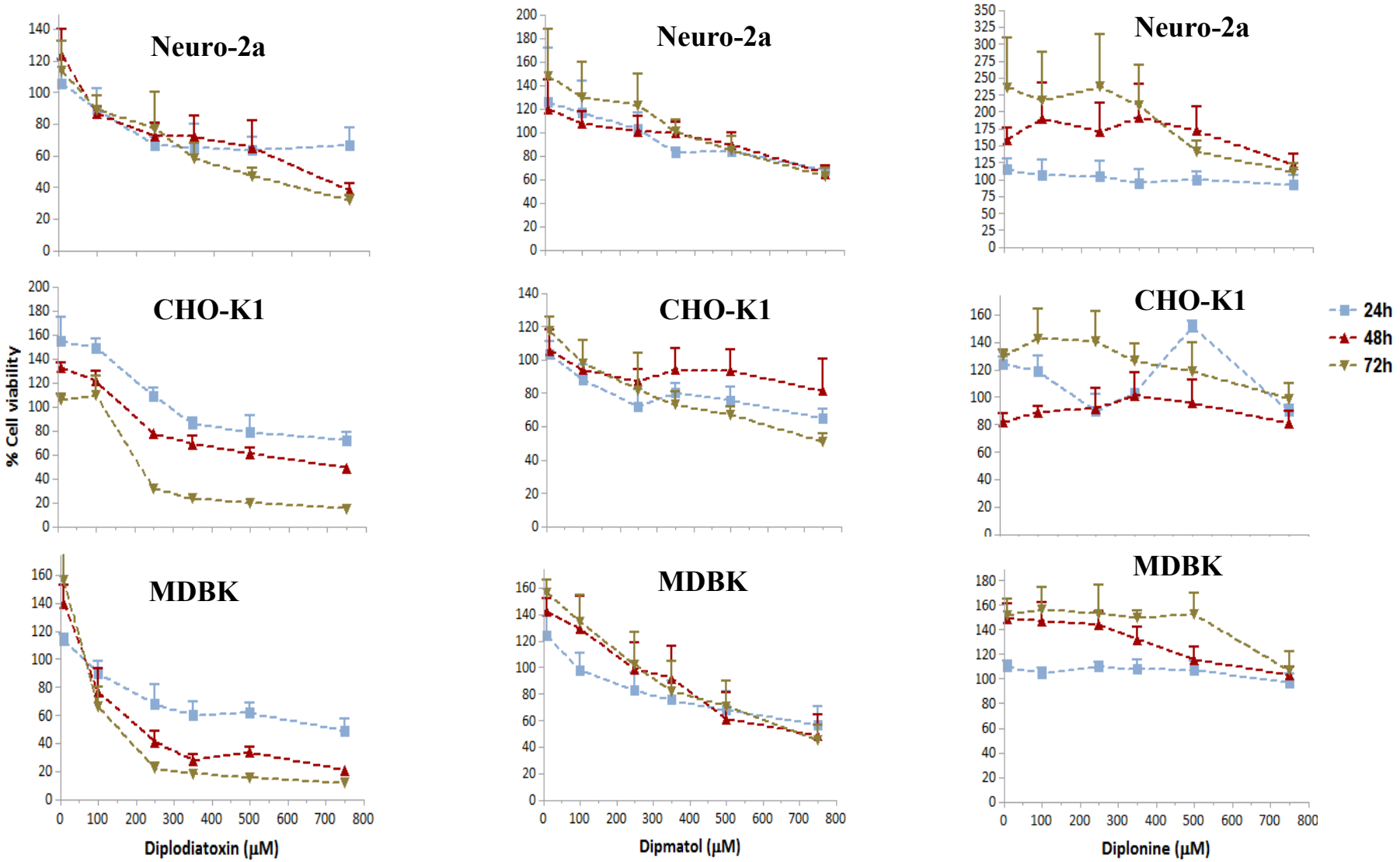

Figure 19. Assessment of cell viability using MTT assay following exposure of Neuro-2a, CHO-K1 and MDBK cells to diplodiatoxin, dipmatol and diplonine for 24, 48 and 72 h. Results are presented as percentage of control.

Table 2

EC_{50} values obtained from MTT assay after exposure of Neuro-2a, CHO-K1 and MDBK cell lines to diplodiatoxin, dipmatol and diplonine for 24, 48 and 72 h. (-) indicates no EC_{50} values (EC_{50} >750 µM) obtained with the toxin concentration range used

	EC_{50} (µM)								
	Diplodiatoxin			**Dipmatol**			**Diplonine**		
Cell line	**24h**	**48h**	**72h**	**24h**	**48h**	**72h**	**24h**	**48h**	**72h**
Neuro-2a	-	614±10.6	466±7.3	-	-	-	-	-	-
CHO-K1	-	663±4.2	219±8.4	-	-	-	-	-	-
MDBK	660±7.9	230±11.9	147±8.6	-	686±17.5	686±15.4	-	-	-

3.3.4 Protein measurement assay

Protein synthesis is a continuous function in actively growing cultured cells which requires complex cellular mechanisms and is subject to inhibition by a wide variety of toxic substances. Thus protein synthesis is a sensitive and general indicator of cell damage (Shopsis & Eng, 1985). Figure 20 depicts the BSA standard curves used to determine the protein concentrations in this study. The correlation coefficient (R^2) of the standard curves was greater than 0.98. A concentration- and time-dependent cytotoxic response was only observed on CHO-K1 cells exposed to diplodiatoxin and dipmatol (Fig. 21). There was no concentration-dependent cytotoxic response observed on the three cell lines after exposure to diplonine.

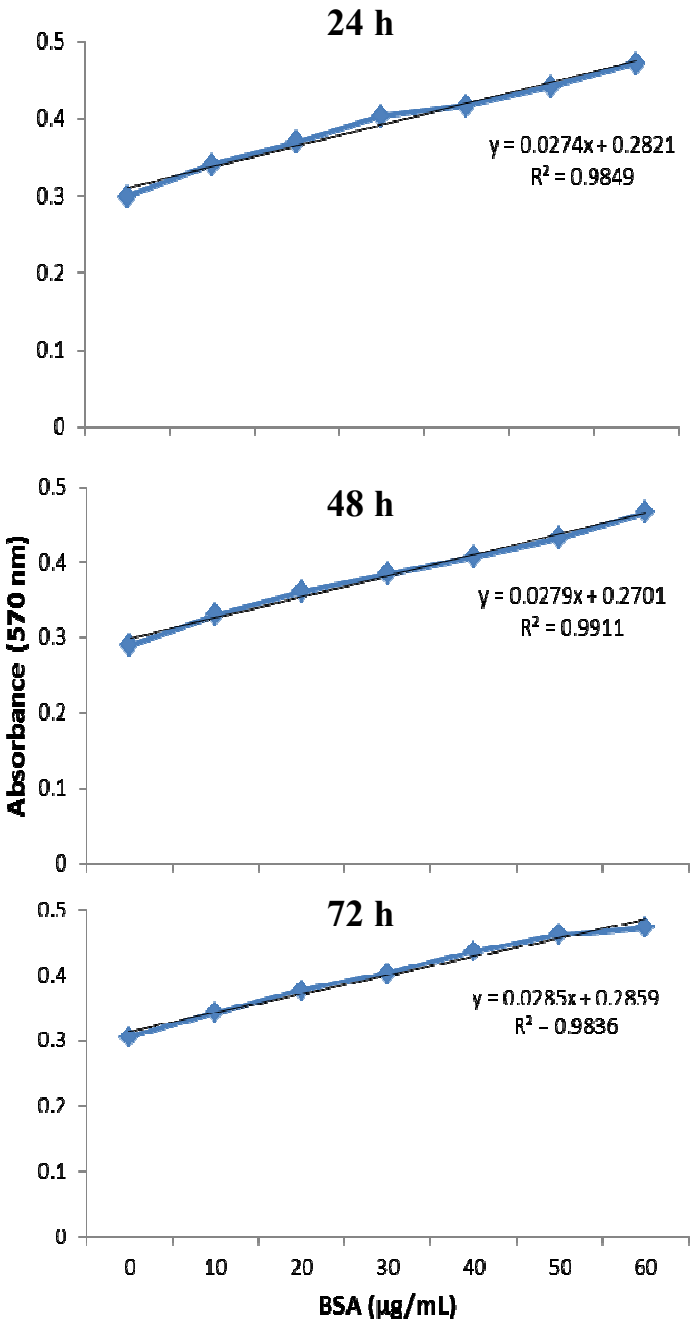

Figure 20. Standard curves compiled using bovine serum albumin (BSA) for 24, 48 and 72 h toxin exposure periods and used to determine protein concentrations. Duplicate measurements were carried out for each BSA concentration.

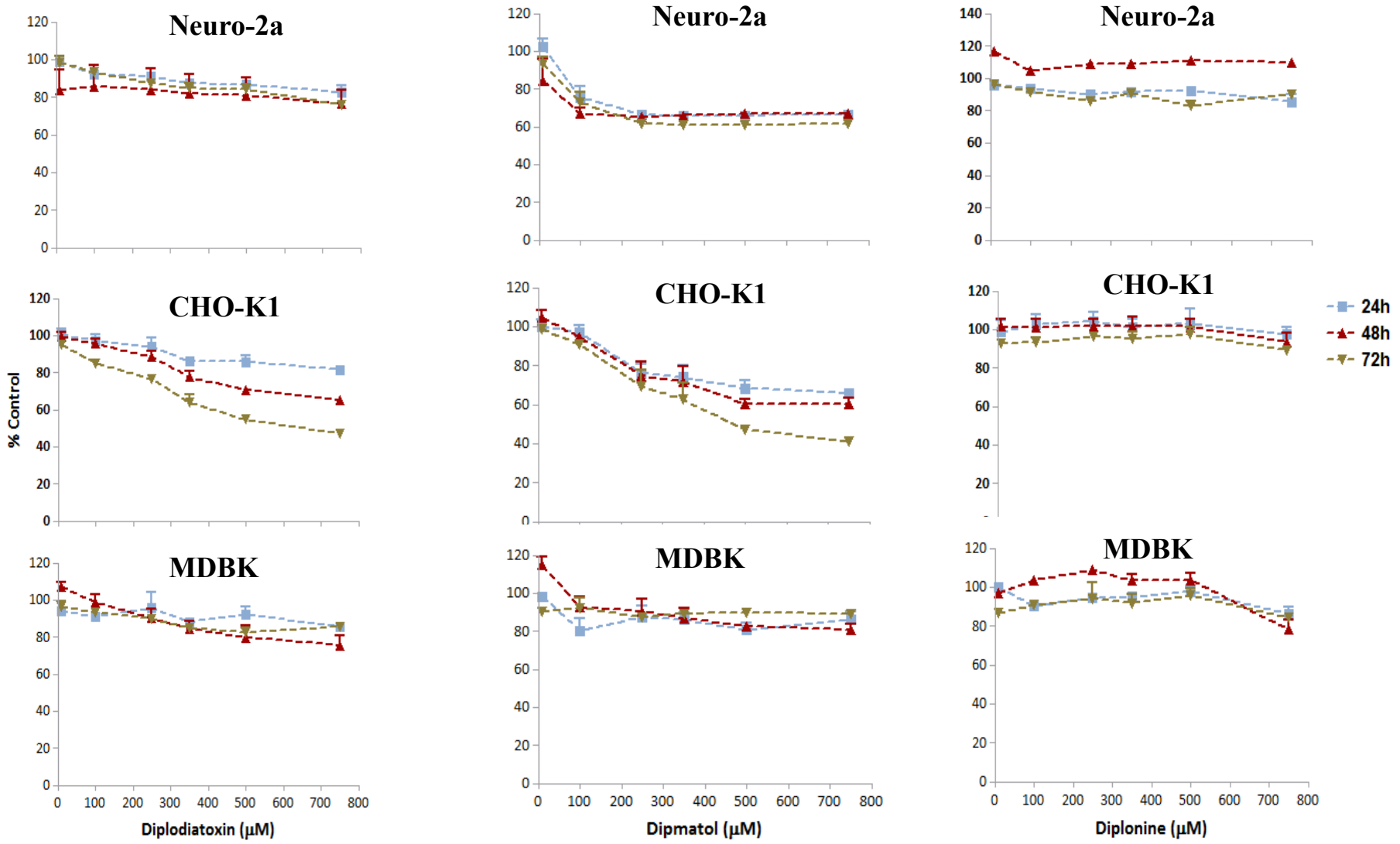

Figure 21. Assessment of cell viability using the Bradford protein assay following exposure of Neuro-2a, CHO-K1 and MDBK cells to diplodiatoxin, dipmatol and diplonine for 24, 48 and 72 h. Results are presented as percentage of control.

This is the first study where *in vitro* cytotoxicity induced by diplodiatoxin, dipmatol and diplonine were compared. The RTCA xCELLigence system has been successfully used previously in the dynamic monitoring of cell proliferation and cytotoxicity following exposure to toxic compounds (Xing et al., 2006; Boyd et al., 2008; Xia et al., 2008; Ózsvári et al., 2010). The cytotoxicity results obtained using the MTT assay confirmed the results of the xCELLigence assay. Previous studies reported consistent results when the colorimetric (MTT, XTT (2,3-bis(2-methoxy-4-nitro-5-sulphophenyl)-5-carboxanilide-2H-tetrazolium), neutral red uptake) and real-time electronic monitoring (xCELLigence) assays were compared (Ózsvári et al., 2010; Kustermann et al., 2013). In the current study the Bradford protein assay was the least sensitive to determine cytotoxicity induced by the three *S. maydis* metabolites. Fotakis and Timbrell (2006) also concluded that the protein assay is less sensitive in detecting cytotoxicity in hepatoma cells after exposure to cadmium chloride when compared with the MTT and neutral red assays. The lack of sensitivity of this assay could be attributed to the fact that dead cells also contain various forms of proteins in them.

Diplodiatoxin was the most cytotoxic *S. maydis* metabolite to the Neuro-2a, CHO-K1 and MDBK cells followed by dipmatol. Diplonine was not cytotoxic to the three cell lines. This lack of cytotoxicity was unexpected and indicates that diplonine might require metabolic activation to induce toxicity. Diplodiosis, a neurotoxic disease of ruminants and mycotoxins synthesized by *S. maydis*, induces *status spongiosis* in the white matter of the cerebrum and cerebellum of foetuses exposed during the second and third trimester of gestation (Prozesky et al., 1994). Therefore, the neuroblastoma (Neuro-2a) and bovine-derived (MDBK) cell lines were selected to investigate the *in vitro* cytotoxicity of the three *S. maydis* metabolites. The ovarian (CHO-K1) cell line was added for comparison. Based on the EC_{50} results the MDBK cell line was the most sensitive for *in vitro* cytotoxicity testing of the *S. maydis* metabolites.

CHAPTER 4

IN VITRO NECROTIC EFFECTS INDUCED BY DIPLODIATOXIN, DIPMATOL AND DIPLONINE

4.1 INTRODUCTION

In addition to the cytotoxicity assays discussed in Chapter 3, the other assays currently employed in evaluating cytotoxicity are based on the exclusion of certain dyes, such as trypan blue and fluorescent dyes (e.g. propidium iodide and ethidium bromide), from viable cells with functional and intact cellular membranes. The assays used in measuring the activities of released cytoplasmic enzymes into the surrounding medium following damage of the plasma membrane include the lactate dehydrogenase (LDH), glyceraldehyde-3-phosphate dehydrogenase, various transaminases and creatine phosphokinase leakage assays (Nieminen et al., 1992; Kim et al., 2009). These suites of cytotoxicity assays are indicative of the necrotic cell death pathway.

Lactate dehydrogenase, with a molecular mass of 140 000 Da, is a stable cytoplasmic enzyme expressed constitutively in all mammalian cells and is rapidly released into the extracellular medium when the plasma membrane is damaged. The advantages of this assay include reliability, speed and ease in evaluation (Decker & Lohmann-Matthes, 1988; Fotakis & Timbrell, 2006). The major disadvantage of this assay is that it might underestimate cellular damage since the initial sites of damage for many cytotoxic substances are intracellular. Cells may be irreversibly damaged and in the process of dying while the plasma

membrane is still intact (Hansen et al., 1989; Fotakis & Timbrell, 2006). In long-term exposure experiments, the marker enzyme activity might be degraded after release into the extracellular environment, thus underestimating the cytotoxicity measurement (Riss & Moravec, 2004).

Propidium iodide (PI) is a fluorescent dye, with a molecular weight of 668.4 Da, which intercalates into double-stranded nucleic acids and absorb blue-green light at 493 nm and fluoresce red light at 630 nm (Nieminen et al., 1992). It is excluded from viable cells, but can readily penetrate plasma membranes of dead or dying cells and non-enzymatically bind to nuclear and cellular DNA where the cell membrane has been compromised (Liao et al., 2011). The PI staining assays are based on the premise that the fluorogenic dye binds stoichiometrically to nucleic acids in such a way that fluorescence emission becomes proportional to the DNA content of the cells (Riccardi & Nicoletti, 2006). The PI assays are simple and rapid to perform and also allow reproducible and quantitative measurements (Nicoletti et al., 1991).

In this chapter, the necrotic effects induced by the three *S. maydis* toxins (i.e. diplodiatoxin, dipmatol and diplonine) were investigated on mouse neuroblastoma (Neuro-2a), Chinese hamster ovary (CHO-K1) and Mardin-Darby bovine kidney (MDBK) cell cultures. The LDH leakage and PI flow cytometry assays were utilized.

4.2 MATERIALS AND METHODS

4.2.1 Materials

All materials used in the necrosis experiments were purchased from Sigma Aldrich, South Africa, unless otherwise stated.

4.2.2 *Stenocarpella maydis* metabolites

Diplodiatoxin ($C_{18}H_{28}O_4$; molecular weight: 308 g/mol) (Steyn et al., 1972), dipmatol ($C_{15}H_{27}O_5$; molecular weight: 287 g/mol) (Ackerman et al., 1995) and diplonine ($C_6H_{11}NO_3$; molecular weight: 145 g/mol) (Snyman et al., 2011) were utilized.

4.2.3 Maintenance of cell cultures

The Neuro-2a, CHO-K1 and MDBK cells were obtained from the American Type Culture Collection (ATCC). The cells were grown in DMEM (Dulbecco's modified Eagle's medium) (Neuro-2a cells) or DMEM and Ham's F-12 Nutrient Mixture (CHO-K1 and MDBK cells) supplemented with 10% foetal calf serum, 100 U/mL penicillin, 100 µg/mL streptomycin and 2.5 µg/mL amphotericin B (Fungizone) in a humidified atmosphere of 5% CO_2 at 37 °C. The cells were cultured in 75 cm^2 cell culture flasks.

4.2.4 Exposure of cell cultures to *Stenocarpella maydis* metabolites

The cell cultures were seeded at a density of 1 x 10^6 cells/mL. After attaching to the wells (24 h post culturing), cells were exposed to 500 µL of diplodiatoxin, dipmatol and diplonine at concentrations of 100, 350 and 750 µM. Necrotic effects of diplonine were

evaluated using the LDH assay only due to the lack of cytotoxicity induced by this metabolite. The stock solutions of the toxic metabolites were prepared in DMSO. The working solutions of the toxins were prepared in the corresponding cell culture media. Control wells were prepared by adding 500 µL of the corresponding culture medium.

4.2.5 Lactate dehydrogenase (LDH) assay

Plasma membrane integrity was evaluated by measuring the LDH activity using the commercially available CytoTox-ONE™ homogeneous membrane integrity assay kit (Promega, USA). The LDH released into culture medium, following treatment of the cells with the *S. maydis* toxins, was measured with an enzymatic reaction that involves the conversion of resazurin into resorufin (Promega Technical Bulletin). At the end of the exposure period, 100 µL of the cell culture medium was removed from each experimental well and transferred into a 96-well opaque-walled tissue culture plate. An equal volume (100 µL) of the CytoTox-ONE™ reagent was added to 100 µL medium-containing wells and the plate was incubated overnight at room temperature. At the end of the incubation, 50 µL of stop solution was added to each well and the fluorescence was measured using the Fluoroskan Ascent FL reader (Thermo Electron Corporation, USA) at 560 nm excitation and 590 nm emission wavelengths. Results were analyzed with the GraphPad Prism software (version 4.0). The LDH release was estimated as the percentage absorbance of sample relative to control. Three independent experiments were carried out with two replicate wells for each toxin concentration.

4.2.6 Propidium iodide (PI) flow cytometry

To evaluate plasma membrane damage, the method accompanying the Annexin V-FITC apoptosis detection kit (Sigma-Aldrich) was followed. The PI solution was used to stain cells with damaged plasma membranes. At the end of the exposure period, cells were trypsinized by adding 500 µL trypsin-versene EDTA to each well. Cells were transferred to sterile 2 mL tubes and 1 mL Dulbecco's PBS (DPBS) was added to each tube. Tubes containing cells were centrifuged at 3 000 rpm for 3 min leaving a pellet in the bottom of the tubes and the supernatant was discarded. The wash step with DPBS was repeated once. Cells were resuspended by adding 1 mL of the binding buffer to each tube. 500 µL of cell suspension was transferred to sterile 2 mL tubes. Ten µL of PI solution was added to each cell suspension and tubes were incubated for 10 min at room temperature and protected from light. Fluorescence of the cells was measured immediately (i.e. 10 000 events were captured per sample) using the Cytomics FC 500 flow cytometer (Beckman Coulter, USA) and analyzed with Kaluza 1.1 software. Results were analyzed with GraphPad Prism software (version 4.0). The PI uptake was estimated as the percentage fluorescence of sample relative to control. Two independent experiments were carried out for each toxin concentration.

4.2.7 Statistical analysis

A factorial analysis of variance (ANOVA) was used for analysis of the LDH and PI flow cytometry datasets which included the toxins (diplodiatoxin and dipmatol) and cell types (Neuro-2a, CHO-K1 and MDBK). Standardized values for both datasets were tested for normality deviations using Shapiro-Wilk's test. In cases where there was strong evidence against normality due to skewness, outliers were removed until the data was symmetrically or normally distributed. Pearson's correlation (r) was used to determine the linear correlation

between different factors of the LDH and PI flow cytometry assays. Correlation was considered significant when $p \leq 0.0001$ (SAS/STAT version 9.2).

4.3 RESULTS AND DISCUSSION

4.3.1 LDH assay

Determination of the plasma membrane integrity following treatment of Neuro-2a, CHO-K1 and MDBK cells with the three *S. maydis* toxins (i.e. diplodiatoxin, dipmatol and diplonine) was carried out using the LDH leakage assay. In summary, Figure 22 shows that diplodiatoxin and dipmatol affected the plasma membrane integrity of the three cell lines at the highest toxin concentration used and that diplonine did not have any effect on the plasma membrane integrity of the cells.

A significant difference ($p < 0.05$) in LDH leakage was observed following treatment of the three cell lines with 750 µM of diplodiatoxin. The LDH released at this concentration ranged from 236±10 – 260±7% for Neuro-2a, 109±1 – 155±8% for CHO-K1 and 125±16 – 195±12% for MDBK cells (Fig. 22).

A concentration-dependent release in LDH was measured following treatment of Neuro-2a cells with dipmatol. The LDH leakage recorded for this cell line ranged from 95±10 – 123±16% for 100 µM concentration, 140±25 – 170±6% for 350 µM concentration and 188±5 – 259±7% for 750 µM concentration. There was a significant difference ($p < 0.05$) in LDH leakage after treatment of CHO-K1 and MDBK cells with the highest concentration (750 µM)

of dipmatol at the three exposure periods. The LDH released at this concentration ranged from 118±2 – 174±5% and 165±6 – 194±14% for CHO-K1 and MDBK cells, respectively (Fig. 22).

There was no significant release of LDH enzyme recorded for Neuro-2a, CHO-K1 and MDBK cells treated with diplonine, indicating that diplonine did not have an effect on the plasma membrane of the three cell lines used at the specified concentration and exposure periods (Fig. 22).

4.3.2 PI flow cytometry

Cells with damaged plasma membranes following exposure to the *S. maydis* toxins were detected by their ability to absorb the PI dye which was intercalated into their nuclei. In summary, diplodiatoxin and dipmatol affected the plasma membrane integrity of the three cell lines at the highest toxin concentration used (Fig. 23). In addition, uptake of PI dye by the MDBK cell line following treatment with 750 µM of diplodiatoxin and dipmatol at 24 and 48 h was significantly different ($p < 0.05$) to that of Neuro-2a and CHO-K1 cells.

A concentration-dependent uptake of the PI dye was measured after treatment of Neuro-2a cells with diplodiatoxin. The highest PI uptake was recorded following treatment of the three cell lines with 750 µM of diplodiatoxin and the measured PI uptake ranged from 174±24 – 299±28% for Neuro-2a, 155±2 – 242±5% for CHO-K1 and 151±12 – 202±19% for MDBK cells (Fig. 23).

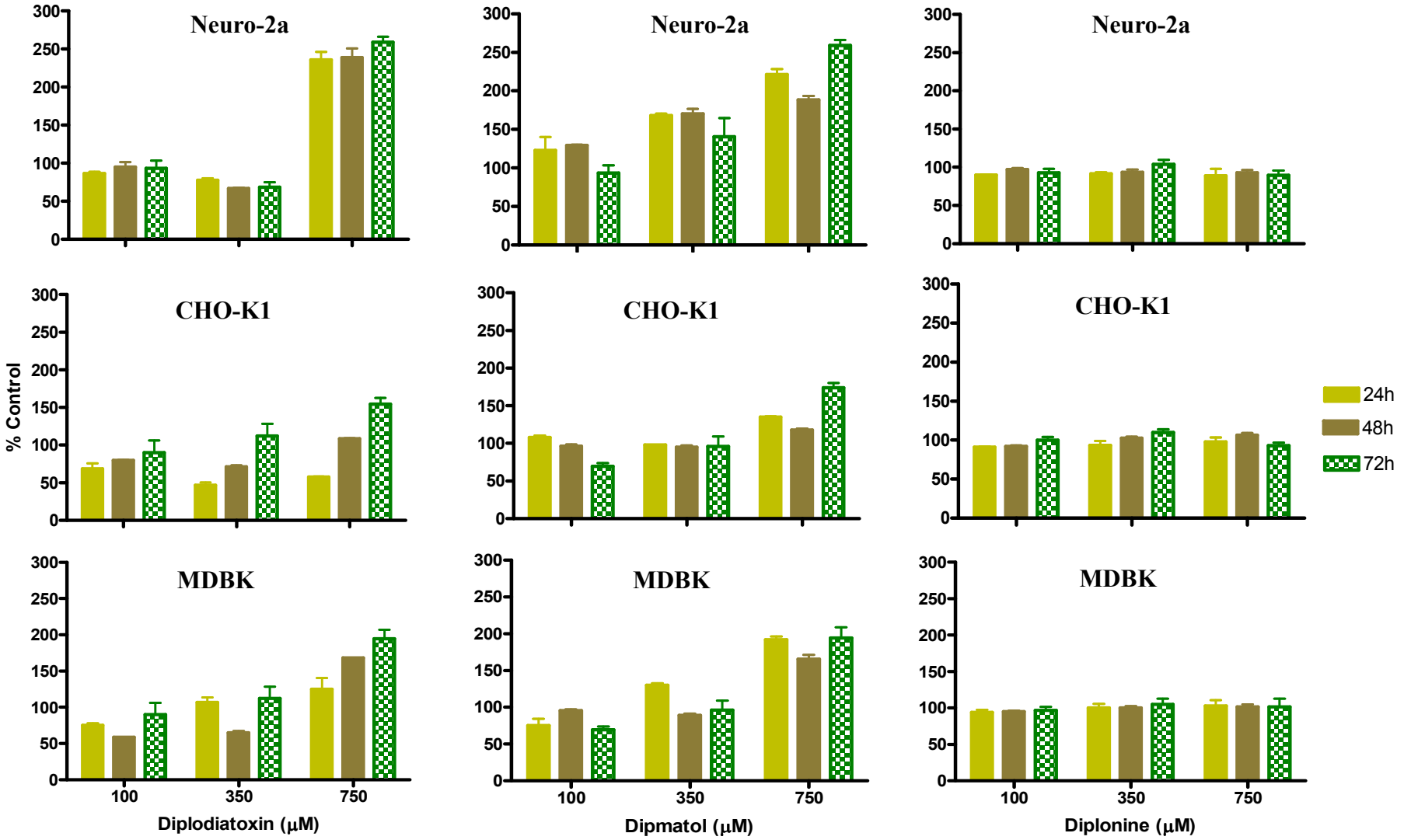

Figure 22. Lactate dehydrogenase (LDH) enzyme leakage following exposure of Neuro-2a, CHO-K1 and MDBK cells to diplodiatoxin, dipmatol and diplonine for 24, 48 and 72 h. Results are presented as percentage of control.

A concentration-dependent uptake of the PI dye was recorded after treatment of Neuro-2a cells with dipmatol and the highest PI uptake was measured for 350 µM (113±4 – 140±19%) and 750 µM (103±32 – 205±45%) toxin concentrations. The significant PI uptake recorded for CHO-K1 cells was at 750 µM dipmatol concentration and ranged from 134±2 – 163±1%. The highest PI uptake recorded for MDBK cells (142±10%) was at 24h exposure period with the highest dipmatol concentration.

Monitoring of plasma membrane integrity is most commonly used as an indicator of cell viability since the plasma membrane is essential in cell functioning (Niemenin et al., 1992). As a result, the inability of cells to retain cytoplasmic enzymes, such as LDH, as well as the failure to exclude certain dyes, such as PI, from entering the cell reflects irreversible plasma membrane damage and is generally accepted as an indicator of the necrotic cell death pathway (Korzeniewski & Callewaert, 1983).

Exposure of Neuro-2a, CHO-K1 and MDBK cells to 750 µM of diplodiatoxin and dipmatol affected the plasma membrane integrity of the cell lines. In contrast, diplonine had no effect on the plasma membrane integrity of the three cell lines. Additionally, a significant positive linear correlation ($r = 0.45256$; $p < 0.0001$) was found between the LDH and PI flow cytometry assays. Other studies have also reported a linear correlation between the LDH release and PI uptake in Mardin-Darby canine kidney (MDCK) cells exposed to mercuric chloride ($HgCl_2$) (Gores et al., 1988) and in hepatocytes exposed to cadmium (Cd) (Koizumi et al., 1996).

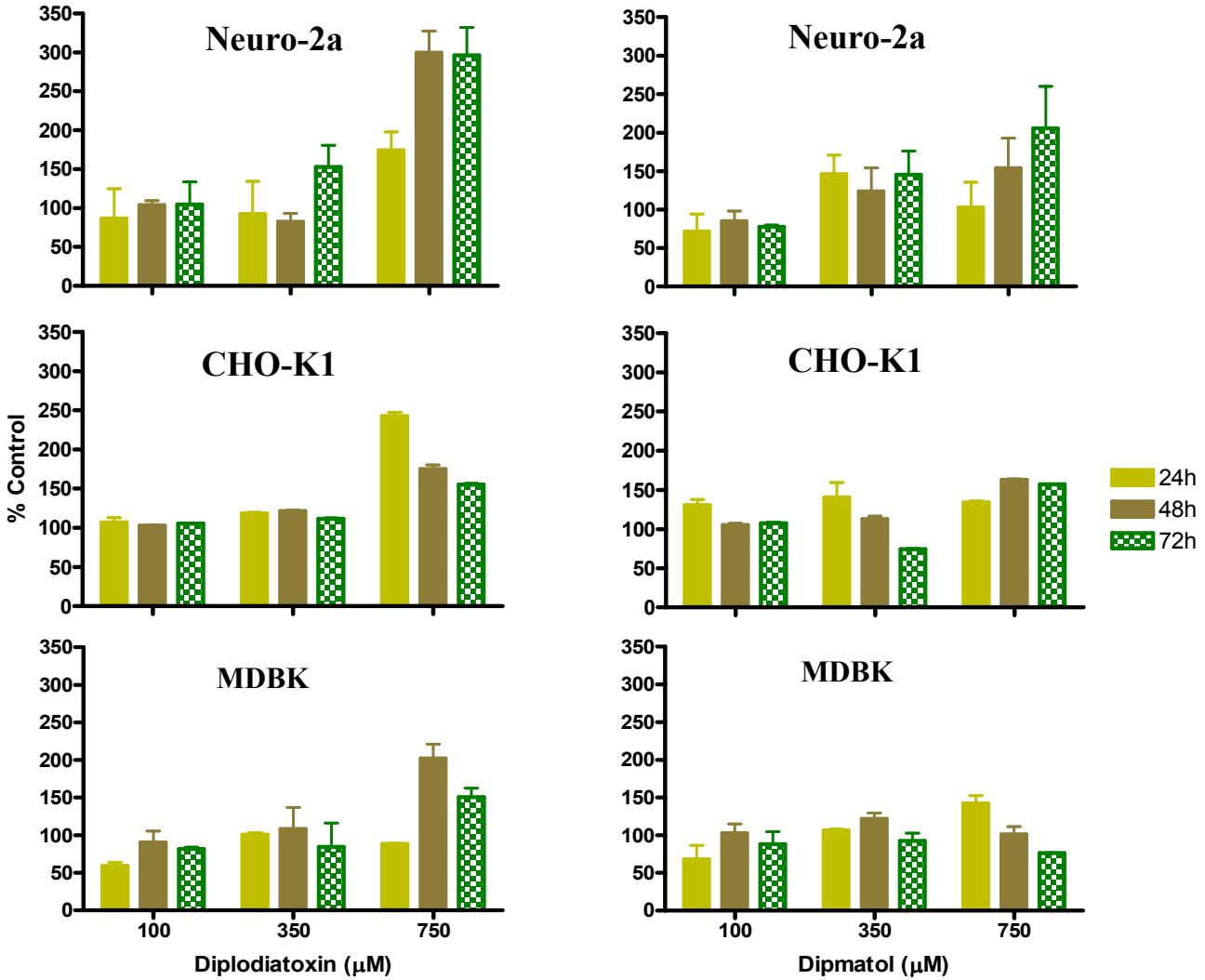

Figure 23. Propidium iodide (PI) uptake (flow cytometry) following exposure of Neuro-2a, CHO-K1 and MDBK cells to diplodiatoxin and dipmatol for 24, 48 and 72 h. Results are presented as percentage of control.

Studies investigating the use of LDH and PI assays in cytotoxicity testing have reported that nuclear staining with PI dye occurred at an early stage while LDH leakage occurred at a later stage (Nieminen et al., 1992; Koizumi et al., 1996). The extent of membrane damage was reported by Liao et al. (2011) to be related to the variation in membrane components (i.e. membrane protein and phospholipids) of the different cell types.

It was concluded that diplodiatoxin and dipmatol, at high concentrations, exerted their toxicity via the necrotic cell death pathway.

CHAPTER 5

IN VITRO APOPTOTIC EFFECTS INDUCED BY DIPLODIATOXIN AND DIPMATOL

5.1 INTRODUCTION

Apoptosis is an important, highly conserved and well controlled process of cell death that is induced by a variety of physiological and pathological conditions (Zhang et al., 1998). It has been established that caspases (cysteine-requiring aspartate proteases) and mitochondria play a critical role in apoptosis (Sawai & Domae, 2011). The most common biochemical/molecular assays used to detect apoptosis include the measurement of caspase activity, binding of Annexin V to phosphatidylserine, detection of DNA fragmentation and Western blot assays (Denecker et al., 2001; Riccardi & Nicoletti, 2006; Krysko et al., 2008; Sawai & Domae, 2011).

Fluorogenic substrates are widely used in determining the activity of caspases (Denecker et al., 2001). The peptide substrate acetyl-Asp-Glu-Val-Asp-7-amino-4-methylcoumarin (Ac-DEVD-AMC) was initially identified as the preferred fluorogenic substrate for caspase enzymes. Hydrolysis of the peptide substrate by caspase-3/7 releases the fluorescent AMC moiety which can be measured using a fluorometer (Thornberry et al., 1997). The caspase assays are rapid and sensitive. The major disadvantage of these assays is that the substrate specificity can be lost outside a certain concentration range (Talanian et al., 1997).

Acquisition of surface changes, such as the externalization of phosphatidylserine (PS), in dying cells is considered as an early and critical event in apoptosis (Vermes et al., 1995). Phosphatidylserine is an amino-phospholipid that is found on the inner surface of the plasma membrane of living cells (Krysko et al., 2006). During apoptotic cell death, PS is actively translocated to the outer surface of the plasma membrane while the membrane integrity remains intact. Once outside of the plasma membrane, PS facilitates the recognition and engulfment of the dying cells by phagocytes (Krysko et al., 2004). Phosphatidylserine exposure lasts from the onset of apoptosis until the final stages, when the cell is broken up into apoptotic bodies (van Engeland et al., 1998). Annexin V, a calcium-dependent phospholipid-binding protein, conjugated to various fluorochromes (such as fluorescein isothiocyanate (FITC), phycoerythrin and carbocyanines) is commonly used in detecting apoptosis due to its high binding affinity for PS (Krysko et al., 2006). Annexin V does not bind to normal viable cells since it is unable to penetrate the phospholipid bilayer (Koopman et al., 1994). The major disadvantage of using Annexin V in detecting apoptosis is that its activity is affected by high calcium concentrations (Trahtemberg et al., 2007).

The purpose of this study was to evaluate the apoptotic effects induced by the two *S. maydis* metabolites (i.e. diplodiatoxin and dipmatol) on mouse neuroblastoma (Neuro-2a), Chinese hamster ovary (CHO-K1) and Mardin-Darby bovine kidney (MDBK) cell cultures using the caspase-3/7 and Annexin V flow cytometry assays.

5.2 MATERIALS AND METHODS

5.2.1 Materials

All materials used in the apoptosis experiments were purchased from Sigma Aldrich, South Africa, unless otherwise stated.

5.2.2 *Stenocarpella maydis* metabolites

Diplodiatoxin ($C_{18}H_{28}O_4$; molecular weight: 308 g/mol) (Steyn et al., 1972) and dipmatol ($C_{15}H_{27}O_5$; molecular weight: 287 g/mol) (Ackerman et al., 1995) were utilized.

5.2.3 Maintenance of cell cultures

The Neuro-2a, CHO-K1 and MDBK cells were obtained from the American Type Culture Collection (ATCC). The cells were grown in DMEM (Dulbecco's modified Eagle's medium) (Neuro-2a cells) or DMEM and Ham's F-12 Nutrient Mixture (CHO-K1 and MDBK cells) supplemented with 10% foetal calf serum, 100 U/mL penicillin, 100 µg/mL streptomycin and 2.5 µg/mL amphotericin B (Fungizone) in a humidified atmosphere of 5% CO_2 at 37 °C. The cells were cultured in 75 cm^2 cell culture flasks.

5.2.4 Exposure of cell cultures to *Stenocarpella maydis* metabolites

The cell cultures were seeded at a density of 1 x 10^6 cells/mL. After attaching to the wells (24 h post culturing), cells were exposed to 500 µL of diplodiatoxin and dipmatol at concentrations of 100, 350 and 750 µM. The stock solutions of the toxic metabolites were prepared in DMSO. The working solutions of the toxins were prepared in the corresponding

cell culture media. Control wells were prepared by adding 500 µL of the corresponding culture medium.

5.2.5 Caspase-3/7 assay

Apoptosis was evaluated by measuring the activity of the caspase-3/7 enzymes using the commercially available APO-ONE® homogeneous caspase-3/7 assay kit (Promega, USA). After exposure of cell cultures to the *S. maydis* toxins, caspase-3/7 activity was measured with an enzymatic reaction that involves cleavage of the non-fluorescent caspase substrate Z-DEVD-R110 (rhodamine 110, bis-[N-CBZ-L-aspartyl-L-glutamyl-L-valyl-L-aspartic acid amide]) by caspase-3/7 to form the fluorescent rhodamine 110. The amount of fluorescent rhodamine 110 generated is proportional to the amount of caspase-3/7 cleavage activity present in a sample (Promega Technical Bulletin). At the end of the exposure period, 100 µL of the cell culture medium was removed from each experimental well and transferred into a 96-well opaque-walled tissue culture plate. An equal volume (100 µL) of the APO-ONE® reagent was added to 100 µL medium-containing wells and the plate was incubated for an hour at room temperature. At the end of the incubation, fluorescence was measured using the Fluoroskan Ascent FL reader (Thermo Electron Corporation, USA) at 485 nm excitation and 530 nm emission wavelengths. Results were analyzed with GraphPad Prism software (version 4.0). The caspase-3/7 activity was estimated as the percentage fluorescence of sample relative to control. Three independent experiments were carried out with two replicate wells for each toxin concentration.

5.2.6 Annexin V-FITC flow cytometry

The commercially available Annexin V-fluorescein isothiocyanate (FITC) apoptosis detection kit (Sigma Aldrich) was used to measure apoptotic cells. At the end of the exposure period, cells were trypsinized by adding 500 µL trypsin-versene EDTA to each well. Cells were transferred to sterile 2 mL tubes and 1 mL Dulbecco's PBS (DPBS) was added to each tube. Tubes containing cells were centrifuged at 3 000 rpm for 3 min leaving a pellet in the bottom of the tubes and the supernatant was discarded. The wash step with DPBS was repeated once. Cells were resuspended by adding 1 mL of the binding buffer to each tube. 500 µL of cell suspension was transferred to sterile 2 mL tubes. Five µL of Annexin V solution was added to each cell suspension and tubes were incubated for 10 min at room temperature and protected from light. Fluorescence of the cells was measured immediately (i.e. 10 000 events were captured per sample) using the Cytomics FC 500 flow cytometer (Beckman Coulter, USA) and analyzed with Kaluza 1.1 software. Results were analyzed with GraphPad Prism software (version 4.0). The induction of apoptosis (Annexin V activity) was estimated as the percentage fluorescence of sample relative to control. Two independent experiments were carried out for each toxin concentration.

5.2.7 Statistical analysis

A factorial analysis of variance (ANOVA) was used for analysis of the caspase-3/7 and Annexin V flow cytometry datasets which included the toxins (diplodiatoxin and dipmatol) and cell types (Neuro-2a, CHO-K1 and MDBK). Standardized values for both datasets were tested for normality deviations using Shapiro-Wilk's test. In cases where there was strong evidence against normality due to skewness, outliers were removed until the data was symmetrically or normally distributed. Pearson's correlation (r) was used to determine the

linear correlation between different factors of the caspase-3/7 and Annexin V flow cytometry assays. Correlation was considered significant when $p \leq 0.0001$ (SAS/STAT version 9.2).

5.3 RESULTS AND DISCUSSION

5.3.1 Caspase-3/7 assay

The assay detected apoptosis in Neuro-2a, CHO-K1 and MDBK cell lines exposed to the two *S. maydis* toxins (i.e. diplodiatoxin and dipmatol) at high concentrations (Fig. 24).

A significant increase in the caspase-3/7 activity was measured in Neuro-2a and MDBK cells exposed to diplodiatoxin (Fig. 24). High enzyme activities in Neuro-2a cells were recorded at 350 µM (148±47 – 376±46%) and 750 µM (149±14 – 597±69%) toxin concentrations. Caspase activity measured in MDBK cells exposed to 350 µM diplodiatoxin ranged from 376±44 – 509±75%. The caspase activity induced following exposure of CHO-K1 cells to diplodiatoxin was the lowest and significantly different ($p < 0.05$) when compared to those of Neuro-2a and MDBK cells. The highest caspase activity measured in the CHO-K1 cells was after exposure to 350 µM of diplodiatoxin (156±19%) for 48 h.

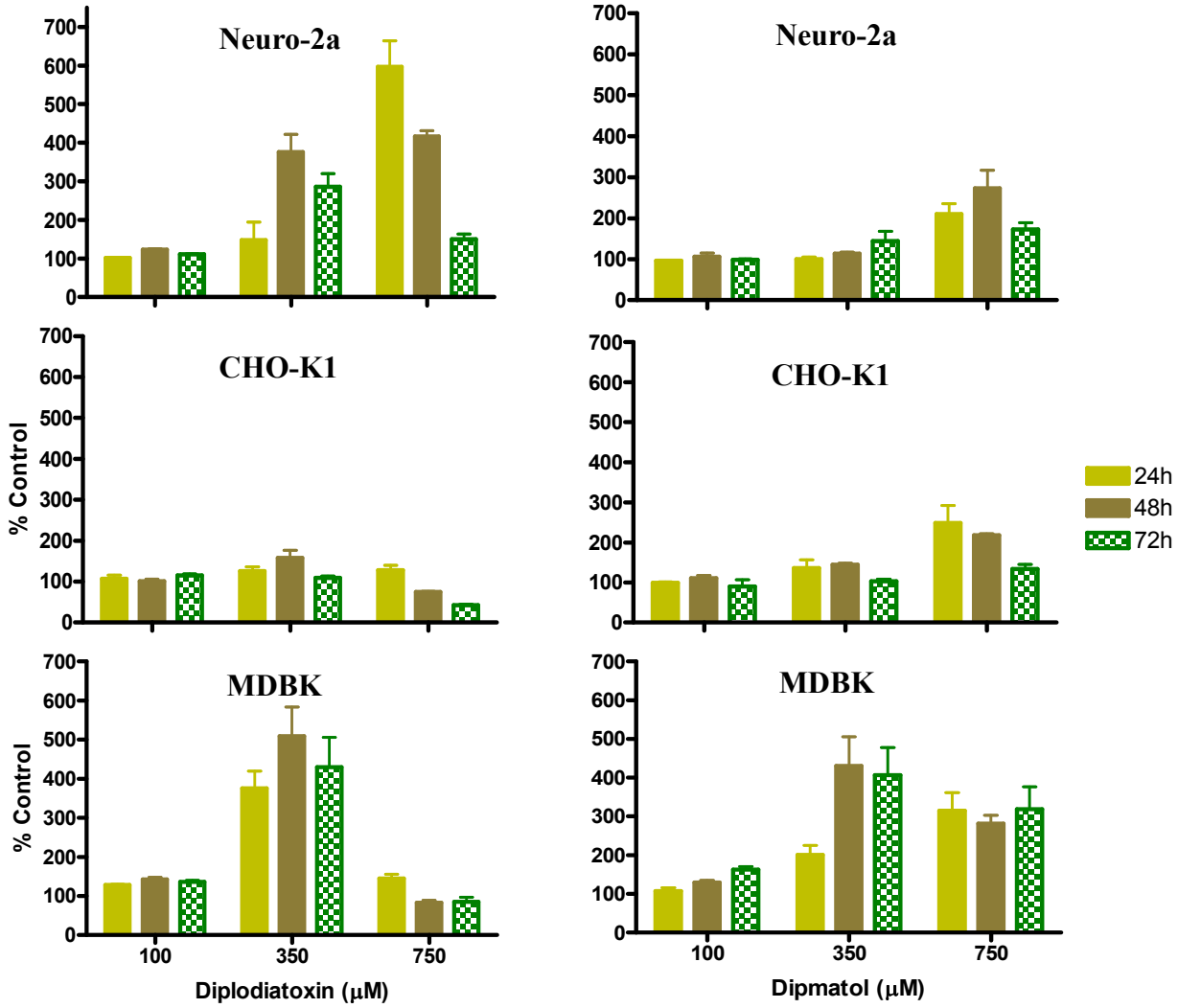

Figure 24. Caspase-3/7 enzyme activity following exposure of Neuro-2a, CHO-K1 and MDBK cells to diplodiatoxin and dipmatol for 24, 48 and 72 h. Results are presented as percentage of control.

A concentration-dependent increase in the caspase-3/7 activity was recorded after exposure of Neuro-2a and CHO-K1 cell cultures to dipmatol (Fig. 24). The highest enzyme activity was measured in Neuro-2a and CHO-K1 cells exposed to 750 µM dipmatol and it ranged from 172±17 – 273±44% and 134±11 – 249±43%, respectively. The caspase activity induced following exposure of MDBK cells to dipmatol was the highest and significantly different ($p < 0.05$) to that of Neuro-2a and CHO-K1 cells. The caspase activity recorded in MDBK cells at the different concentrations of dipmatol ranged from 108±9 – 430±75%.

5.3.2 Annexin V-FITC flow cytometry

Apoptotic cells exposed to diplodiatoxin and dipmatol were detected using Annexin V-FITC flow cytometry assay. Apoptosis was induced in Neuro-2a, CHO-K1 and MDBK cells exposed to the two higher concentrations of diplodiatoxin and dipmatol (Fig. 25).

A concentration-dependent increase in the Annexin V binding activity was recorded following exposure of Neuro-2a, CHO-K1 and MDBK cells to diplodiatoxin (Fig. 25). The highest Annexin V activity was measured at 750 µM of diplodiatoxin concentration and it ranged from 163±14 – 265±31% for Neuro-2a, 160±7 – 170±1% for CHO-K1 and 109±19 – 176±11% for MDBK cells.

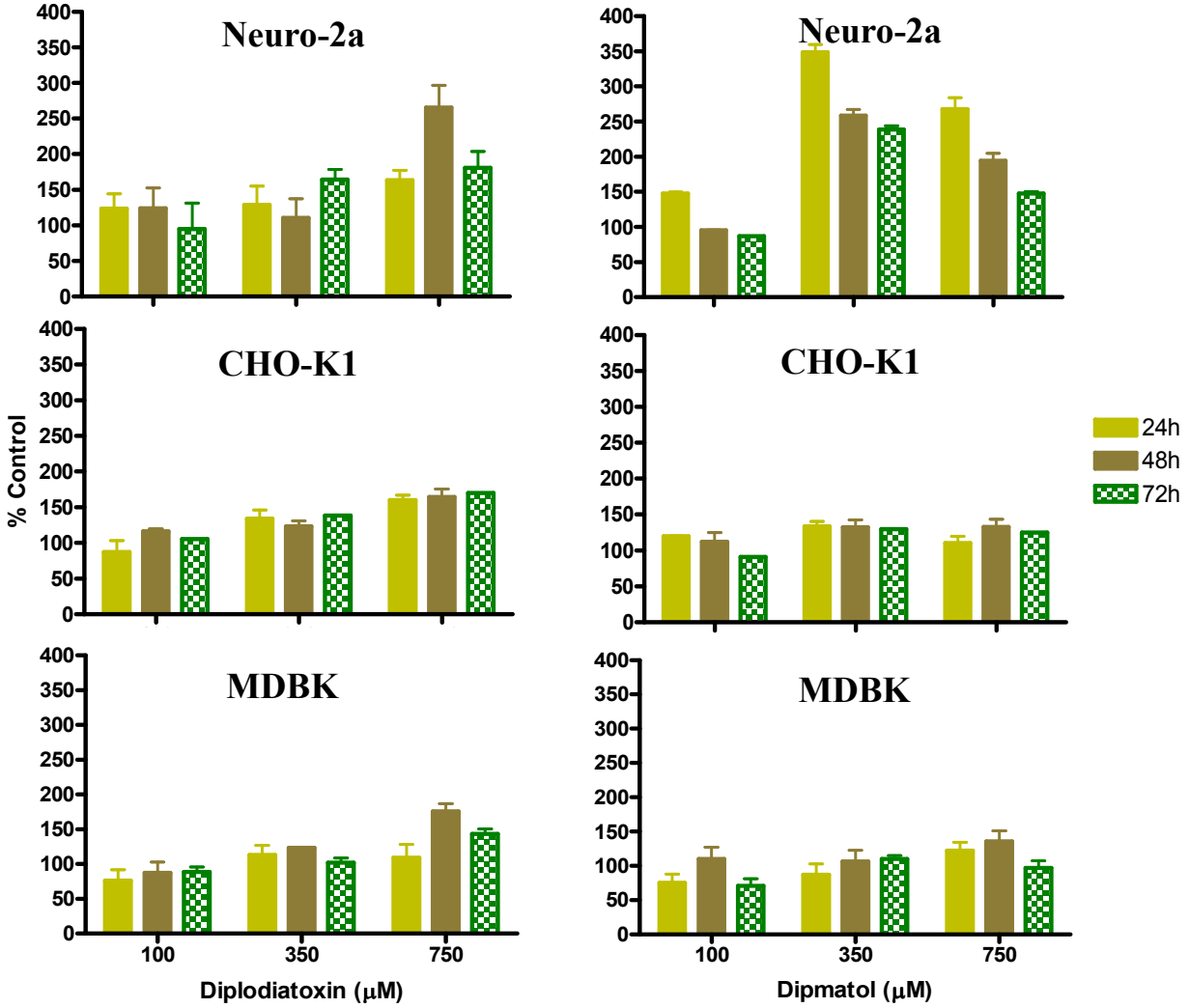

Figure 25. Annexin V activity (flow cytometry) following exposure of Neuro-2a, CHO-K1 and MDBK cells to diplodiatoxin and dipmatol for 24, 48 and 72 h. Results are presented as percentage of control.

High Annexin V binding activities were recorded in Neuro-2a cells at dipmatol concentrations of 350 µM (239±5 – 348±11%) and 750 µM (148±3 – 268±16%) (Fig. 25). Annexin V activities measured in the CHO-K1 and MDBK cells after exposure to dipmatol were significantly lower compared to those of the Neuro-2a cells. The highest Annexin V activity recorded for CHO-K1 and MDBK cells was at an average of 133±9% and 123±15%, respectively.

Apoptosis is one of the most common forms of cell death in eukaryotes (Riccardi & Nicoletti, 2006). In this study, apoptosis was evaluated in the Neuro-2a, CHO-K1 and MDBK cell lines treated with the two *S. maydis* metabolites (i.e. diplodiatoxin and dipmatol) using the caspase-3/7 and Annexin V-FITC flow cytometry assays. Data presented in this chapter indicate that exposure of the three cell lines to 750 µM concentrations of diplodiatoxin and dipmatol induced apoptosis. Additionally, a significant positive linear correlation (r = 0.85850; $p < 0.0001$) was found between the two assays.

The involvement of caspase-3/7 enzymes in apoptosis was previously reported in cultured human melanoma cells exposed to staurosporine (Zhang et al., 2004) and human monocytic leukemia (U937) cells treated with T2-toxin (Huang et al., 2007). A number of studies confirmed Annexin V-FITC flow cytometry to be a useful tool in detecting cells undergoing apoptosis. Annexin V-FITC was used successfully in detecting apoptosis in cultured human hepatocellular carcinoma (HepG2) cells exposed to T-2 toxin (Du et al., 2012) and tacrine (Gao et al., 2014). These studies have also demonstrated a positive correlation between the caspase-3/7 and Annexin V-FITC flow cytometry assays (Du et al., 2012; Gao et al., 2014).

It was concluded that the apoptosis induced by the two *S. maydis* toxins in this study was caspase-dependent.

CHAPTER 6

ULTRASTRUCTURAL CHANGES INDUCED BY DIPLODIATOXIN, DIPMATOL AND DIPLONINE:

A TRANSMISSION ELECTRON MICROSCOPY (TEM) STUDY

6.1 INTRODUCTION

Following injury, from exposure to toxins, cells undergo a series of changes which are collectively recognized as disease processes (Henics & Wheatley, 1999). Most injuries to cells are sublethal and result in altered or new steady states in which the cells are able to survive. However, injuries incurred following a period of irreversible reactions are often lethal and result in cell death (Trump et al., 1997).

At least two modes of cell death can be clearly distinguished, i.e. apoptosis and necrosis. Cells undergoing apoptosis exhibit typical and well-defined morphological changes such as plasma membrane blebbing, chromatin condensation accompanied by margination of chromatin at the nuclear membrane, nuclear fragmentation and formation of apoptotic bodies (Kerr et al., 1972; Kroemer et al., 1998; Loos & Engelbrecht, 2009).

In contrast, necrosis is characterized by rapid cytoplasmic swelling, rupture of the plasma membrane and organelle breakdown (Edinger & Thompson, 2004; Festiens et al., 2006;

Krysko et al., 2008). The fundamental morphological differences between apoptosis and necrosis are summarized in Table 3.

Table 3

Summary of the common morphological features of apoptosis and necrosis

Apoptosis	Necrosis	References
Plasma membrane near-to-intact until late	Loss of plasma membrane integrity	Kroemer et al., 1998; Edinger & Thompson, 2004; Krysko et al., 2008
Subtle changes in plasma membrane (becomes symmetrical before loss of membrane integrity) at later stages		
Chromatin condensation (pyknosis)	Chromatin condenses into small irregular pieces at later stages	
Nuclear fragmentation (karyorrhexis)	Nuclear morphology remains unchanged (intact chromatin)	
Cell shrinkage and protrusion of cytoplasm	Swelling of cytoplasm (oncosis)	
No swelling of mitochondria	Swelling of mitochondria and other cytoplasmic organelles (ER & Golgi)	
Formation of membrane-bound apoptotic bodies of different sizes containing well-preserved but compact cytoplasmic organelles	Cytoplasm becomes electron-lucent and contains vacuoles	

ER = endoplasmic reticulum

Evaluation of subcellular changes using transmission electron microscopy (TEM) has been considered as a '*golden standard'* in the field of cell death research (Krysko et al., 2008). The major advantage of using TEM is that it provides images of the inside of cells, thus allowing investigation of the biological structure and function relationships at cellular and subcellular levels (Unwin & Zampighi, 1980; Unwin & Ennis, 1984). Ultramicroscopy provides more detailed information about cell morphology because of its higher resolution power (0.1 – 0.4 nm). In addition, TEM is considered as the most accurate method for distinguishing apoptosis from necrosis in cell cultures (Krysko et al., 2008). The major

disadvantage of this technique is that it is time consuming and requires the use of expensive equipment.

The purpose of this study was to evaluate the subcellular changes induced by the three *S. maydis* toxins (i.e. diplodiatoxin, dipmatol and diplonine) on mouse neuroblastoma (Neuro-2a), Chinese hamster ovary (CHO-K1) and Mardin-Darby bovine kidney (MDBK) cells using TEM.

6.2 MATERIALS AND METHODS

6.2.1 Materials

All materials used in the preparation and exposure of cells to toxins as well as the TEM processing were purchased from Sigma Aldrich, South Africa, unless otherwise stated.

6.2.2 *Stenocarpella maydis* metabolites

Diplodiatoxin ($C_{18}H_{28}O_4$; molecular weight: 308 g/mol) (Steyn et al., 1972), dipmatol ($C_{15}H_{27}O_5$; molecular weight: 287 g/mol) (Ackerman et al., 1995) and diplonine ($C_6H_{11}NO_3$; molecular weight: 145 g/mol) (Snyman et al., 2011) were utilized.

6.2.3 Maintenance of cell cultures

The Neuro-2a, CHO-K1 and MDBK cells were obtained from the American Type Culture Collection (ATCC). The cells were grown in DMEM (Dulbecco's modified Eagle's

medium) (Neuro-2a cells) or DMEM and Ham's F-12 Nutrient Mixture (CHO-K1 and MDBK cells) supplemented with 10% foetal calf serum, 100 U/mL penicillin, 100 µg/mL streptomycin and 2.5 µg/mL amphotericin B (Fungizone) in a humidified atmosphere of 5% CO_2 at 37 °C. The cells were cultured in 75 cm^2 cell culture flasks.

6.2.4 Exposure of cell cultures to *Stenocarpella maydis* metabolites

The cell cultures were seeded at a density of 1 x 10^6 cells/mL. After attaching to the wells (24 h post culturing), cells were exposed to the highest concentration (750 µM) of diplodiatoxin and dipmatol for 24, 48 and 72 h. Diplonine (750 µM) was only evaluated on MDBK cells due to its lack of cytotoxicity at the concentration range used. Staurosporine (1 µM) and Triton-X (0.01%) were used as positive inducers of apoptosis (Zhang et al., 1998) and necrosis (Weyermann et al., 2005), respectively. The stock solutions of the toxic metabolites were prepared in DMSO. The working solutions of the toxins were prepared in the corresponding cell culture media.

6.2.5 Transmission electron microscopy (TEM)

Subcellular changes characteristic of apoptosis and necrosis in cells exposed to the three *S. maydis* toxins were investigated using TEM based on the modified method of Glauert (1980). At the end of the exposure period, cells were fixed in 2.5% glutaraldehyde in Millonig's buffer for 5 min before scraping the cells off the bottom of the microtitre plates. Detached cells contained in the supernatant were pelleted by centrifugation at 3 000 rpm for 3 min. Both the cells that were scraped off and pelleted were transferred to Eppendorf tubes and fixed for an hour. The cells were post-fixed in 1% osmium tetroxide in Millonig's buffer,

followed by washing and dehydration in buffer and graded alcohols. Cells were then embedded in absolute resin at 60 °C. Pelleting of the cells after each step was achieved by centrifugation at 3 000 rpm for 3 min. Following curing overnight, the ultra-thin sections were prepared and stained with lead citrate and uranyl acetate. The prepared sections were viewed using a Phillips CM10 transmission electron microscope operated at 80 kV.

6.3 RESULTS AND DISCUSSION

For comparison purposes the MDBK cells exposed to media only (i.e. normal/control cells), 1 µM staurosporine (i.e. apoptotic cells) and 0.01% Triton-X (i.e. necrotic cells) for 24, 48 and 72 h are presented in Figure 26. The subcellular changes observed in MDBK cells after exposure for 24, 48 and 72 h to diplodiatoxin, dipmatol and diplonine are shown in Figure 27.

The control MDBK cells showed normal morphology of the cytoplasm and nucleus at 24, 48 and 72 h exposure periods (Fig. 26 A-C). The control MDBK cells contained numerous mitochondria (white arrows) which were distributed throughout the cytoplasm. The cristae of the mitochondria were transversely oriented and the matrix of the mitochondria was slightly more electron-dense than the cytoplasm. Occasional electron-dense granules and vacuoles (V) were observed in the cytoplasm. Intact nuclear and plasma membranes were visible.

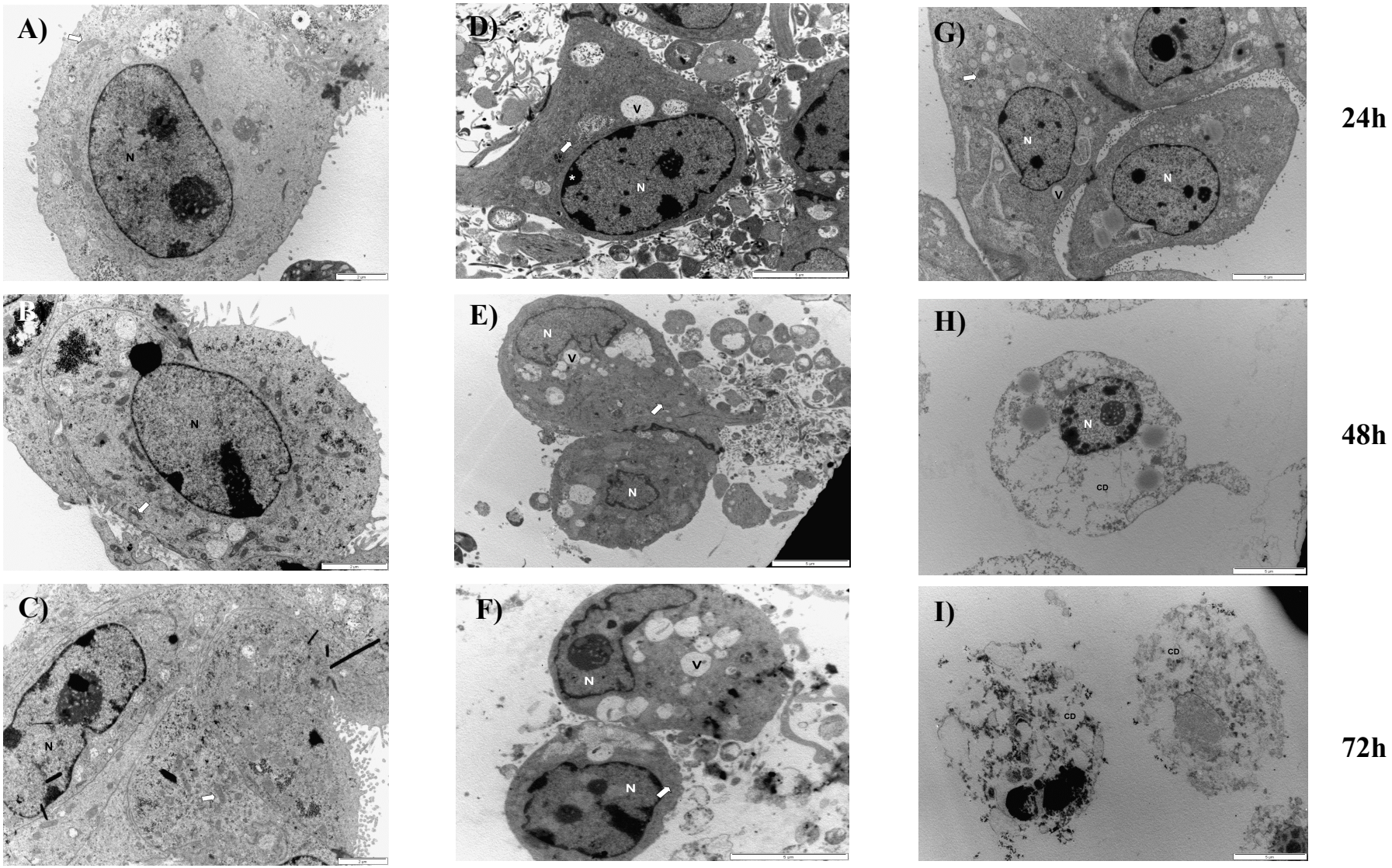

Figure 26. Electron micrographs showing MDBK cells exposed to media (A, B, C), 1 µM staurosporine (D, E, F) and 0.01% Triton-X (G, H, I) for 24, 48 and 72 h. N = nucleus; V = vacuoles; CD = cytoplasmic disruption; arrows = mitochondria; asterisk = chromatin condensation.

The apoptotic MDBK cells showed typical morphology of apoptosis (Fig. 26 D-F) which included the presence of chromatin condensation (white asterisks) and formation of apoptotic bodies. Numerous mitochondria and vacuoles were present in the cytoplasm. The mitochondria showed normal morphology. Both the nuclear and plasma membranes appeared to be intact.

The necrotic MDBK cells showed typical morphology of necrosis (Fig. 26 G-I) which was characterized by the presence of numerous large cytoplasmic vacuoles, the occasional swollen mitochondria and electron-lucent cytoplasm. The nuclear and plasma membranes appeared to be intact at 24 and 48 h treatment periods. At 48 h, most of the cytoplasm appeared to be completely disrupted (CD) and chromatin condensation became visible. Complete disruption of the nuclear and plasma membranes occurred after exposure for 72 h and this was usually accompanied by complete disruption of the cytoplasm.

The MDBK cells exposed for 24 h to diplodiatoxin contained numerous swollen mitochondria and most of these mitochondria had progressed to form electron-dense vacuoles (Fig. 27 A). In addition, a number of electron-lucent vacuoles were also seen. Some of the MDBK cells exhibited abnormal nuclei with fragmented nuclear matrix and chromatin condensation. At this stage, both the nuclear and plasma membranes appeared to be intact.

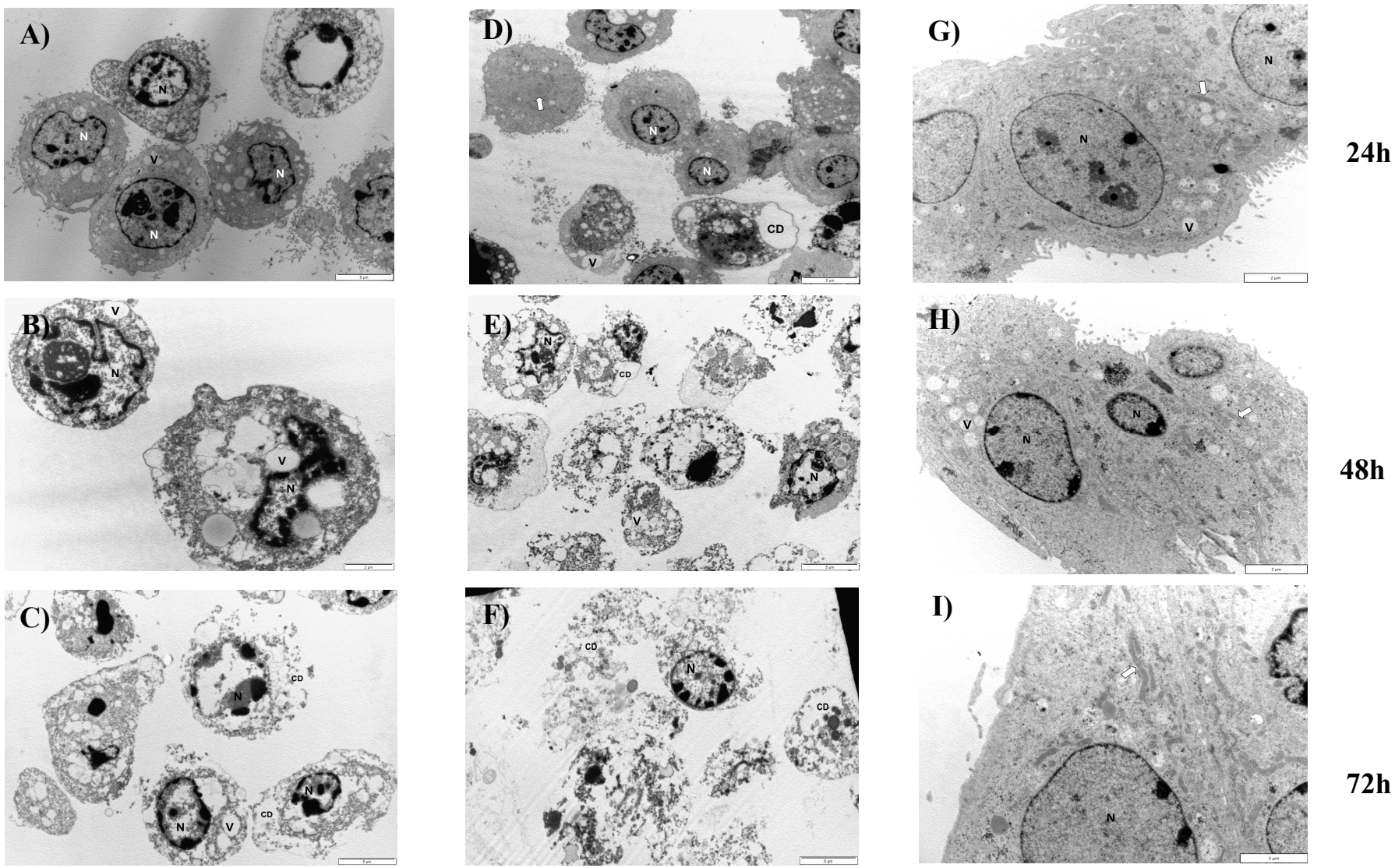

Figure 27. Electron micrographs showing MDBK cells exposed to 750 µM of diplodiatoxin (A, B, C), dipmatol (D, E, F) and diplonine (G, H, I) for 24, 48 and 72 h. N = nucleus; V = vacuoles; CD = cytoplasmic disruption; arrows = mitochondria.

The subcellular damage seemed to be progressive and at 48 h of exposure of MDBK cells to diplodiatoxin, the number and size of the electron-lucent vacuoles increased and protrusion of the cytoplasm was also observed (Fig. 27 B). Less electron-dense vacuoles were seen and there was complete disappearance of the mitochondria. Changes in the nuclear morphology were more evident and included invagination of the nuclear membrane and increased chromatin condensation. The plasma membrane appeared to be intact at 48 h of exposure. After 72 h, the electron-lucent cytoplasmic vacuoles progressed to complete disruption of the cytoplasm (Fig. 27 C). Fragmentation of the nucleus with increased chromatin condensation in most of the MDBK cells was prominent at this stage. Disruption in some parts of the plasma membrane was noticed in most of the cells.

The MDBK cultures treated with dipmatol for 24 h contained a large number of swollen mitochondria and electron-lucent cytoplasmic vacuoles (Fig. 27 D). The nuclei of most of the cells appeared normal with intact membranes and slight chromatin condensation. The cells that were more severely damaged exhibited nuclear fragmentation and some degree of cytoplasmic disruption. At this stage, the majority of the MDBK cells had intact plasma membranes. Distinct changes were visible at 48 h of exposure to dipmatol and included the complete disappearance of mitochondria, nuclear fragmentation accompanied by chromatin condensation and increase in the presence of electron-lucent vacuoles in the cytoplasm (Fig. 27 E). At this exposure period, numerous cells appeared to have intact nuclear and plasma membranes. Complete disruption of the cells together with the loss of nuclear and plasma membranes were evident after 72 h of exposure to dipmatol. Electron-dense cytoplasmic fragments/bodies were visible all around the field of focus. Only a few cells contained nuclei with intact membranes.

The major subcellular change observed after exposure of MDBK cells to diplonine was the progressive increase in length of the mitochondria with prolonged exposure (Fig. 27 G-I). The mitochondria were distributed in the entire cytoplasm. A few electron-lucent vacuoles and electron-dense granules were visible in the cytoplasm at the different exposure periods. Exposure to diplonine appeared to have caused no major changes in the nuclear morphology as well as the nuclear and plasma membranes of the cells.

Figure 28 demonstrates the subcellular changes observed in Neuro-2a cells after exposure to media only (i.e. normal/control cells), 1 µM staurosporine (i.e. apoptotic cells) and 0.01% Triton-X (i.e. necrotic cells) for 24, 48 and 72 h. Normal morphology of the cytoplasm and nucleus was observed in the control Neuro-2a cells throughout the exposure periods (Fig. 28 A-C). The control Neuro-2a cells contained numerous normal mitochondria and electron-dense granules in their cytoplasm. The nuclear and plasma membranes were intact.

The apoptotic Neuro-2a cells contained a large number of cytoplasmic electron-lucent vacuoles at 24 h of exposure to staurosporine (Fig. 28 D). There were electron-dense contents inside the vacuoles. Few mitochondria were visible in the cytoplasm. Dark-stained round granules/structures were distributed in most of the cytoplasm. The nucleus appeared normal with intact membrane. However, in other cells chromatin condensation appeared to have occupied the entire nucleus. At this stage of exposure, the plasma membrane was intact.

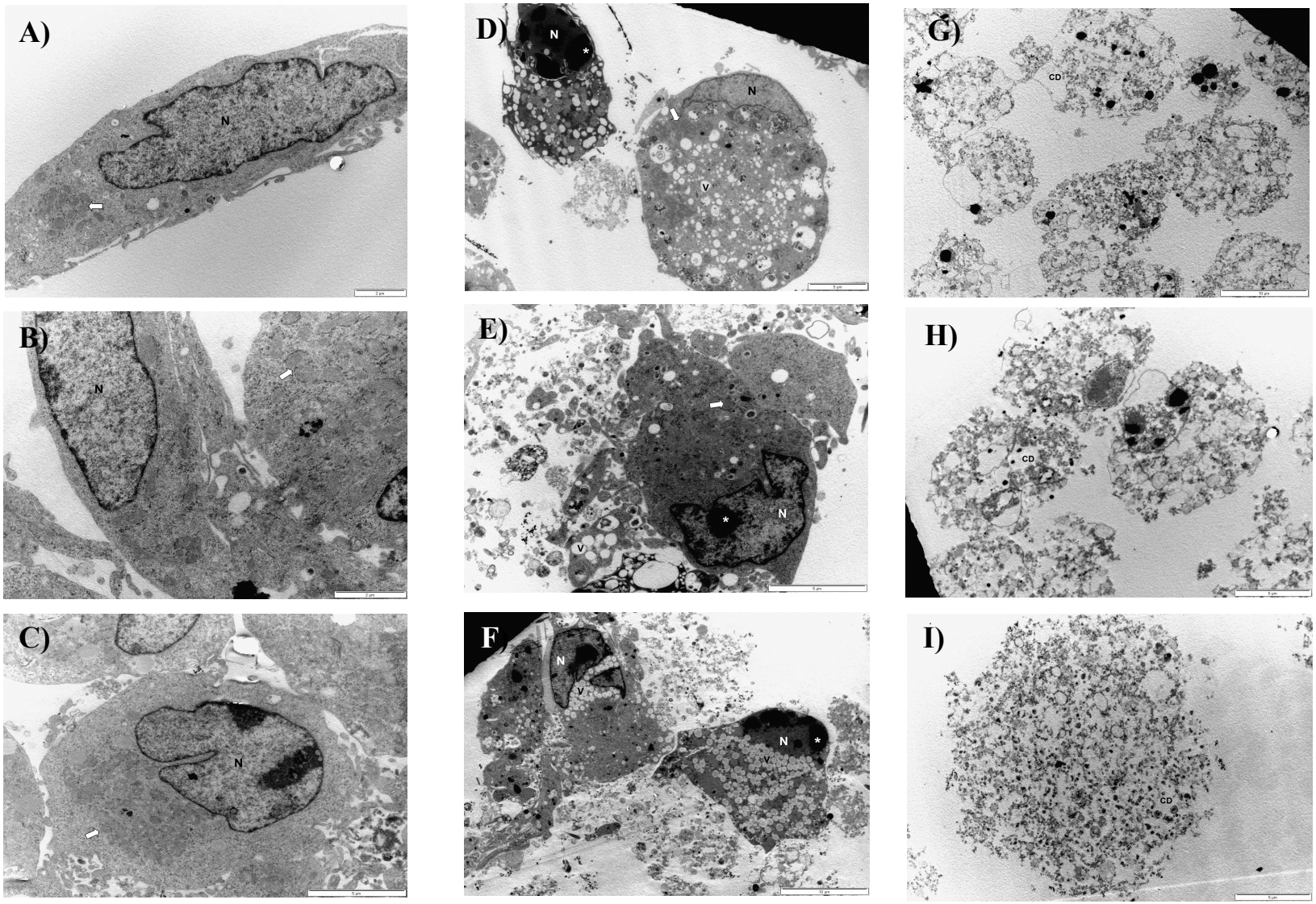

Figure 28. Electron micrographs showing Neuro-2a cells exposed to media (A, B, C), 1 µM staurosporine (D, E, F) and 0.01% Triton-X (G, H, I) for 24, 48 and 72 h. N = nucleus; V = vacuoles; CD = cytoplasmic disruption; arrows = mitochondria; asterisk = chromatin condensation.

The typical morphology of apoptosis in Neuro-2a cells was most evident at 48 and 72 h of exposure to staurosporine and included the presence of apoptotic bodies and chromatin condensation. Mitochondria were visible in the cytoplasm at 48 h (Fig. 28 E). The nuclear and plasma membranes appeared to be intact at 48 and 72 h. A large number of electron-lucent cytoplasmic vacuoles were visible at 72 h of exposure (Fig. 28 F).

The necrotic Neuro-2a cells showed typical morphology of necrosis (Fig. 28 G-I) which included the presence of large cytoplasmic vacuoles that progressed to complete cytoplasmic disruption with prolonged exposure. Chromatin condensation was seen in some of the necrotic cells. Damage to the nuclear and plasma membranes intensified with prolonged exposure until there were no visible membranes remaining (Fig. 28 I).

The subcellular changes observed in Neuro-2a cells following treatment with diplodiatoxin and dipmatol for 24, 48 and 72 h are shown in Figure 29. Numerous vacuoles and granules were visible in the cytoplasm of the cells after exposure for 24 h to diplodiatoxin (Fig. 29 A). Some of the cells were binucleated with intact nuclear membranes. Mitochondria were not visible in the cytoplasm at 24 h. At this stage of exposure, the plasma membrane was intact. The most notable changes at 48 h of exposure to diplodiatoxin included the disappearance of nuclei and mitochondria as well as the presence of numerous electron-lucent vacuoles (Fig. 29 B). A large number of electron-dense granules/structures were seen in the cytoplasm. The plasma membrane was still intact after 48 h of exposure with a few apoptotic body-like structures outside of the cell.

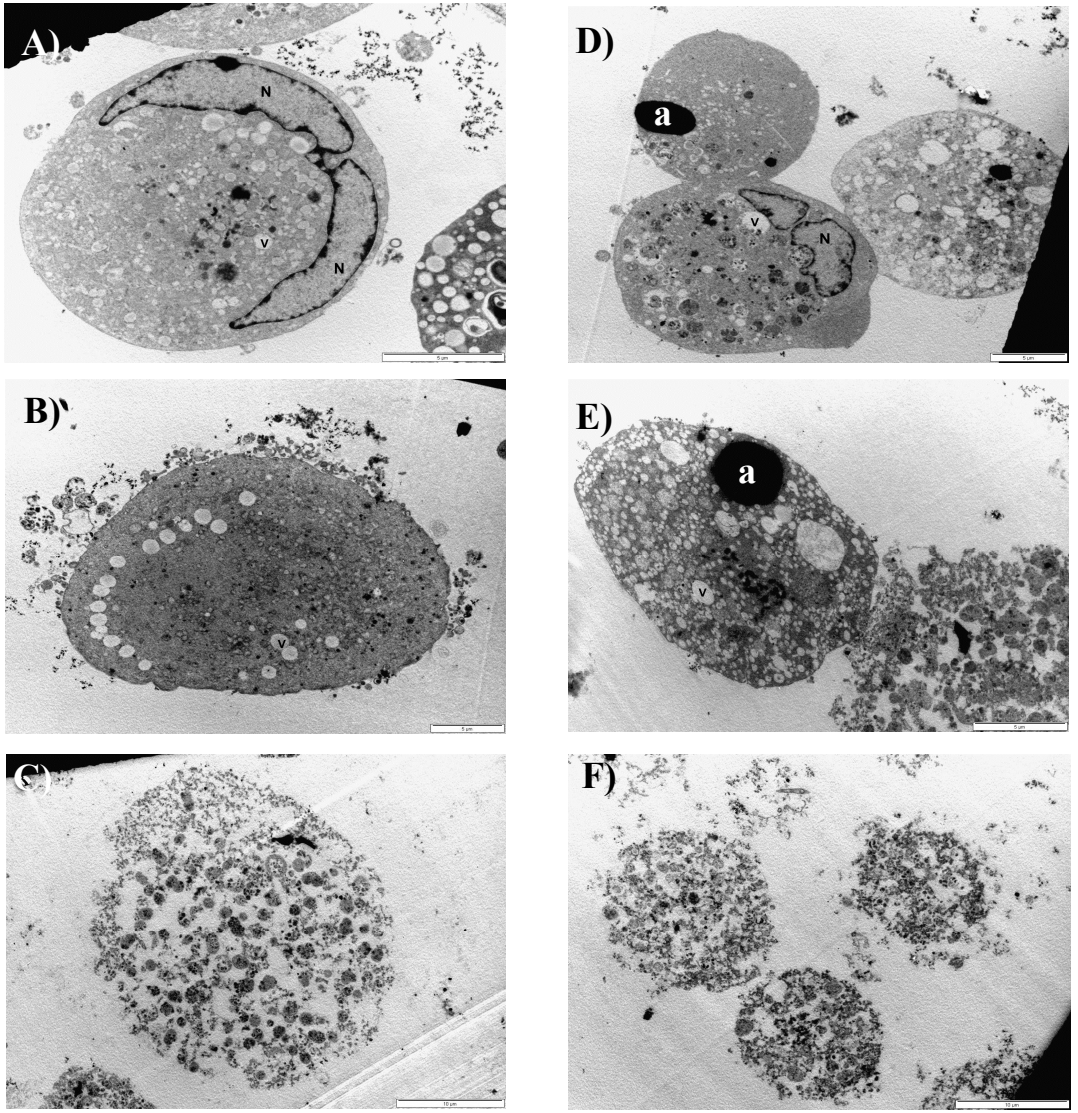

Figure 29. Electron micrographs showing Neuro-2a cells exposed to 750 µM of diplodiatoxin (A, B, C) and dipmatol (D, E, F) for 24, 48 and 72 h. N = nucleus; V = vacuoles; a = staining artefact.

Complete disruption of the cells accompanied by the loss of plasma membrane was evident after 72 h of exposure of Neuro-2a cells to diplodiatoxin (Fig. 29 C). Electron-dense apoptotic body-like structures were distributed in the fragmented cytoplasm.

The Neuro-2a cultures treated with dipmatol for 24 h contained numerous vacuoles and electron-dense round structures in the cytoplasm (Fig. 29 D). Most of the cells did not contain any nuclei, however, some cells were binucleated. The plasma membrane appeared to be intact at this stage. A large number of vacuoles were visible in the cytoplasm at 48 h of exposure to dipmatol (Fig. 29 E). Complete disappearance of nuclei and mitochondria was evident. The plasma membrane of some cells appeared to be intact while other cells appeared to be completely disrupted. At 72 h, complete disruption of the cells was observed and apoptotic body-like structures constituted the fragmented cytoplasm (Fig. 29 F).

The subcellular changes observed in CHO-K1 cells after exposure to media only (i.e. normal/control cells), 1 µM staurosporine (i.e. apoptotic cells) and 0.01% Triton-X (i.e. necrotic cells) for 24, 48 and 72 h are shown in Figure 30. The control CHO-K1 cells showed normal morphology of the cytoplasm and nucleus throughout the exposure periods (Fig. 30 A-C). Numerous mitochondria were distributed in the cytoplasm. Few electron-dense granules and vacuoles were visible in the cytoplasm. The nuclear and plasma membranes were intact at 24, 48 and 72 h.

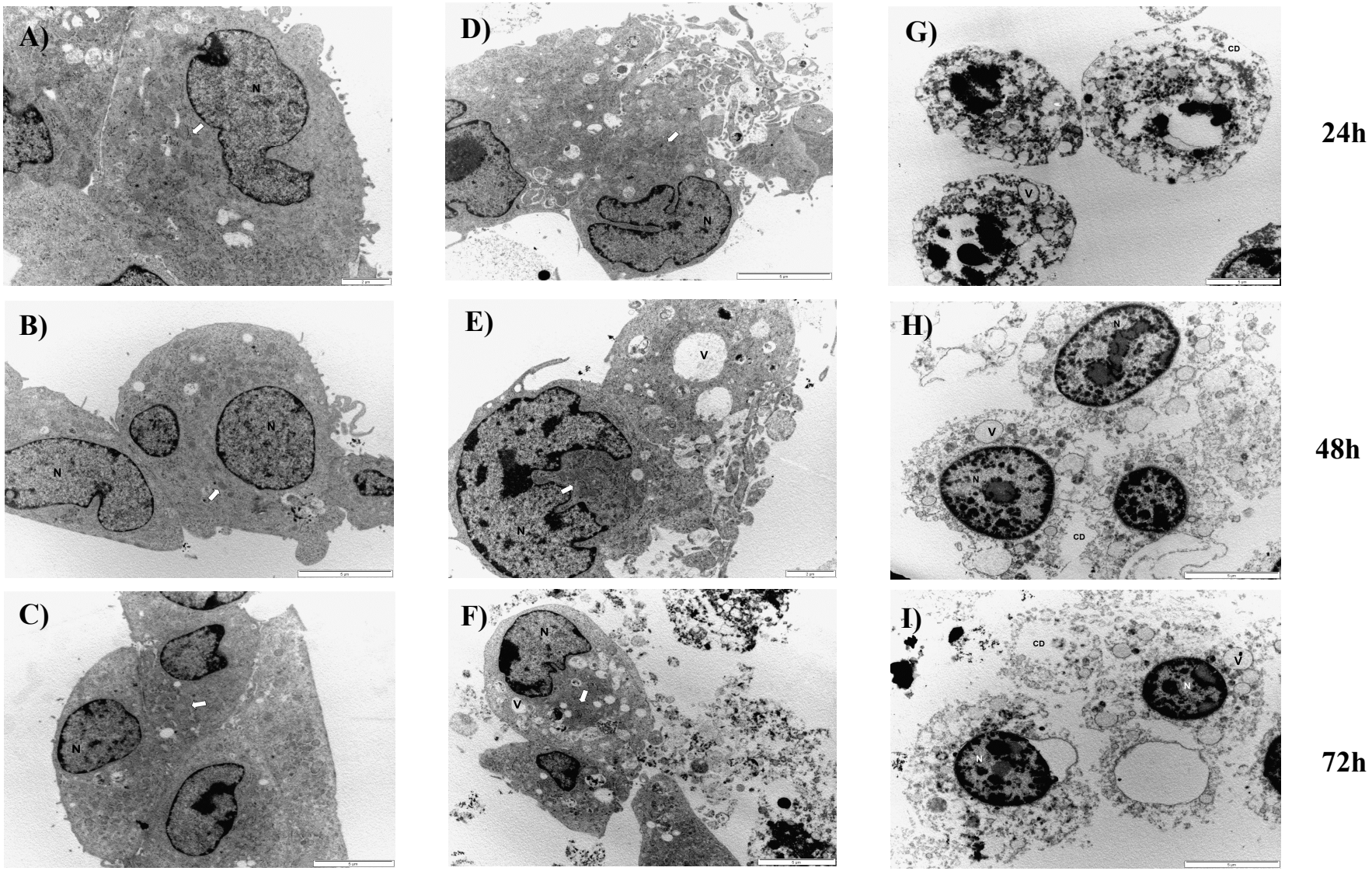

Figure 30. Electron micrographs showing CHO-K1 cells exposed to media (A, B, C), 1 µM staurosporine (D, E, F) and 0.01% Triton-X (G, H, I) for 24, 48 and 72 h. N = nucleus; V = vacuoles; CD = cytoplasmic disruption; arrows = mitochondria.

Typical apoptotic morphology characterized by the presence of apoptotic bodies and chromatin condensation was evident in the CHO-K1 cells exposed to staurosporine (Fig. 30 D-F). Invagination of the nuclear membrane was seen in most of the nuclei. Numerous mitochondria and vacuoles were present in the cytoplasm. Both the nuclear and plasma membranes appeared intact.

The necrotic CHO-K1 cells showed typical morphology of necrosis (Fig. 30 G-I) which included the presence of large cytoplasmic vacuoles that progressed to complete cytoplasmic disruption with prolonged exposure. Nuclear fragmentation accompanied by chromatin condensation was most evident at 24 h (Fig. 30 G). The plasma membrane was intact at 24 h exposure. Complete disruption of the plasma membrane was most prominent at 48 and 72 h.

Figure 31 shows the subcellular changes observed in CHO-K1 cells exposed to diplodiatoxin and dipmatol for 24, 48 and 72 h. The most noticeable changes in CHO-K1 cells exposed to diplodiatoxin included the complete disappearance of mitochondria and the fragmentation of nucleus and cytoplasm (Fig. 31 A-C). The nuclear and plasma membranes appeared to be intact at 24 h of exposure to diplodiatoxin (Fig. 31 A). Disruption of the cytoplasm intensified with prolonged exposure to the toxin (Fig. 31 B & C). The plasma membrane of most of the cells appeared to be intact at 48 and 72 h, however, disruption in some parts of the plasma membrane was noticed. Complete disruption of the nucleus and nuclear membrane was not seen in all cells, some cells had nuclei with nuclear membrane that appeared to be intact even at 72 h of toxin exposure (Fig. 31 C).

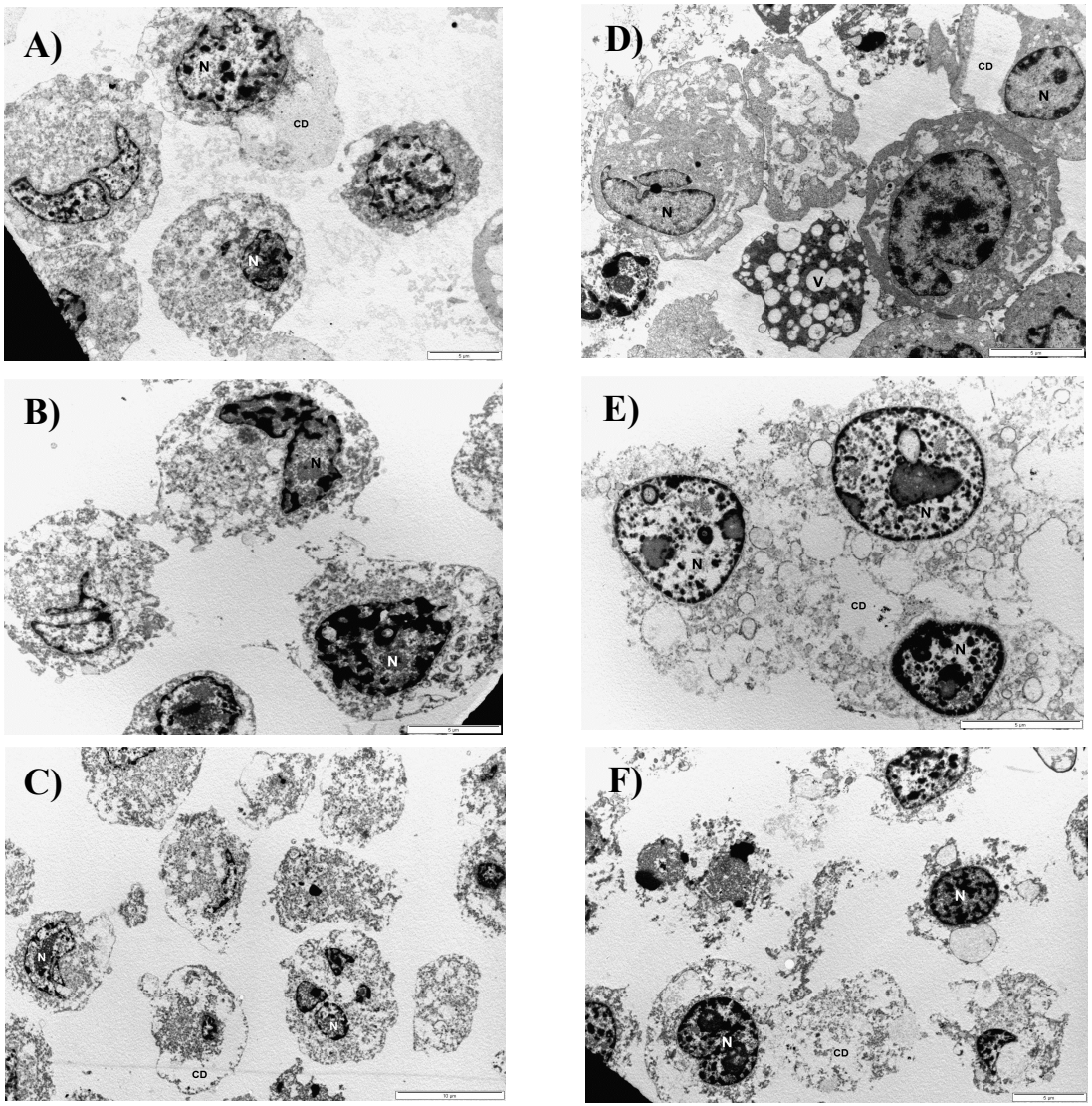

Figure 31. Electron micrographs showing CHO-K1 cells exposed to 750 µM of diplodiatoxin (A, B, C) and dipmatol (D, E, F) for 24, 48 and 72 h. N = nucleus; V = vacuoles; CD = cytoplasmic disruption.

The CHO-K1 cultures exposed for 24 h to dipmatol contained numerous electron-lucent vacuoles which had progressed to complete disruption of the cytoplasm in some instances (Fig. 31 D). At this stage, there was complete disappearance of the mitochondria and the nuclear and plasma membranes appeared to be intact. Complete disruption of the cytoplasm and plasma membrane was observed with prolonged exposure (Fig. 31 E & F). The nuclear membrane appeared to be intact in most of the CHO-K1 cells exposed to dipmatol at 48 and 72 h. Fragmentation of the nuclear matrix was evident in these cells.

Except for the elongation of mitochondria, no major subcellular changes were observed following treatment of MDBK cells with diplonine. The most remarkable subcellular changes observed in MDBK, Neuro-2a and CHO-K1 cell cultures treated with diplodiatoxin and dipmatol for 24, 48 and 72 h were abnormal/swollen mitochondria which progressed to from cytoplasmic vacuoles, nuclear fragmentation and complete disruption of the cytoplasm accompanied by nuclear and plasma membrane disintegration. In general, these subcellular changes were consistent with the morphological changes characteristic of the necrotic cell death pathway. The plasma membranes of the MDBK cells exposed to diplodiatoxin and the plasma membranes of CHO-K1 cells exposed to diplodiatoxin and dipmatol were retained the longest and even at 72 h some membrane integrity was still observed. Apoptotic body-like structures were mainly visible in the Neuro-2a cells treated with the two *S. maydis* toxins. Nuclear fragmentation observed in the damaged cells was usually accompanied by chromatin condensation, subcellular changes which are indicative of apoptosis. The subcellular damage observed in the cells intensified with prolonged exposure to the toxins.

One of the first *in vitro* changes induced by diplodiatoxin and dipmatol included morphological alterations to the mitochondria. Mitochondria have been reported to play an important role in oxidative phosphorylation (Green & Reed, 1998), maintenance of calcium ion levels in cellular compartments (Kroemer & Reed, 2000) and facilitation of apoptotic and necrotic cell death pathways (Kroemer et al., 1998).

The second major subcellular change observed in this study was the progression of mitochondrial damage to cytoplasmic vacuoles with prolonged exposure to diplodiatoxin and dipmatol. Formation of cytoplasmic vacuoles from damaged mitochondria following exposure to toxic substances has been reported previously (Pollanen et al., 1990; Henics & Wheatley, 1997; Carranza-Rosales et al., 2005). In most cases, vacuolation occurs after a stimulus and leads to an increase in size and number of vacuoles in the cytoplasm. Up to a certain threshold, vacuolation is fully reversible and cells can recover to full functionality. However, beyond this threshold, due to continued exposure to certain toxins, the process of vacuolation is irreversible and the structural damage caused by vacuolation leads to cell death (Henics & Wheatley, 1999).

Nuclear fragmentation accompanied by chromatin condensation was the third major subcellular change observed in this study. Caspases, especially caspase-3 and -7 enzymes, are responsible for cleaving various death substrates involved in regulation of nuclear changes during apoptosis (Robertson et al., 2000). Caspase-3 enzyme is capable of cleaving the poly-(ADP-ribose) polymerase (PARP), DNA-dependent protein kinase (DNA-PK) and lamin, which are protein substrates responsible for maintaining the genomic integrity. The PARP and DNA-PK proteins have also been implicated in cellular DNA repair processes (Nagata,

2000). Chromatin condensation was reported to occur as a result of the loss of structural integrity of the nuclear matrix (Susin, et al., 2000).

It was concluded that diplodiatoxin and dipmatol, at high concentrations, induced subcellular changes indicative of both necrotic and apoptotic cell death pathways.

CHAPTER 7

GENERAL DISCUSSION AND CONCLUSIONS

The mechanism of action of the currently known *S. maydis* metabolites is poorly understood. *In vivo* models have been used previously to investigate the toxicity of the three *S. maydis* metabolites i.e. diplodiatoxin, dipmatol and diplonine (Steyn et al., 1972; Ackerman et al., 1995; Rahman et al., 2002; Rao et al., 2003; Snyman et al., 2011). Cell-based assays have been widely used as suitable replacement models for animal experimentation in pre-clinical research, drug development and toxicological testing (Xing et al., 2006). In this study, the toxicity and mechanism of action of diplodiatoxin, dipmatol and diplonine were investigated using *in vitro* cell cultures, namely the Neuro-2a, CHO-K1 and MDBK cells.

Cytotoxicity of the three *S. maydis* metabolites was initially assessed using the xCELLigence assay, which provided real-time analysis of the cell-toxin interactions. The cytotoxicity measured using this method is considered to reflect the true biological status of the cells in real-time, since there is no addition of chemicals, dyes or radiation indicators after exposure of the cells to toxins of interest (Xing et al., 2006). Subsequently, cytotoxicity was assessed by the ability of the cultured cells to reduce MTT, a measure of the activity of the mitochondrial succinate dehydrogenase and other cytoplasmic enzymes (Liu et al., 1997), and as the total protein concentration which was indicative of growth and survival of the cells (Viluksela et al., 1996).

A concentration-dependent cytotoxicity was observed when the three cell lines were exposed to diplodiatoxin and dipmatol. The cytotoxicity results obtained indicate that diplodiatoxin and dipmatol affected the activity of the mitochondrial dehydrogenase enzyme. Inhibition of enzymes, such as the mitochondrial succinate dehydrogenase involved in the mitochondrial electron transfer chain reactions, due to damage of the mitochondria has been linked to depletion of ATP synthesis which is crucial to the viability of cells (Schulze-Osthoff et al., 1992). The lowest EC_{50} values were obtained with MDBK cells exposed to diplodiatoxin (EC_{50} = 147 µM at 72 h) and dipmatol (EC_{50} = 686 µM at 72 h). It was concluded that diplodiatoxin was more toxic than dipmatol.

To better understand the mechanism(s) involved in the concentration-dependent cytotoxicity observed on the three cell lines exposed to the *S. maydis* metabolites, necrotic and apoptotic cell death pathways were investigated. The LDH and PI flow cytometry assays used in this study showed that exposure of Neuro-2a, CHO-K1 and MDBK cells to 750 µM of diplodiatoxin and dipmatol affected the plasma membrane integrity of the cell lines. In contrast, diplonine had no effect on the plasma membrane integrity of the three cell lines at comparable concentrations. Apoptosis, evaluated by caspase-3/7 and Annexin V-FITC flow cytometry assays, was induced in the three cell lines exposed to diplodiatoxin and dipmatol at high concentrations. These results indicate that diplodiatoxin and dipmatol, at high concentrations, exerted their cellular toxicity via both apoptosis and necrosis.

Results presented in this study concur with previous studies reporting on the induction of both apoptosis and necrosis following exposure of cells to toxins (Denecker et al., 2001; Sawai & Domae, 2011; Gao et al., 2014). In their study, Gao et al. (2014) found that both

necrosis and apoptosis contributed to the tacrine-induced death of HepG2 cells and concluded that tacrine-induced apoptosis was the main cause. Denecker et al. (2001) demonstrated that in murine fibrosarcoma (L929sA) cells treated with tumor necrosis factor (TNF), the release of active caspases into the culture supernatant coincided with the release of LDH. Dual staining (i.e. Annexin-V positive/PI positive) of both apoptotic and primary necrotic U937 cells treated with TNF was reported by Sawai and Domae (2011). The occurrence of both apoptotic and necrotic cell death pathways could be attributed to the fact that during the early stages of apoptosis, phosphatidylserine is actively externalized to the outer surface of the plasma membrane resulting in the recognition and engulfment of the dying cells (Krysko et al., 2008). Thus, the apoptotic cells are rapidly removed before the plasma membrane integrity is lost. However, under *in vitro* conditions where phagocytes are absent, the apoptotic cells are not removed and therefore proceed to secondary necrosis (Krysko et al., 2008). Hence, under these conditions, both apoptosis and necrosis are manifested.

The apoptosis recorded in this study was caspase-dependent and this was demonstrated by the activation of caspase-3/7 enzymes following exposure of the three cell lines to diplodiatoxin and dipmatol at high concentrations. In their study, Du et al. (2012) reported an increased expression of caspase-3 and -9 enzymes after treatment of HepG2 cells with trichothecenes. An increase in caspase activity was reported with staurosporine-induced apoptosis in CHO-K1 cells (Zhang et al., 1998). On the other hand, apoptosis has also been suggested to occur via caspase-independent mechanisms (Zhang et al., 2004).

The two main apoptotic pathways i.e. extrinsic and intrinsic apoptosis, have been described in detail in Chapter 2. The extrinsic pathway is initiated by binding of death ligands

to cell surface receptors resulting in the formation of DISC, whereas the intrinsic apoptosis is triggered by intracellular signals such as cellular and DNA damage (Danial & Korsmeyer, 2004; Meier & Vousden, 2007). Mitochondria are central to both apoptotic pathways and also play a critical role in the regulation of necrotic cell death (Sawai & Domae, 2011). Activation of mitochondria is controlled by the Bcl-2 family of proteins (e.g. Bcl-2, Bax, Bak and BH3) (Shimizu et al., 1996; Schultze-Osthoff, 2008). Initiation of the caspase cascades is central in apoptosis regulation. Once activated, initiator caspases (e.g. caspase-2, -8, -9 and -10) cleave and activate downstream effector caspases (e.g. caspase-3, -6 and -7), which are responsible for cleaving various death substrates that eventually set apoptosis into full action (Franke et al., 2010).

Finally, TEM was used to correlate the cell death pathways evaluated in this study with their typical morphology. Necrotic cells typically show cytoplasmic vacuolation, swelling of mitochondria, rupture of both nuclear and plasma membranes and appear as faintly stained cells with nuclear ghosts (Vermes et at., 1995). In contrast, apoptotic cells show chromatin condensation, nuclear fragmentation and formation of apoptotic bodies. The cell membrane of apoptotic cells remain intact, although it may often show some blebbing (Loos & Engelbrecht, 2009).

Mitochondrial damage, cytoplasmic vacuolation and nuclear fragmentation, including the formation of apoptotic bodies in Neuro-2a cells, were the major subcellular changes induced by diplodiatoxin and dipmatol *in vitro*. No major subcellular changes were observed in MDBK cells exposed to diplonine, except for the elongation of mitochondria. The cytotoxicity of the two *S. maydis* metabolites observed in this study could be mainly

attributed to mitochondrial damage as indicated by both the cytotoxicity (xCELLigence, MTT and protein measurement assays) and TEM results. Following the formation of cytoplasmic vacuoles from the damaged mitochondria, a point of irreversible cellular damage was reached which eventually led to the activation of the apoptotic and necrotic cell death pathways. The subcellular changes observed in the three cell lines after exposure to diplodiatoxin and dipmatol support the results obtained with the apoptotic and necrotic assays. The results of this study indicate that mitochondrial damage could be central in the development of diplodiosis, since no gross lesions, except *status spongiosis*, are noticeable.

The following conclusions were made from the results obtained:

1. Diplodiatoxin and dipmatol induced a concentration-dependent cytotoxicity in Neuro-2a, CHO-K1 and MDBK cells. The cytotoxicity order was: diplodiatoxin > dipmatol. Diplonine was not cytotoxic at comparable concentrations.

2. Based on the EC_{50} results, it is recommended that the MDBK cell line should be considered as a suitable *in vitro* model for cytotoxicity and other toxicological, biochemical, and molecular investigations of the *S. maydis* metabolites.

3. Diplodiatoxin and dipmatol, at high concentrations, exerted their toxicity via caspase-dependent apoptosis and necrosis.

4. Mitochondrial damage, cytoplasmic vacuolation and nuclear fragmentation were the major subcellular changes observed.

5. Mitochondrial damage appeared to be central in the toxicity induced by the two *S. maydis* metabolites.

FUTURE STUDIES

Future studies should focus on:

- Inducing diplodiosis in the target animals (cattle and sheep) using toxic *S. maydis* metabolites.
- Comparing the electron microscopy lesions in animals poisoned naturally and experimentally by *S. maydis* with the lesions induced by the purified mycotoxins.
- Investigating if metabolic activation will increase the toxicity of diplonine.
- Investigating if cellular damage will be induced by diplonine in freshly isolated primary neuronal (e.g. oligodendrocytes) cells.
- Elucidating in detail the roles of apoptosis and necrosis (even autophagy) in the toxicity of the *S. maydis* metabolites.
- Developing analytical tools for detection and quantification of the *S. maydis* toxins in maize commodities.

REFERENCES

ACKERMAN, L.G.J., COMBRINK, S., HORAK, R.M., KUHN, M., LEARMONTH, R.L., LÜBBEN, A., MAHARAJ, V.J. & RABIE, C.J. 1995. A novel hydroxylated fatty acid isolated from cultures of *Diplodia maydis* on maize. In: Book of Abstract-Poster B1, 5th Frank Warren National Organic Chemistry Conference, 4-7 April 1995, Aventura Aldam Resort, Ventersburg, Free State, South Africa.

ADAMS, J.M. & CORY, S. 1998. The Bcl-2 protein family: arbiters of cell survival. *Science* 281: 1322-1326.

ATANDA, S.A., AINA, J.A., AGODA, S.A., USANGA, O.E. & PESSU, P.O. 2012. Mycotoxin management in agriculture: a review. *Journal of Animal Science Advances* 2: 250-260.

BARROCAS, E.N., MACHADO, J. da C., ALMEIDA, M.F., de BOTELHO, L.S., PINHO, É.V. & VON, de R. 2012. Sensibility of the PCR technique in the detection of *Stenocarpella* sp. associated with maize seeds. Associação Brasileira de Tecnologia de Sementes (ABRATES), Brasília, Brazil, *Revista Brasileira de Sementes* 34(2): 218-224.

BARROS, E., CRAMPTON, M., MARAIS, G. & LEZAR, S. 2008. A DNA-based method to quantify *Stenocarpella maydis* in maize. *Maydica* 53: 125-129.

BEASLEY, V.R. 2011. Photophysiology and clinical manifestations of mycotoxin and phycotoxin poisoning. *Egyptian Journal of Natural Toxins* 8(1-2): 103-133.

BENNETT, J.W. 1987. Mycotoxins, mycotoxicoses and mycopathology. *Mycopathologia* 100: 3-5.

BENNETT, J.W. & KLICH, M. 2003. Mycotoxins. *Clinical Microbiology Reviews* 16(3): 497-516.

BENSCH, M.J. 1995. An evaluation of inoculation techniques inducing *Stenocarpella maydis* ear rot on maize. *South African Journal of Plant and Soil* 12: 172-174.

BERGMANN, A. 2007. Autophagy and cell death: No longer at odds. *Cell* 131: 1032-1034.

BLAKEMORE, E.J.A., JACCOUD FILHO, D.S. & REEVES, J.C. 1994. PCR for the detection of *Pyrenophora* species, *Fusarium moniliforme*, *Stenocarpella maydis* and the *Phomopsis/Diaporthe* complex. In: Schots, A., Dewey, F.M. & Oliver, R. (Eds.). *Modern assays for plant pathogenic fungi: Identification, Detection and Quantification*. CAB International, Oxford, U.K.

BLOUNT, W.P. 1961. Turkey "X" disease. *Turkeys* 9: 52-77.

BORENFREUND, E. & PUERNER, J.A. 1985. Toxicity determined *in vitro* by morphological alterations and neutral red absorption. *Toxicology Letters* 24: 110-124.

BOYD, J.M., HUANG, L., XIE, L., MOE, B., GABOS, S. & LI, X-F. 2008. A cell-microelectronic sensing technique for profiling cytotoxicity of chemicals. *Analytica Chimica Acta* 615: 80-87.

BRADFORD, M.M. 1976. A rapid and sensitive method for the quantification of microgram quantities of protein utilizing the principle of protein dye binding. *Analytical Biochemistry* 72: 248-254.

CARRANZA-ROSALES, P., SAID-FERNÁNDEZ, S., SEPÚLVEDA-SAAVEDRA, J., CRUZ-VEGA, D.E. & GANDOLFI, A.J. 2005. Morphologic and functional alterations

induced by low doses of mercuric chloride in kidney OK cell line: ultrastructural evidence for an apoptotic mechanism of damage. *Toxicology* 210: 111-121.

CHAMBERS, K.R. 1982. Some aspects of root and stalk rot of maize. In: Proceedings of the 5th South African Maize Breeding Symposium. Department of Agriculture and Water Supply Technical Communication 182, pp. 50-53.

CIEGLER, A. & BENNETT, J.W. 1980. Mycotoxins and mycotoxicoses. *BioScience* 30(8): 512-515.

COLLINS, J.A., SCHANDL, C.A., YOUNG, K.K., VESELY, J. & WILLINGHAM, M.C. 1997. Major DNA fragmentation is a late event in apoptosis. *The Journal of Histochemistry and Cytochemistry* 45(7): 923-934.

COMPTON, S.J. & JONES, C.G. 1985. Mechanism of dye response and interference in the Bradford protein assay. *Analytical Biochemistry* 151(2): 369-374.

COULOMBE, R.A. 1993. Biological action of mycotoxins. *Journal of Dairy Science* 76: 880-891.

CUTLER, H.G., CRUMLEY, F.G., COX, R.H., COLE, R.J., DORNER, J.W., SPRINGER, J.P., LATTERELL, F.M., THEAN, J.E. & ROSSI, A.E. 1980. Chaetoglobosin K: A new plant growth inhibitor and toxin from *Diplodia macrospora*. *Journal of Agricultural and Food Chemistry* 28: 139-142.

DANIAL, N.N. & KORSMEYER, S.J. 2004. Cell death: critical control points. *Cell* 116: 205-219.

DARVALL, P.M. 1964. Mouldy corn cobs, a danger to cows. *Queensland Agricultural Journal* 90: 692-693.

DEBATIN, K.M. & KRAMMER, P.H. 2004. Death receptors in chemotherapy and cancer. *Oncogene* 23: 2950-2966.

DECKER, T., LOHMANN-MATTHES, M.L. 1988. A quick and simple method for the quantification of lactate dehydrogenase release in measurements of cellular cytotoxicity and tumor necrosis factor (TNF) activity. *Journal of Immunological Methods* 115: 61-69.

DEL RIO, M.L. & DEL RIO, L. 1991. Dispersion of *Stenocarpella maydis* (Berk.) Sutton in maize crops. *CEIBA* 32: 133-140.

DENECKER, G., VERCAMMEN, D., STEEMANS, M., VANDEN BERGHE, T., BROUCKAERT, G., VAN LOO, G., ZHIVOTOVSKY, B., FIERS, W., GROOTEN, J., DECLERCQ, W. & VANDENABEELE, P. 2001. Death receptor-induced apoptotic and necrotic cell death: differential role of caspases and mitochondria. *Cell Death and Differentiation* 8: 829-840.

DEPARTMENT OF AGRICULTURE, FORESTRY AND FISHERIES (DAFF). 2013. Trends in the Agricultural Sector. http://www.daff.gov.za/docs/statsinfo/Trends13.pdf.

DEPARTMENT OF AGRICULTURE, FORESTRY AND FISHERIES (DAFF). 2014. Crop Estimates Committee. R.D. Dredge: http://www.daff.gov.za/crop estimates. Date of access: 16 September 2014.

DU, R.H., CUI, J.T., WANG, T., ZHANG, A.H. & TAN, R.X. 2012. Trichothecin induces apoptosis of HepG2 cells via caspase-9 mediated activation of the mitochondrial death pathway. *Toxicon* 59: 143-150.

DURRELL, L.W. 1923. Dry rot of corn. *Iowa Agricultural Experimental Station Research Bulletin 77*: 31.

EDINGER, A.L. & THOMPSON, C.B. 2004. Death by design: apoptosis, necrosis and autophagy. *Current Opinion in Cell Biology* 16: 663-669.

EISENBRAND, G., POOL-ZOBEL, B., BAKER, V., BALLS, M., BLAAUBOER, B.J., BOOBIS, A., CARERE, A., KEVEKORDES, S., LHUGUENOT, J-C., PIETERS, R. & KLEINER, J. 2002. Methods of *in vitro* toxicology. *Food and Chemical Toxicology* 40: 193-236.

ELLIS, C.E., NAICKER, D., BASSON, K.M., BOTHA, C.J., MEINTJES, R.A. & SCHULTZ, R.A. 2010. Cytotoxicity and ultrastructural changes in H9c2 (2-1) cells treated with pavetamine, a novel polyamine. *Toxicon* 55: 12-19.

FESTIENS, N., VANDEN BERGHE, T. & VANDENABEELE, P. 2006. Necrosis, a well-orchestrated form of cell demise: Signalling cascades, important mediators and concominant immune response. *Biochimica et Biophysica Acta* 1757: 1371-1387.

FLETT, B.C. & WEHNER, F.C. 1991. Incidence of *Stenocarpella* and *Fusarium* cob rots in monoculture maize under different tillage systems. *Journal of Phytopathology* 133: 327-333.

FLETT, B.C., WEHNER, F.C. & SMITH, M.F. 1992. Relationship between maize stubble placement in soil and survival of *Stenocarpella maydis*. *Journal of Phytopathology* 134: 33-38.

FLETT, B.C. & MCLAREN, N.W. 1994. Optimum disease potential for evaluating resistance to *Stenocarpella maydis* ear rot in corn hybrids. *Plant Disease* 78: 587-589.

FLETT, B.C., BENSCH, M.J., SMIT, E. & FOURIE, D. 1996. A field guide for identification of maize diseases in South Africa. ARC–Grain Crops Institute, Potchefstroom, South Africa.

FLETT, B.C., MCLAREN, N.W. & WEHNER, F.C. 1998. Incidence of ear rot pathogens under alternating corn tillage systems. *Plant Disease* 82: 781-784.

FLETT, B.C. 1999. Epidemiology and management of maize ear rot. PhD thesis (Agric.), University of Pretoria.

FLETT, B.C., MCLAREN, N.W. & WEHNER F.C. 2001. Incidence of *Stenocarpella maydis* ear rot of corn under crop rotation systems. *Plant Disease* 85: 92-94.

FORSBY, A., ANDERSSON, M. & LEWAN, L. 1991. The cytotoxicity of 22 sesquiterpenoid unsaturated dialdehydes, as determined by the neutral red absorption assay and by protein determination. *Toxicology In Vitro* 5(1): 9-14.

FOTAKIS, G. & TIMBRELL, J.A. 2006. *In vitro* cytotoxicity assays: Comparison of LDH, neutral red, MTT and protein assay in hepatoma cell lines following exposure to cadmium chloride. *Toxicology Letters* 160: 171-177.

FRANKE, J.C., PLÖTZ, M., PROKOP, A., GEILEN, C.C., SCHMALZ, H-G. & EBERLE, J. 2010. New caspase-independent but ROS-dependent apoptosis pathways are targeted in melanoma cells by iron-containing cytosine analogue. *Biochemical Pharmacology* 79: 575-586.

FRESHNEY, I. 2001. Application of cell cultures to toxicology. *Cell Biology and Toxicology* 17: 213-230.

FUENTES-PRIOR, P. & SALVESEN, G.S. 2004. The protein structures that shape caspase activity, specificity, activation and inhibition. *Biochemical Journal* 384: 201-232.

GAO, C., DING, Y., ZHONG, L., JIANG, L., GENG, C., YAO, X. & CAO, J. 2014. Tacrine induces apoptosis through lysosome- and mitochondria-dependent pathway in HepG2 cells. *Toxicology In Vitro* 28: 667-674.

GLAUERT, A.M. 1980. Fixation, dehydration and embedding of biological specimens. In: Glauert, A.M. (ed.). *Practical methods in electron microscopy*, Vol. 3, pp. 91. Elsevier Biomedical Press, North-Holland.

GONZALEZ, R. & TARLOFF, J. 2001. Evaluation of hepatic subcellular fractions for Alamar Blue and MTT reductase activity. *Toxicology In Vitro* 15: 257-259.

GORES, G.J., NIEMINEN, A.L., FLEISHMAN, K.E., DAWSON, T.L., HERMAN, B. & LEMSTERS, J.J. 1988. Extracellular acidosis delays onset of cell death in ATP-depleted hepatocytes. *American Journal of Physiology* 255: 315-322.

GREEN, D.R. & REED, J.C. 1998. Mitochondria and apoptosis. *Science* 281: 1309-1312.

HAMACHER-BRADY, A., BRADY, N.R. & GOTTLIEB, R.A. 2006. The interplay between pro-death and pro-survival signalling pathways in myocardial ischemia/reperfursion injury: Apoptosis meets autophagy. *Cardiovascular Drugs Therapy* 20: 445-462.

HAN, S.I., KIM, Y.S. & KIM, T.H. 2008. Role of apoptotic and necrotic cell death under physiologic conditions. *Biochemistry and Molecular Biology Reports* 41: 1-10.

HANSEN, M.B., NIELSEN, S.E. & BERG, K. 1989. Re-examination and further development of a precise and rapid dye method for measuring cell growth/cell kill. *Journal of Immunological Methods* 119: 203-210.

HARBELL, J.W., KOONTZ, S.W., LEWIS, R.W., LOVELL, D. & ACOSTA, D. 1997. Cell cytotoxicity assays. *Food and Chemical Toxicology* 35: 79-126.

HENICS, T. & WHEATLEY, D.N. 1997. Vacuolar cytoplasmic phase separation in cultured mammalian cells involves the microfilament network and reduces motional properties of intracellular water. *International Journal of Experimental Pathology* 78: 343-354.

HENICS, T. & WHEATLEY, D.N. 1999. Cytoplasmic vacuolation, adaptation and cell death: A view on new perspectives and features. *Biology of the Cell* 91: 485-498.

HORVATH, S. 1980. Cytotoxicity of drugs and diverse chemical agents to cell cultures. *Toxicology* 16: 59-66.

HUANG, P., AKAGAWA, K., YOKOYAMA, Y., NOHARA, K., KANO, K. & MORIMOTO, K. 2007. T-2 toxin initially activates caspase-2 and induces apoptosis in U937 cells. *Toxicology Letters* 170: 1-10.

HUSØY, T., SYVERSEN, T. & JENSSEN, J. 1993. Comparison of four *in vitro* cytotoxicity tests: the MTT assay, NR assay, uridine incorporation and protein measurements. *Toxicology In Vitro* 7(2): 149-154.

ICHIHARA, A., KAWAGISHI, H., TOKUGAWA, N. & SAKAMURA, S. 1986. Stereoselective total synthesis and stereochemistry of diplodiatoxin, a mycotoxin from *Diplodia maydis*. *Tetrahedron Letters* 27(12): 1347-1350.

KELLERMAN, T.S., RABIE, C.J., VAN DER WESTHUIZEN, G.C.A., KRIEK, N.P.J. & PROZESKY, L. 1985. Induction of diplodiosis, a neuromycotoxicoses, in domestic ruminants with cultures of indigenous and exotic isolates of *Diplodia maydis*. *Onderstepoort Journal of Veterinary Research* 52: 35-42.

KELLERMAN, T.S., PROZESKY, L., SCHULTZ, R.A., RABIE, C.J., VAN ARK, H., MAARTENS, B.P. & LÜBBEN, A. 1991. Perinatal mortality in lambs of ewes exposed to cultures of *Diplodia maydis* (= *Stenocarpella maydis*) during gestation. *Onderstepoort Journal of Veterinary Research* 58: 297-308.

KELLERMAN, T.S., NAUDÉ, T.W. & FOURIE, N. 1996. The distribution, diagnoses and estimated economic impact of plant poisonings and mycotoxicoses in South Africa. *Onderstepoort Journal of Veterinary Research* 63: 65-90.

KELLERMAN, T.S., COETZER, J.A.W., NAUDÉ, T.W. & BOTHA, C.J. 2005. *Plant poisoning and mycotoxicoses of livestock in Southern Africa*, 2nd ed. Oxford University Press, Cape Town.

KERR, J.F.R., WHYLLIE, A.H. & CURRIE, A.R. 1972. Apoptosis: A basic biological phenomenon with wide-ranging implications in tissue kinetics. *British Journal of Cancer* 26: 239-257.

KIM, H., YOON, S.C., LEE, T.Y. & JEONG, D. 2009. Discriminative cytotoxicity assessment based on various cellular damages. *Toxicology Letters* 184: 13-17.

KITANAKA, C. & KUCHINO, Y. 1999. Caspase-independent programmed cell death with necrotic morphology. *Cell Death Differentiation* 6: 508-515.

KOEHLER, B. 1942. Natural mode of entrance of fungi into corn ears and some symptoms that indicate infection. *Journal of Agricultural Research* 64: 421-442.

KOIZUMI, T., SHIRAKURA, H., KUMAGAI, H., TATSUMOTO, H. & SUZUKI, K.T. 1996. Mechanism of cadmium-induced cytotoxicity in rat hepatocytes: cadmium-induced active oxygen-related permeability changes of the plasma membrane. *Toxicology* 114: 125-134.

KOOPMAN, G., REUTELINGSPERGER, C.P.M., KUIJTEN, G.A.M., KEEHNEN, R.M.J., PALS, S.T. & VAN OERS, M.H.J. 1994. Annexin V for flow cytometric detection of phosphatidylserine expression on B cells undergoing apoptosis. *Blood* 84(5): 1415-1420.

KORZENIEWSKI, C. & CALLEWAERT, D.M. 1983. An enzyme-release assay for natural cytotoxicity. *Journal of Immunological Methods* 64: 313:320.

KROEMER, G., DALLAPORTA, B. & RESCHE-REGON, M. 1998. The mitochondrial death/life regulator in apoptosis and necrosis. *Annual Review of Physiology* 60: 619-642.

KROEMER, G. & REED, J.C. 2000. Mitochondrial control of cell death. *Nature Medicine* 6: 513-519.

KRYSKO, O., DE RIDDER, L. & CORNELISSEN, M. 2004. Phosphatidyleserine exposure during early primary necrosis (oncosis) in JB6 cells as evidenced by immunogold labeling technique. *Apoptosis* 9: 495-500.

KRYSKO, D.V., D'HERDE, K. & VANDENABEELE, P. 2006. Clearance of apoptotic and necrotic cells and its immunological consequences. *Apoptosis* 11(10): 1709-1726.

KRYSKO, D.V., VANDEN BERGHE, T., D'HERDE, K. & VANDENABEELE, P. 2008. Apoptosis and necrosis: detection, discrimination and phagocytosis. *Methods* 44: 205-221.

KUSTERMANN, S., BOESS, F., BUNESS, A., SCHMITZ, M., WATZELE, M., WEISER, T., SINGER, T., SUTER, L. & ROTH, A. 2013. A label-free, impedance-based real time assay to identify drug-induced toxicities and differentiate cytostatic from cytotoxic effects. *Toxicology In Vitro* 27: 1589-1595.

LATTERELL, F.M. & ROSSI, A.E. 1983. *Stenocarpella macrospora* (=*Diplodia*) and *S. maydis* (=*Diplodia*) compared as pathogens of corn. *Plant Disease* 67: 725-729.

LEVINE, B. & KROEMER, G. 2008. Autophagy in the pathogenesis of disease. *Cell* 132: 27-42.

LEZAR, S. & BARROS, E. 2010. Oligonucleotide microarray for the identification of potential mycotoxigenic fungi. *BMC Microbiology* 10: 87-101.

LIAO, T.T., JIA, R.W., SHI, Y.L., JIA, J.W., WANG, L. & CHUA, H. 2011. Propidium iodide staining method for testing the cytotoxicity of 2,4,6-trichlorophenol and perfluorooctane sulfonate at low concentrations with Vero cells. *Journal of Environmental Science and Health Part A* 46: 1769-1775.

LIU, Y., PETERSON, D.A., KIMURA, H. & SCHUBERT, D. 1997. Mechanism of cellular 3-(4,5-dimethylthiazol-2-yl)-2,5-diphenyltetrazolium bromide (MTT) reduction. *Journal of Neurochemistry* 69: 581-593.

LOCKSHIN, R.A. & ZAKERI, Z. 2004. Caspase-independent cell death? *Oncogene* 23: 2766-2773.

LOOS, B. & ENGELBRECHT, A-M. 2009. Cell death. A dynamic response concept. *Autophagy* 5(5): 1-14.

LOS, M., WESSELBORG, S. & SCHULZE-OSTHOFF, K. 1999. The role of caspases in development, immunity, and apoptotic signal transduction: lessons from knockout mice. *Immunity* 10: 629-639.

LOUW, W.K.A. 1969. Toxic metabolites of *Diplodia maydis* (Berk.) Sacc. M.Sc. (Agric.) Thesis, University of Pretoria.

MAGGON, K.K., GUPTA, S.K. & VENKITASUBRAMANIAN, T.A. 1977. Biosynthesis of aflatoxins. *Bacteriology Reviews* 41: 822-855.

MARASAS, W.F.O. 1977. The genus *Diplodia*. In: Wyllie, T.D. & Moorehouse, L.G. (Eds.). *Mycotoxic Fungi, Mycotoxins, Mycotoxicoses. An Encyclopedic Handbook*, Vol. 1, pp. 28-36. Marcel Decker, Inc., New York.

MARASAS, W.F.O., GELDERBLOM, W.C.A., SHEPHARD, G.S. & VISMER, H.F. 2012. Mycotoxicological research in South Africa 1910-2011. *World Mycotoxin Journal* 5(1): 89-102.

MARIÑO, G. & LÓPEZ-OTÍN, C. 2004. Autophagy: molecular mechanisms, physiological functions and relevance in human pathology. *Cellular and Molecular Life Sciences* 61: 1439-1454.

MCNEW, G.L. 1937. Crown infection of corn by *Diplodia zeae. Iowa Agriculture Experimental Station Research Bulletin* pp. 216.

MEIER, P. & VOUSDEN, K.H. 2007. Lucifer's labyrinth-ten years of path finding in cell death. *Molecular Cell* 28: 746-754.

MILLER, J.H. 1952. The presence of internal mycelium in corn grains in relation to external symptoms of corn ear rot. *Phytopathology* 4: 286.

MITCHELL, D.T. 1919. Poisoning of cattle by *Diplodia*-infected maize. *South African Journal of Science* 16: 446-452.

MOSMANN, T. 1983. Rapid colorimetric assay for cellular growth and survival: application to proliferation and cytotoxicity assays. *Journal of Immunological Methods* 65: 55-63.

MOUTON, M. 2014. Resistance in maize inbred lines to the major ear rot pathogens and their mycotoxins. MSc thesis (Plant Path.), Stellenbosch University.

NAGATA, S. 2000. Apoptotic DNA fragmentation. *Experimental Cell Research* 256 12-18.

NICOLETTI, I., MIGLIORATI, G., PAGLIACCI, M.C., GRIGNANI, F. & RICCARDI, C. 1991. A rapid and simple method for measuring thymocyte apoptosis by propidium iodide staining and flow cytometry. *Journal of Immunological Methods* 139: 271-279.

NIEMINEN, A. L., GORES, G.J., BOND, J.M., IMBERTI, R., HERMAN, B. & LEMASTERS, J.J. 1992. A novel cytotoxicity screening assay using a multiwell fluorescence scanner. *Toxicology and Applied Pharmacology* 115: 147-155.

NILES, A.L., MORAVEC, R.A. & RISS, T.L. 2008. Update on *in vitro* cytotoxicity assays for drug development. *Expert Opinion on Drug Discovery* 3(6): 655-669.

NOWELL, D.C. 1997. Studies on ear rot and grey leaf spot of maize in South Africa. PhD thesis (Plant Path.), University of KwaZulu-Natal.

ODRIOZOLA, E., ODEÓN, A., CANTON, G., CLEMENTE, G. & ESCANDÉ, A. 2005. *Diplodia maydis*: a cause of death of cattle in Argentina. *New Zealand Veterinary Journal* 53(2): 160-161.

ORRENIUS, S., ZHIVOTOVSKY, B. & NICOTERA, P. 2003. Regulation of cell death: the calcium-apoptosis link. *Nature Reviews Molecular Cell Biology* 4: 552-565.

ÓZSVÁRI, B., PUSKÁS, L.G., NAGY, L.I., KANIZSAI, I., GYURIS, M., MADÁCSI, R., FEHÉR, L.Z., GERÖ, D. & SZABÓ, C. 2010. A cell-microelectronic sensing technique for the screening of cytoprotective compounds. *International Journal of Molecular Medicine* 25: 525-530.

POLLANEN, M.S., QUINN, B.A., WOLLENBERG, G.K. & HAYES, M.A. 1990. Reversible mitochondrial swelling in cultured rat hepatocytes exposed to 1,2-dimethylhydrazine. *Experimental and Molecular Pathology* 52: 170-178.

PROZESKY, L., KELLERMAN, T.S., SWART, D.P., MAARTENS, B.P. & SCHULTZ, R.A. 1994. Perinatal mortality in lambs of ewes exposed to cultures of *Diplodia maydis* (=*Stenocarpella maydis*) during gestation. A study of the central nervous system lesions. *Onderstepoort Journal of Veterinary Research* 61: 247-253.

RABIE, C.J., VAN RENSBURG, S.J., KRIEK, N.P.J. & LÜBBEN, A. 1977. Toxicity of *Diplodia maydis* to laboratory animals. *Applied and Environmental Microbiology* 34(2): 111-114.

RABIE, C.J., KELLERMAN, T.S., KRIEK, N.P.J., VAN DER WESTHUIZEN, G.C.A. & DE WET, P.J. 1985. Toxicity of *Diplodia maydis* in farm and laboratory animals. *Food and Chemical Toxicology* 23(3): 349-353.

RAHMAN, M.F., RAO, S.K. & ACHAR, P.N. 2002. Effect of diplodiatoxin (*Stenocarpella maydis*) on some enzymatic profiles in male and female rats. *Ecotoxicology and Environmental Safety* 52: 267-272.

RAO, K.R., ACHAR, P.N. & RAHMAN, M.F. 2003. Biochemical changes in liver and serum of diplodiatoxin (*Stenocarpella maydis*) treated male and female rats. *Drug and Chemical Toxicology* 26(4): 231-243.

RICCARDI, C. & NICOLETTI, I. 2006. Analysis of apoptosis by propidium iodide staining and flow cytometry. *Nature Protocols* 1(3): 1458-1461.

RIET-CORREA, F., RIVERO, R., ORDRIOZOLA, E., ADRIEN, M.D., MEDEIROS, R.M.T. & SCHILD, A.L. 2013. Mycotoxicoses of ruminants and horses. *Journal of Veterinary Diagnostic Investigation* 25(6): 692-708.

RISS, T.L. & MORAVEC, R.A. 2004. Use of multiple assay endpoints to investigate the effects of incubation time, dose of toxin, and plating density in cell-based cytotoxicity assays. *Assay and Drug Development Technologies* 2(1): 51-61.

ROBERTSON, J.D., ORRENIUS, S. & ZHIVOTOVSKY, B. 2000. Review: Nuclear events in apoptosis. *Journal of Structural Biology* 129: 346-358.

ROGERS, K.D., CANNISTRA, J.C., GLOER, J.B. & WICKLOW, D.T. 2014. Diplodiatoxin, chaetoglobosins and diplonine associated with a field outbreak of *Stenocarpella* ear rot in Illinois. *Mycotoxin Research* 30: 61-70.

SABATER-VILAR, M., MAAS, R.F.M., DE BOSSCHERE, H., DUCATELLE, R. & FINK-GREMMELS, J. 2004. Patulin produced by an *Aspergillus clavatus* isolated from feed containing malting residues associated with a lethal neurotoxicosis in cattle. *Mycopathologia* 158: 419-426

SABERI, B., SHINOHARA, M., YBANEZ, M.D., HANAWA, N., GAARDE, W.A., KAPLOWITZ, N. & HAN, D. 2008. Regulation of H_2O_2-induced necrosis by PKC and AMP-activated kinase signalling in primary cultured hepatocytes. *American Journal of Physiology-Cell Physiology* 295: 50-63.

SAIKUMAR, P., DONG, Z., MIKHAILOV, V., DENTON, M., WEINBERG, J.M. & VENKATACHALAM, M.A. 1999. Apoptosis: definition, mechanisms, and relevance to disease. *American Journal of Medicine* 107: 489-506.

SAWAI, H. & DOMAE, N. 2011. Discrimination between necrosis and apoptosis by necrostatin-1 in annexin V-positive/propidium iodide-negative cells. *Biochemical and Biophysical Research Communications* 411: 569-573.

SCHULTZ, R.A., SNYMAN, L.D., BASSON, K.M. & LABUSCHAGNE, L. 2009. The use of guinea pig model in detecting diplodiosis, a neuromycotoxicosis of ruminants. In: Riet-Correa, F., Pfister, J., Schild, A.L. & Wierenga, T. (Eds.). *Poisonous by Plants, Mycotoxins and Related Toxins*, Proceedings of the 8th International Symposium on Poisonous Plants, João Pessoa-Paraiba, Brazil, May 4-8, 2009, CABI: Oxfordshire, U.K., pp. 520-523.

SCHULZE-OSTHOFF, K., BAKKER, A.C., VANHAESEBROECK, B., BEYAERT, R., JACOB, W.A. & FIERS, W. 1992. Cytotoxic activity of tumor necrosis factor is mediated by early damage of mitochondrial functions. *The Journal of Biological Chemistry* 267 (8): 5317-5323.

SCHULZE-OSTHOFF, K. 2008. How cells die: Apoptosis and other cell death pathways. In: Rode, H-J. (Ed.). *Apoptosis, Cytotoxicity and Cell Proliferation*, 4th ed. Roche Diagnostics GmbH, Germany.

SCHWEICHEL, J.U. & MERKER, H.J. 1973. The morphology of various types of cell death in prenatal tissues. *Teratology* 3: 253-266.

SHIMIZU, S., EGUCHI, Y., KAMIIKE, W., ITOH, Y., HASEGAWA, J-I., YAMABE, K., OTSUKI, Y., MATSUDA, H. & TSUJIMOTO, Y. 1996. Induction of apoptosis as well as necrosis by hypoxia and predominant prevention of apoptosis by Bcl-2 and Bcl-X_L[1]. *Cancer Research* 56: 2161-2166.

SHIMIZU, S., NARITA, M. & TSUJIMOTO, Y. 1999. Bcl-2 family proteins regulate the release of apoptogenic cytochrome c by the mitochondrial channel VDAC. *Nature* 399: 483-487.

SHOPSIS, C. & ENG, B. 1985. Rapid cytotoxicity testing using a semi-automated protein determination on cultured cells. *Toxicology Letters* 26: 1-8.

SHURTLEFF, M.C. 1980. *Compendium of corn diseases*, 2nd ed., pp. 105. American Phytopathological Society, St. Paul, MN, USA.

SNYMAN, A.J. 1991. Factors affecting production and germination of *Stenocarpella maydis* propagules. MSc thesis (Agric.), University of Pretoria.

SNYMAN, L.D., KELLERMAN, T.S., VLEGGAAR, R., FLETT, B.C., BASSON, K.M. & SCHULTZ, R.A. 2011. Diplonine, a neurotoxin isolated from cultures of the fungus *Stenocarpella maydis* (Berk.) Sacc. that induces diplodiosis. *Journal of Agricultural and Food Chemistry* 59: 9039-9044.

STEYN, P.S., WESSELS, P.L., HOLZAPFEL, C.W., POTGIETER, D.J.J. & LOUW, W.K.A. 1972. The isolation and structure of a toxic metabolite from *Diplodia maydis* (BERK.) SACC. *Tetrahedron* 28: 4775-4785.

SUSIN, S.A., DAUGAS, E., RAVAGNAN, L., SAMEJIMA, K., ZAMZAMI, N., LOEFFLER, M., COSTANTINI, P., FERRI, K.F., IRINOPOULOU, T., PRÉVOST, M-C., BROTHERS, G., MAK, T.W., PENNINGER, J., EARNSHAW, W.C. & KROEMER, G. 2000. Two distinct pathways leading to nuclear apoptosis. *Journal of Experimental Medicine* 192(4): 571-579.

SUTTON, B.C. 1964. Coelomycetes III. *Mycological Papers* 97: 16-22.

SUTTON, B.C. 1980. *The Coelomycetes: Fungi imperfecti with pycnidia, acervuli and stromata*. Commonwealth Mycological Institute, Kew, Surrey, U.K.

TALANIAN, R.V., QUINLAN, C., TRAUTZ, S., HACKETT, M.C., MANKOVICH, J.A., BANACH, D., GHAYUR, T., BRADY, K.D. & WONG, W.W. 1997. Substrate specificities of caspase family proteases. *Journal of Biological Chemistry* 272(15): 9677-9682.

TAYLOR, R.C., CULLEN, S.P. & MARTIN, S.J. 2008. Apoptosis: controlled demolition at the cellular level. *Nature Reviews Molecular Cell Biology* 9: 231-241.

THEILER, A. 1927. Die Diplodiosis der Rinder und Scafe in Süd-Afrika. *Deutschen Tierärztlichen Wochenschrift* 35: 395-399.

THORNBERRY, N.A., RANO, T.A., PETERSON, E.P., RASPER, D.M., TIMKEY, T., GARCIA-CALVO, M., HOUTZAGER, V.M., NORDSTROM, P.A., ROY, S., VAILLANCOURT, J.P., CHAPMAN, K.T. & NICHOLSON, D.W. 1997. A combinatorial approach defines specificities of members of the caspase family and granzyme B. Functional relationships established for key mediators of apoptosis. *Journal of Biological Chemistry* 272(29): 17907-17911.

TRAHTEMBERG, U., ATALLAH, M., KRISPIN, A., VERBOVETSKI, I. & MEVORACH, D. 2007. Calcium, leukocyte cell death and the use of annexin V: fatal encounters. *Apoptosis* 12(10): 1769-1780.

TRUMP, B.F., BEREZESKY, I.K., CHANG, S.H. & PHELPS, P.C. 1997. The pathways of cell death: Oncosis, apoptosis and necrosis. *Toxicologic Pathology* 25: 82-88.

TURNER, N.W., SUBRAHMANYAM, S. & PILETSKY, S.A. 2009. Analytical methods for determination of mycotoxins: A review. *Analytica Chimica Acta* 632: 168-180.

UHLIG, S., BOTHA, C.J., VRÅLSTAD, T., ROLÉN, E. & MILES, C.O. 2009. Indole-diterpenes and ergot alkaloids in *Cynodon dactylon* (Bermuda grass) infected with *Claviceps cynodontis* from an outbreak of tremors in cattle. *Journal of Agricultural and Food Chemistry* 57: 11112-11119.

UNWIN, P.N.T. & ZAMPIGHI, G. 1980. Structure of the junction between communicating cells. *Nature* 283: 545-549.

UNWIN, P.N.T. & ENNIS, P.D. 1984. Two configurations of a channel-forming membrane protein. *Nature* 307: 609-613.

VALENTIN, I., LHUGUENOT, J-C. & CHANGNON, M.C. 2000. Uridine uptake inhibition as a cytotoxicity test for a human hepatoma cell line (HepG2 cells): comparison with the neutral red assay. *Biochimica et Biophysica Acta* 794: 373-380.

VAN DER BIJL, P.A. 1914. Preliminary investigation on the deterioration of maize infected with *Diplodia zeae* (Schw.) Lev. *Transactions of the Royal Society of South Africa* 4(1): 231-239.

VAN ENGELAND, M., NIELAND, L.J.W., RAMAEKERS, F.C.S., SCHUTTE, B. & REUTELINGSPERGER, C.P.M. 1998. Annexin V-affinity assay: A review on an apoptosis detection system based on phosphatidylserine exposure. *Cytometry* 31: 1-9.

VAN RENSBURG, J.B.J. & FERREIRA, M.J. 1997. Resistance of elite maize inbred lines resistant to *Diplodia* ear rot, caused by *Stenocarpella maydis* (Berk) Sutton. *South African Journal of Plant and Soil* 14: 89-92.

VAN RENSBURG, J.B.J. & FLETT, B.C. 2010. A review of research achievements on maize stem borer, *Busseola fusca* (Fuller) and *Diplodia* ear rot caused by *Stenocarpella maydis* (Berk. Sutton). *South African Journal of Plant and Soil* 27: 74-80.

VERMES, I., HAANEN, C., STEFFENS-NAKKEN, H. & REUTELINGDPERGER, C. 1995. A novel assay for apoptosis flow cytometric detection of phosphatidylserine expression on early apoptotic cells using fluorescein labelled annexin V. *Journal of Immunological Methods* 184: 39-51.

VILUKSELA, M., VAINIO, P.J. & TUOMINEN, R.K. 1996. Cytotoxicity of macrolide antibiotics in a cultured human liver cell line. *Journal of Antimicrobial Chemotherapy* 38: 465-473.

WEYERMANN, J., LOCHMANN, D. & ZIMMER, A. 2005. A practical note on the use of cytotoxicity assays. *International Journal of Pharmaceutics* 288: 369-376.

WICKLOW, D.T., ROGERS, K.D., DOWD, P.F. & GLOER, J.B. 2011. Bioactive metabolites from *Stenocarpella maydis*, a stalk and ear rot pathogen of maize. *Fungal Biology* 115: 133-142.

XIA, Z. & ACHAR, P.N. 2001. Random amplified polymorphic DNA and polymerase chain reaction markers for the differentiation and detection of *Stenocarpella maydis* in maize seeds. *Journal of Phytopathology* 149: 35-44.

XIA, M., HUANG, R., WITT, K.L., SOUTHALL, N., FOSTEL, J., CHO, M-H., JADHAV, A., SMITH, C.S., INGLESE, J., PORTIER, C.J., TICE, R.R. & AUSTIN, C.P. 2008. Compound cytotoxicity profiling using quantitative high-throughput screening. *Environmental Health Perspectives* 116(3): 284-291.

XING, J.Z., ZHU, L., JACKSON, J.A., GABOS, S., SUN, X-J., WANG, X-B. & Xu, X. 2005. Dynamic monitoring of cytotoxicity on microelectronic sensors. *Chemical Research in Toxicology* 18: 154-161.

XING, J.Z., ZHU, L., GABOS, S. & XIE, L. 2006. Microelectronic cell sensor assay for detection of cytotoxicity and prediction of acute toxicity. *Toxicology In Vitro* 20: 995-1004.

ZHANG, G., YAN, G., GURTU, V., SPENCER, C. & KAIN, S.R. 1998. Caspase inhibition prevents staurosporine-induced apoptosis in CHO-K1 cells. *Apoptosis* 3: 27-33.

ZHANG, X.D., GILLESPIE, S.K. & HERSEY, P. 2004. Staurosporine induces apoptosis of melanoma by both caspase-dependent and -independent apoptotic pathways. *Molecular Cancer Therapeutics* 3(2): 187-197.

APPENDIX 1

Table A

xCELLigence instrument programming schedule for proliferation experiments

Sequence	Step	No. of Sweeps	Interval	Total Time
1	Step_1	1	1 min	1 min
2	Step_2-1	30	1 min	0.5 h
	Step_2-2	12	5 min	1 h
	Step_2-3	12	10 min	2 h
	Step_2-4	41	30 min	20.5 h
	Step_2-5	72	1 h	72 h

Table B

xCELLigence instrument programming schedule for cytotoxicity experiments

Sequence	Step	No. of Sweeps	Interval	Total Time
1	Step_1	1	1 min	1 min
2	Step_2-1	30	1 min	0.5 h
	Step_2-2	12	5 min	1 h
	Step_2-3	12	10 min	2 h
	Step_2-4	41	30 min	20.5 h
3	Step_3-1	30	1 min	0.5 h
	Step_3-2	12	5 min	1 h
	Step_3-3	12	10 min	2 h
	Step_3-4	41	30 min	20.5 h
	Step_3-5	144 (72)	30 min (1 h)	72 h